HEAT TRANSFER AND FRICTION LOSS ANALYSIS OF NON-WOOD FIBER SUSPENSIONS IN CLOSED CONDUIT FLOW

SAMIRA GHAREHKHANI

FACULTY OF ENGINEERING
UNIVERSITY OF MALAYA
KUALA LUMPUR

2016

HEAT TRANSFER AND FRICTION LOSS ANALYSIS OF NON-WOOD FIBER SUSPENSIONS IN CLOSED CONDUIT FLOW

Samira Gharehkhani

THESIS SUBMITTED IN FULFILMENT OF THE REQUIREMENTS FOR THE DEGREE OF DOCTOR OF PHILOSOPHY

FACULTY OF ENGINEERING
UNIVERSITY OF MALAYA
KUALA LUMPUR

2016

UNIVERSITY OF MALAYA

ORIGINAL LITERARY WORK DECLARATION

Name of Candidate: Samira Gharehkhani

Registration/Matric No: KHA 120061

Name of Degree: **DOCTOR OF PHILOSOPHY**

Title of Project Paper/Research Report/Dissertation/Thesis ("this Work"):

Heat transfer and friction loss analysis of non-wood fiber suspensions in closed conduit flow

Field of Study: **HEAT TRANSFER**

I do solemnly and sincerely declare that:

(1) I am the sole author/writer of this Work;
(2) This Work is original;
(3) Any use of any work in which copyright exists was done by way of fair dealing and for permitted purposes and any excerpt or extract from, or reference to or reproduction of any copyright work has been disclosed expressly and sufficiently and the title of the Work and its authorship have been acknowledged in this Work;
(4) I do not have any actual knowledge nor do I ought reasonably to know that the making of this work constitutes an infringement of any copyright work;
(5) I hereby assign all and every rights in the copyright to this Work to the University of Malaya ("UM"), who henceforth shall be owner of the copyright in this Work and that any reproduction or use in any form or by any means whatsoever is prohibited without the written consent of UM having been first had and obtained;
(6) I am fully aware that if in the course of making this Work I have infringed any copyright whether intentionally or otherwise, I may be subject to legal action or any other action as may be determined by UM.

Candidate's Signature Date:

Subscribed and solemnly declared before,

Witness's Signature Date:

Name:

Designation:

ABSTRACT

Study of the behavior of pulp fiber suspension flow is one of the most significant scientific interests as addition of small amount of fiber to the water changes the flow behavior considerably. Pulp and paper mills are the major industries using the fiber suspensions. However, the tendency of using non-wood fibers as one of the alternative sources is going to be increased, the lack of knowledge about the non-wood fiber suspension flow in pipe raised some concerns regarding the handle of non-wood pulp suspension in different processes. There is no significant reporting about non- wood pulp suspension flow in the pipelines. Therefore, the investigation of the non-wood fiber suspension in pipe flow, such as heat transfer and pressure drop trends seem necessary to obtain. A set up was built in order to evaluate the heat transfer and pressure drop characteristics of flowing pulp fiber suspensions. A number of experiments were conducted for different types of non-wood pulp fibers (Kenaf, Rice straw and Empty fruit bunches fibers). The results show that most of the fiber and paper properties could be correlated with both h_c and pressure drop data. Using this strategy, the papermakers can predict and monitor the paper quality at the stock delivery step (delivery pipe). In order to investigate another objective of this study, a series of experiments were performed to examine the effect of presence of additives e.g. cationic polyacrylamide (CPAM), potato starch and nanocrystalline cellulose (NCC) in pulp suspension on pressure loss and drag reduction phenomena. Among these polymers the hydrodynamic behavior of NCC as a new generation of additives is less known and there is no any report on pipe flow behavior of NCC/pulp mixture. The results revealed that the pulp mixture containing 150 ppm NCC produced higher drag reduction level than pulp suspension alone. The findings in present work can shed light on flow mechanism of non-wood fibers suspensions and their mixtures with polymers in pipe flow.

ABSTRAK

Kajian mengenai kelakuan aliran pulpa terapung adalah salah satu kepentingan saintifik yang amat penting disebabkan penambahan sedikit serat ke atas air merubah kelakuan aliran dengan ketara. Kilang pulpa dan kertas adalah industri utama yang menggunakan gentian terapung. Dalam dekad kebelakangan ini permintaan untuk menggunakan gentian bukan kayu telah meningkat, yang mana penggunakan gentian bukan kayu dalam industri memberi kesan kurang memudaratkan kepada alam sekitar melalui pemeliharaan hutan semula jadi dan pokok-pokok, dan mengurangkan sisa bahan tumbuhan. Walaupun kecenderungan untuk menggunakan gentian bukan kayu sebagai sumber alternatif akan meningkat, kekurangan pengetahuan tentang aliran apungan serat bukan kayu dalam paip menimbulkan beberapa kebimbangan mengenai pengendalian apungan bukan kayu dalam proses pembuatan kertas. Lebih-lebih lagi, disebabkan reka bentuk awal saluran paip adalah berdasarkan apungan serat kayu, persoalan yang terlintas di fikiran adalah sama ada data reka bentuk yang sedia ada adalah mencukupi untuk menggunakan apungan pulpa bukan kayu dalam saluran paip. Oleh itu, permintaan untuk menyiasat berkenaan sifat aliran bukan kayu dalam paip seperti pemindahan haba dan trend kejatuhan tekanan adalah perlu. Satu pelantar ujikaji telah dibina untuk menilai pemindahan haba apungan pulpa dan memaparkan kelakuan kejatuhan tekanan bagi apungan tersebut. Satu reka bentuk eksperimen sistematik telah dijalankan ke atas pelbagai jenis pulpa bukan kayu. Ujianujian telah dilakukan dengan tatacara seperti itu untuk mengaitkan sifat-sifat kertas dengan kedua- dua nilai pekali pemindahan haba dan kejatuhan tekanan. Dalam usaha untuk menyiasat objektif seterusnya dalam kajianini, satu siri eksperiment elah dijalankan untuk mengkaji kesan kehadiran polimercth. polyacrylamidekationik (CPAM), kanji kentang dan nanokristal selulosa (NCC) di dalam apungan pulpa terhadap fenomena kehilangant ekanan dan pengurangan seretan. Keputusan menunjukkan pengurangan seretan di dalam campuran

pulpa dan bahan tambahan, dan apungan pulpa sahaja. Antara polimer ini tingkah laku hidrodinamik NCC sebagai bahan tambahan generasi barua dalah kurang diketahui dan tidak ada apa-apa laporan mengenai tingkah laku aliran paip bagi campuran NCC / pulpa. Keputusan menunjukkan bahawa campuran pulpa yang mengandungi 150 ppm NCC menghasilkan tahap pengurangan seretan lebih tinggi daripada apungan pulpa sahaja. Penemuan dalam kajian ini boleh memberi penerangan tentang mekanisme aliran gentian-gentian apungan bukan kayu dan campuran mereka dengan polimer dalam aliran paip.

ACKNOWLEDGEMENT

When it comes to acknowledgement of the people who have been helpful during the PhD, it becomes a difficult task to express the appreciation by writing in just one or two pages.

My special words of thanks should go to my husband, Farid Seyed Shirazi for his endless love and nonstop supports. My deepest and sincerest appreciation to my parents, sisters and my little princess Farnick for their lovely encouragement.

I would like to salute and acknowledge my supervisors, Dr. Salim Newaz Kazi, Dr. Ahmad Badarudin and Dr. Rushdan Ibrahim; for their kind assistance, support, critical advice and their encouragement to improve my dissertation.

I specially thank Elham Montazer, Hooman Yarmand, Maryam Hosseini, Dr. Mohd Nashrul Mohd Zubir, Dr. Reza Safaei, who have been always supportive and friendly to me and they have helped me a lot in my project.

I am pleased to acknowledge the financial support from Ministry of Higher Education of Malaysia (MOHE), grant number UM.C/HIR/MOHE/ENG/45.

Finally, thank you GOD for your blessing through my life and for all the things I have been given.

Table of Contents

List of Figures

List of Tables

List of Symbols and Abbreviations

A	Area, m^2
C	Concentration, %
C_p	Specific heat, J/kg K
D	Inner diameter of the tube, m
f	Friction factor
H	Head loss (m)
h	Heat transfer coefficient, KW/m2 K
I	Current, Amp
k	Thermal conductivity, W/m K
l	Length of the tube, m
$\dot{m}$	Mass flow rate, kg/s
Nu	Nusselt number,
P	Power, Watts
Pr	Prandtl number
Q	Heat flow, Watts
$\dot{q}$	Heat flux, W/m^2
Re	Reynolds number,
T	Temperature, °C
u	Velocity, m/s
x	Distance of thermocouple from the inner surface of pipe.

Greek symbols

Δp	Pressure drop
ε	Surface roughness
λ	Wall thermal conductivity

μ	Viscosity, kg/m^2 s
ρ	Density, kg/m^3
τ	Shear stress
ω	Fiber coarseness, kg/m

Subscripts

b	Bulk
i	Inlet
m	Mass
o	Outlet
t	Thermocouple
w	Wall

List of Appendices

CHAPTER 1 INTRODUCTION

1.1 Background and motivation

Diversity of application of fiber suspension in different industries such as food processing, textile and composites attracted significant attentions to study the behavior of fiber suspension flow. No industries other than pulp and paper industry are using the fiber suspension in large volume. The investigation on flow behavior of various processes containing the fiber suspension transportation such as washing, screening and refining is critical to the design of the typical paper mill (Pande, Rao, Kapoor, & Roy, 1999)

The major raw material in papermaking is pulp consists of cellulose fibers which come from wood and non-wood plants (Gharehkhani, Sadeghinezhad, et al., 2015). Due to the rising global demand for fibrous material, worldwide shortage of trees in many areas, and increasing environmental awareness, non-wood fibers have become one of the important alternative sources of fibrous material for the 21st century (Pirmahboub, Talebizadeh-Rafsanjani, Charani, & Morvaridi, 2015). In most cases the non-wood materials such as crops, agriculture residues, grasses and tree leaves which do not have immediate beneficial applications in many communities have been proposed to be potential sources of pulp. In many of the Southeast Asian countries such as India, China, and Thailand, non-wood plants have become a major source of fiber (Mossello, Harun, Tahir, et al., 2010).

The problem associated with the flow of non-wood pulp suspensions is that the design of the pipelines in the pulp and paper mills has been done by considering the wood pulp transportation and not the non-wood pulp suspension (Pande et al., 1999). Therefore, study on the non-wood pulp flow can shed light on the design of pulp and paper mill's pipelines.

Fibers in water change the rheological behavior of the water. The interactions between the fibers and hydrodynamic disturbance to the flow field results in an increase in viscosity. It is notable that the behavior of the pulp suspension deviates from Newtonian behavior. The fibers/filament presence in the low concentration suspension is as the individual particles which can bend and absorb turbulent energy. Further increase in fiber concentration results in the formation of flocs and fiber networks (Duffy, 2006).

The flow of non-wood pulp suspension in a pipe can be studied by means of heat transfer coefficient (h_c) and pressure drop behavior where these two parameters can be used to correlate the quality of the paper.

In the case of heat transfer coefficient, once a value of h_c is linked to the acceptable paper product qualities, then this could be used as a pulp quality parameter or indicator (Kazi, Duffy, & Chen, 2014b). It is known that heat transfer coefficient depends on fiber concentration, fiber type and specifications and velocity range as well.

The flow behavior in pipe flow can be divided in three different regimes: Plug, mixed, and turbulent (Jäsberg, 2007). One of the interesting phenomena occurred in turbulent pulp flow is drag reduction when the pressure drop of a water–additive system is lower than the pressure drop of the water alone flowing at the similar flow rate (Kazi et al., 2014b). Fundamentally, it is important to investigate the drag reduction in the fiber slurry to obtain insight into pulp suspension turbulence. In paper making industries the water-soluble polymers having molecular mass greater than about 4 million grams per mole as the retention agents are commonly used additives. The polymer also can cause drag reduction, so in a mixture of pulp and polymer in suspension the drag reduction can be induced by fiber/polymer.

1.2 Objective of study

This project aims to study the flow of non-wood pulp suspension in a straight pipe for certain applications. The objectives in this study are defined as follows:

- To investigate the pressure loss and heat transfer coefficient of non-wood pulp suspension in pipe flow
- To correlate the fiber and paper quality with heat transfer coefficient and pressure loss data.
- To analyze the effect of conventional and new generation additives on friction loss in pipeline flow.

1.3 Organization of the thesis

Chapter 1 highlights the problems existing in this area which provides the motivation for this project, and the objectives of this research.

Chapter 2 presents the literature review which covers the fibers structures, properties of fibers and papers, definition of beating as a mechanical action in paper making process and its effect on fiber and paper properties, and heat transfer and pressure loss studies of fiber suspensions. The efforts which have been made by others to investigate the effect of additives on pressure drop of fiber suspensions are presented in this chapter. Moreover, studies on preparation of NCC and its properties as a new generation of additives are reviewed in the present chapter.

Chapter 3 is related to the materials and methods. The test rig used for experiments and data acquisition is explained in detail. Materials are introduced and synthesis process of NCC, pulp suspension making, and procedures for fiber and paper characterizations are explained. Details of experimental conditions and procedures are presented in the current chapter.

Chapter 4 first provides the water run data in the form of Nusselt number and pressure loss, and comparison between obtained data with existing correlations. Then the heat transfer and pressure loss studies e.g., effect of fiber concentration of pulp samples from different sources and beating process on h_c and pressure drop data are discussed in details. Relationship of h_c and pressure drop data with fiber and paper properties are studied. Moreover, effect of additives on pressure loss are presented and thoroughly discussed.

Chapter 5 provides a concise summary of important outcomes of this work. This chapter also includes recommendation for future studies in the current research area.

CHAPTER 2 LITERATURE REVIEW

2.1 Fiber and paper properties

Modification of the pulp or fiber quality to improve the paper features is one of the most significant scientific challenges in the paper industries. Pulp consists of cellulose fibers which come from wood and non-wood plants, and it is the major raw material in papermaking. The main sources for wood pulps are softwood (e.g., spruce, pine) and hardwood (e.g., eucalyptus, aspen) trees, and for non-wood are crops and agriculture residues (Gharehkhani, Sadeghinezhad, et al., 2015).

The cell wall structure (see Figure 2.1(a-d)) of different species is generally composed of cellulose, hemicelluloses and lignin. Cellulose is a polysaccharide consisting of glucose units (Pokhrel, 2010). The cellulose molecule with several chains organized into elementary fibrils, which are the narrowest fibrils (diameter of 3.5 nm). Each elementary fibril can consists of as high as 40 cellulose chains. The aggregation of elementary fibrils forms the microfibrils having diameters between 10-35 nm (Chinga-Carrasco, 2011; Sixta, 2008). Finally, the macrofibrils are other units which are shaped by the microfibrils aggregations (Figure2.1(b)) (Abe & Yano, 2009; Donaldson, 2007). Macrofibrills are twisted around the cell wall axis which introduced the term "microfibrillar angle (MFA)", (Figure 2.1(a)) (Barnett & Bonham, 2004; Pulkkinen, 2010; Wathén, 2006). A smaller fibril angle is beneficial for paper strength (Blomstedt, 2007; Courchene, Peter, & Litvay, 2006). Cellulose has crystalline structure while hemicellulose has amorphous structure. Hemicellulose surrounds cellulose microfibrils. Hemicellulose has a lower strength than cellulose and can be easily hydrolyzed. It is a polymer of neutral polysaccharides present in the plant cell wall matrix and can be divided into xylans, mannans, β-glucans with mixed linkages, and xyloglucans. Details information about the above mentioned polysaccharides and amount of them in different

species can be found in literatures (Ebringerova, Hromadkova, & Heinze, 2005; Sixta, 2008). The third component of the cell wall is Lignin. Lignin acts as glue and binds the different layers of cell wall (Sutton, Joss, & Crossely, 2000). Lignin is a hydrophobic substance and can be removed by the chemical pulping and bleaching. Low amount of lignin in the raw material makes it as a good candidate for paper making. All of these components are present in the different layers of cell wall. The cell wall can be divided into different layers: middle lamella, primary cell wall, secondary cell wall and Lumen (Figurer 2.1(a)) (Sjöström 1993). Middle lamella acts as a cementing substance between the cells and has highest concentration of lignin (Shafiei Sabet, 2013). The middle lamella (ML) surrounds the primary wall (P). P layer is thin and flexible. It consists mainly of hemicelluloses and lignin and a loose aggregation of microfibrils which oriented randomly in this layer. Cellulose chains are twisted along the axis of glucan chains and are held by hydrogen bonds between the chains (Sixta, 2008; Thomas et al., 2013). Secondary wall is located between the primary wall and lumen. It sometimes consists of three distinct layers: S1, S2 and S3 (Bergander & Salmén, 2002; Meier, 1962). The most of fiber mass belongs to the S2 layer, the MFA in the S2 is 10-30^{o} while the S1 layer has a high microfibril angle (50-70^{o}). The S3 layer is thin with fairly horizontal microfibrils (MFA is 70-90^{o}) (Blomstedt, 2007). The last layer in the cell wall is Lumen (w) which is the hollow core and can hold the moisture (water or water vapor). Fibers with large lumen tend to be flatten to rribons during pulping which result in good strength properties. Scanning microscopic image of cell wall layers and microfibrils can be seen in Figure 2.1 (c and d).

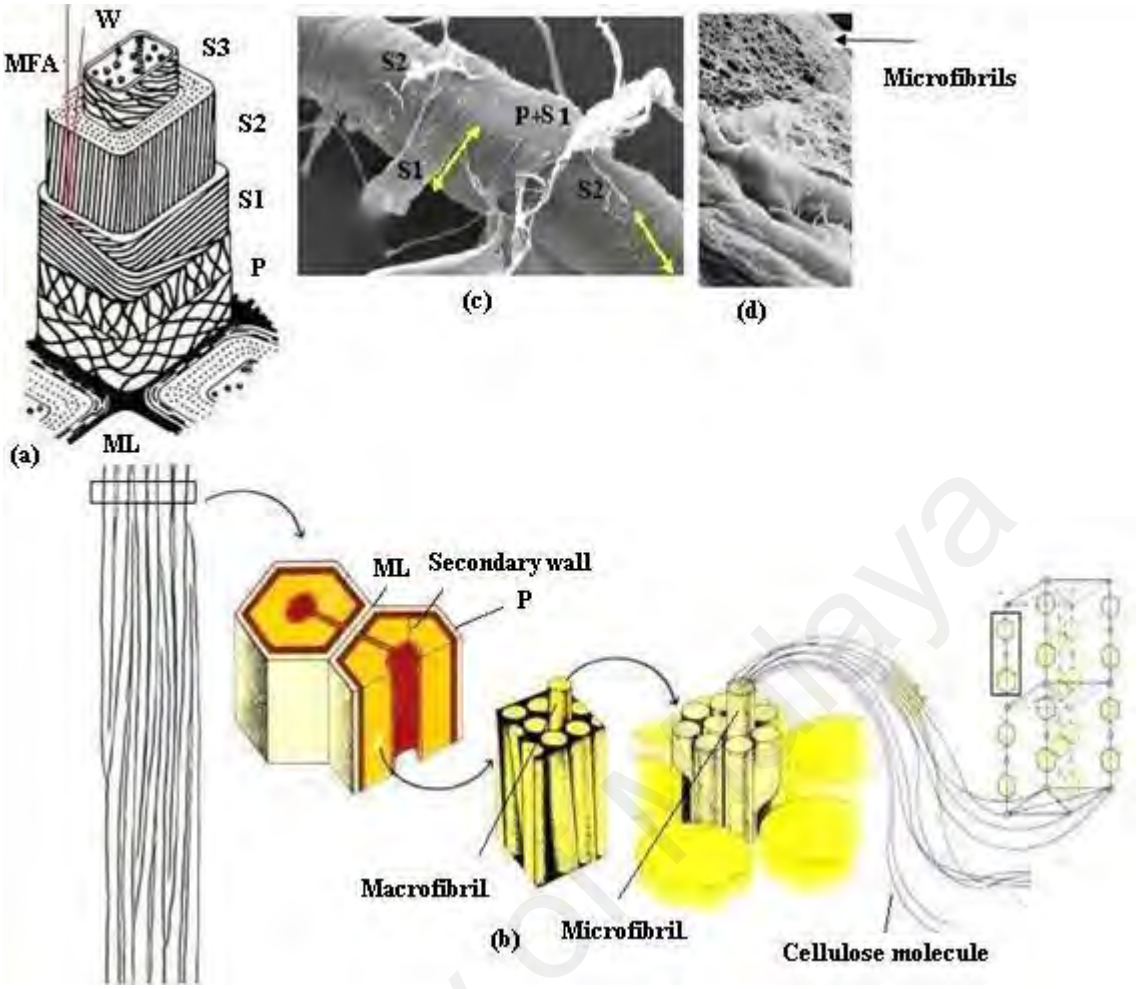

Figure 2.1: Fiber unit structure: (a) schematic of cell wall layers (middle lamella (ML), primary wall (P), secondry wal (S1, S2, S3) and lumen (W); (b) fibrillar structure of cell wall; (c and d) scanning microscopic image of cell wall layers and microfibrils ((Chinga-Carrasco, 2011; Gharehkhani, Sadeghinezhad, et al., 2015; Page, 1989a); Sixta, 2008).

To produce the pulp from the raw materials, different pulping processes can be performed on the chips or small parts which have been produced by the chipping of timber or other parts of plant. Depending on the pulping processes the wood pulps are categorized as mechanical pulp, chemical pulp (e.g., Kraft, Sulfite pulps) and Chemithermomechanical pulp (CTMP). Mechanical pulps are produced from raw material by application of mechanical energy. The mechanical pulps have good print quality. Thermomechanical pulps (TMP) are one of the popular types of mechanical pulps which are produced by processing the wood chips using the high temperature steam and mechanical refining. Chemical pulps are almost pure celluloses which are produced by the heat and chemical treatment. During the treatment of raw material with

chemicals, a large amount of lignin is extracted from the material. The chemical pulps can be classified to Kraft and Sulfite pulps. Kraft pulp or sulfate pulp, is obtained by the treatment of the chips with a mixture of sodium hydroxide and sodium sulfide and sulfite pulp is formed during the pulping process by using the various salts of sulfurous acid. CTMPs are produced by the combination of chemical and mechanical treatments. They need less mechanical energy, and the chemical treatment is performed with lower temperature and shorter time. The CTMPs have good strength. Among different types of pulps, the chemical pulps have the highest share in pulp productions. For instance, in Europe, Kraft pulps account for 65% of total pulp production (Khalil, Bhat, & Yusra, 2012).

2.2 Feasibility of using non-wood fibers for papermaking

Due to the rising global demand for fibrous materials, worldwide shortage of trees in many areas, and increasing environmental awareness, non-wood fibers have become one of the important alternative sources of fibrous materials for the 21st century (Ashori, 2006; Hosseinpour et al., 2010).

The average ratio of non-wood fiber length ranges from 1 mm to 30 mm which depends on plant species and the plant part from which the fiber is derived. Non-woods have lower lignin content (compared to wood), so can be pulped in less time compared to woods. With regards to non-wood fibers for example, jute fiber provides long fiber furnish, where cotton stalks, corn stalks and straw provide short fiber furnish. Yet, fiber length is only one of many criteria that need to be considered when assessing the suitability for papermaking. Furthermore, the chemical and morphological characteristics of non-wood fibers vary by geographical location.

2.3 Physical properties of fibers and papers

Physical properties and dimensional constraints of fiber affect the sheet properties formed by them. The distribution of fiber dimensions, in particular the fiber length and fiber coarseness, are useful for pulp characterization and are often measured using optical techniques (Olson, Robertson, Finnigan, & Turner, 1995).

Fiber length is most commonly parameter which is used to describe the paper sheet properties (Jahan, Chowdhury, & Ni, 2010). Fiber length can be estimated by using the statistical average lengths such as numerical or arithmetic, length-weighted and weight-weighted. The long fibers are more suitable for papermaking. Short fibers formed a denser sheet resulting a decrease in drainage on the paper machine and consequently an increase in energy requirements for drying.

In some rare applications, the reduction of fiber length is a desired effect to improve formation, by decreasing the crowding number (Stoere, Nazhad, & Kerekes, 2001). The shortening of fibers improves sheet formation considerably due to decrease in the crowding number which leads to the lowering of flocculation tendency (Kerekes, Soszynski, & Doo, 2005; Zeng, Retulainen, Heinemann, & Fu, 2012) and smaller sizes of flocs formation (Chen et al., 2012; Ramezani & Nazhad, 2005), thus, contributing to paper uniformity and smoothness. Details of the relationship between the fiber length and the paper properties have been studied in many literatures (Pulkkinen, 2007; Richter et al., 1996; Seth & Page, 1988).

The effect of fiber diameter, wall thickness and coarseness on sheet properties is rather complex and not clearly established. It has been reported that thick-walled fibers form the bulky sheets (Figure 2.2 (a)) with low tensile and high tearing strength. Fibers with narrowest and most symmetrical wall thickness distributions (Figure 2.2 (b)) yield the strongest sheets (Pulkkinen, 2007).

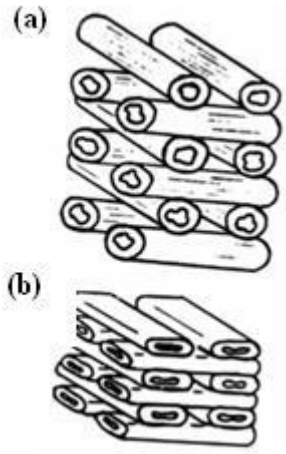

Figure 2.2: (a) Thick walled tend to retain its tubular structure and provide less surface area (b) Thin walled fibers are readily converted into ribbons and provide more surface contact area for bonding (Dutt & Tyagi, 2011).

Tensile strength measures the maximum force per unit width that a paper strip can resist before breaking when applying the load in a direction parallel to the length of the strip (Marin et al., 2009).

Tensile properties of papers are affected by fiber length in a large extent. Moreover, tensile and tear index can be correlated with fiber wall thickness and coarseness (Pulkkinen, 2010). Decrease in fiber length often has negative effect on strength properties of papers (Tschirner, Ramaswamy, & Goel, 2002). The tear strength decreases greatly with a reduction in fiber length. Coarseness also has significant effect on paper properties. Coarseness is defined as the mass per unit length of the fiber. The coarser fibers have thicker walls and lower specific surface area. Coarse and long fibers tend to produce higher tear and tensile resistance than fine fibers do (Sridach, 2010). The coarseness of filaments is generally expressed as denier. The coarseness of a wood fiber depends on its diameter, thickness, and density of its wall. Coarse fibers normally produce paper of higher permeability and have an enhanced capability of absorbing liquids (Duffy, Kazi, & Chen, 2000). Clarke, Ebeling, and Kropholler (1985) proposed a new definition of coarseness based on the mass per unit projected area of fiber as measured by image analysis. The measured quantity is equivalent to the ratio of fiber

coarseness and width and may therefore be considered a measure of fiber grammage (I'Anson, Karademir, & Sampson, 2006).

Another parameter that affects the quality of paper sheets is fiber bonding. Improvement in inter-fiber bonding yielding higher burst and tensile indices (Main et al., 2015) as well as higher apparent density. Apparent density is related to Fiber bonding and flexibility. If the fibers are flexible the sheet will be compact with relatively little pore space. If the fibers are relatively rigid, the sheet will be porous, open and not well bonded.

Flexibility is a key factor as it governs the most physical and optical properties of pulp and paper, including paper formation and paper strength (Fernando, Muhić, Engstrand, & Daniel, 2011; Forgacs, 1963; Paavilainen, 1993; Peng & Johansson, 1996; Petit-Conil, Cochaux, & De Choudens, 1994). The flexible and collapsible fibers giving more close contact which lead to strong bonding (Forsström, Torgnysdotter, & Wågberg, 2005; Lumiainen, 1990; Rusu et al., 2011).

A rigid sheet will concentrate the force on a few fibers in a small area; a flexible sheet will distribute the force over a much larger area and, therefore, a larger number of fibers. Fiber bonding and the total number of fibers that are involved in the sheet rupture have effect on tear index. Tear index is the energy required to propagate an initial tear through several sheets of paper for a fixed distance. The value is reported in g cm/sheet. Longer fibers can produce higher tear and tensile strength papers and decrease sheet density. Moreover in a weakly bonded sheet, since more fibers pull out than break in the tear zone, the tearing resistance is controlled more by the number of bonds that break along the length of the fibers; thus tearing resistance depends strongly on the fiber length (Mossello, Harun, Resalati, et al., 2010).

It was found that flexible fibers form the sheets with more surface area. A very important effect of specific surface is its effect on drainage rate in the papermaking

process. The higher the specific surface the slower the water will be drained from the sheet during its formation. Marius Rusu (2011) showed that fiber bendability increases with the internal fibrillation, and the spruce has a higher increase in flexibility than pine.

Paper has often been referred to as a fibrous network. Micrographs of thin sheets and surfaces have provided some insight into the network structure of paper. The layered nature of paper structure has been observed for some time and more recent developments have enabled the assessment of the internal structure with respect to internal fiber orientation distribution. The quality of paper is limited by the properties of the pulp from which it is derived (Baptista, Costa, Simões, & Amaral, 2014; Gharehkhani, Sadeghinezhad, et al., 2015).

The properties of the sheet mirror the properties of the pulp in many respects. The proportion of fiber types, their physical dimensions (length, diameter and coarseness), mechanical properties (strength and flexibility), optical properties (color and brightness), and chemical properties, are all important and influence the limit of similar properties in a sheet.

As mentioned earlier, non-wood fibers are used in pulp and paper mills. One of the non-wood plants used as a source of paper making is Kenaf (Hibiscus cannabinus L.) Kenaf grows quickly and comparison to other non-wood sources has long fibers (Ashori, 2006; Charani et al., 2013; Nayeri et al., 2013) (Figure 2.3). The southern Asia countries such as India, China, and Thailand account for 90% of world plantation with more than 95% of world production of Kenaf (Mossello, Harun, Tahir, et al., 2010). Various kinds of Kenaf fibers obtained from core, bast or whole are used in pulp and paper industries. The core fibers are shorter than the bast fibers and account for 65% of Kenaf fibrous part (Manzanares, Tenorio, & Ayerbe, 1997; Ververis et al., 2004).

Figure 2.3: Kenaf pulp from Kenaf plant.

Since the core fibers are short and thick, they have low slenderness ratio which resulting the low tearing resistance. Unlike the core fibers, the bast fibers have long length and high slenderness ratio which increase the strength properties of the papers (Saikia, Goswami, & Ali, 1997). Moreover, Bast pulp refines easier than core pulp. By considering the advantages of both core and bast fibers, there is tendency to use the whole stem as a pulp source in papermaking where resulting saving of energy. An enhancement in strength of the recycled fibers was reported by some researchers (Latifah, Ainun, Rushdan, & Mahmudin, 2009) where the old corrugated containers were blended with Kenaf fibers. Kugler (1990) reported that newsprint paper of excellent quality can be made from whole Kenaf stalks. Ververis et al. (2004) have studied the fiber dimensions, lignin and cellulose content of various non-wood fibers and reported that Kenaf is suitable for producing papers of various grades, whereas reed, switchgrass, miscanthus and cotton stalks are suitable for producing mainly writing and printing papers or mixing with conventional wood pulps could produce paper of various uses.

Oil palm (Elaeis guineensis) solid wastes, especially empty fruit bunches (EFB), have great potential to be used as raw materials for the pulp and paper industries. A non-wood fiber source, EFB is the stalk and spikelets of the fruit bunch after removal of fruits (Figure 2.4) and is abundant in south east Asia (Gharehkhani, Shirazi, et al., 2015)

. Malaysia produced 16 million tons of EFB in 2000, which were generally used as mulch for oil palms, converted to bunch ash or discarded as waste (Rushdan, Latifah, Hor, & Mohd Nor, 2007). Its production of oil palm biomass reached to 70 million tons in 2006 (Daud & Law, 2010; Yacob, 2007).

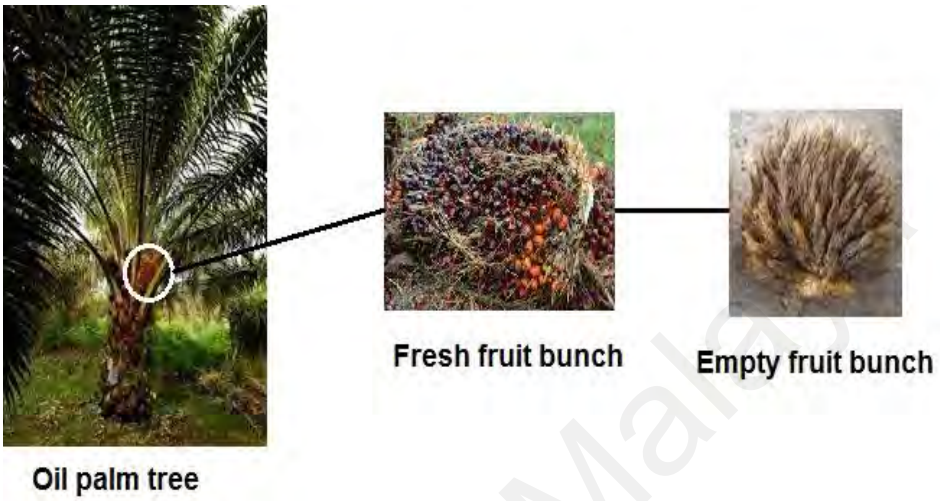

Figure 2.4: Empty fruit bunch from oil palm tree.

Chemically, EFB are similar to hardwood except for their increased pentosan content. The physical properties of paper from EFB are somewhat poorer than those of sulphite paper (Jiménez, Serrano, Rodríguez, & Sánchez, 2009). Wanrosli et al. (2005) observed that in that mixing of old corrugated board with only 20% of unbeaten EFB virgin soda pulp, or with only 10% of beaten EFB virgin pulp is sufficient to completely restore the tensile index of the paper sheets from the recycled fiber. Rushdan et al. (2007) reported that the EFB soda pulp can be blended with recycled pulp from old corrugated container and converted into medium paper commercially. They presented the values of tear index, tensile index and burst index of 5.85 mNm^2/g, 21.37 Nm/g and 1.41 $kPa.m^2/g$ respectively.

Rice for human consumption is of the Asian (*Oryza sativa*) or African variety (*Oryza laberrima*) (Rodríguez et al., 2008). More than 650 million metric tons of paddy was produced in the world at 2013. The greatest producers of rice in 2013 were China (203

million metric tons), India (159.2 million metric tons) and Indonesia (71.28 million metric tons) (http://www.statista.com/statistics).

Therefore, there is a huge amount of rice straw disposal. Traditionally, straw has been burnt on site; this practice generates heavy smoke frequently resulting in breathing, cardiorespiratory and allergic problems in nearby populations, and also it releases large amounts of carbon dioxide to the environment (Rodríguez, Sánchez, Requejo, & Ferrer, 2010). One way to reuse the rice straw is converting it to the pulp (Figure 2.5).

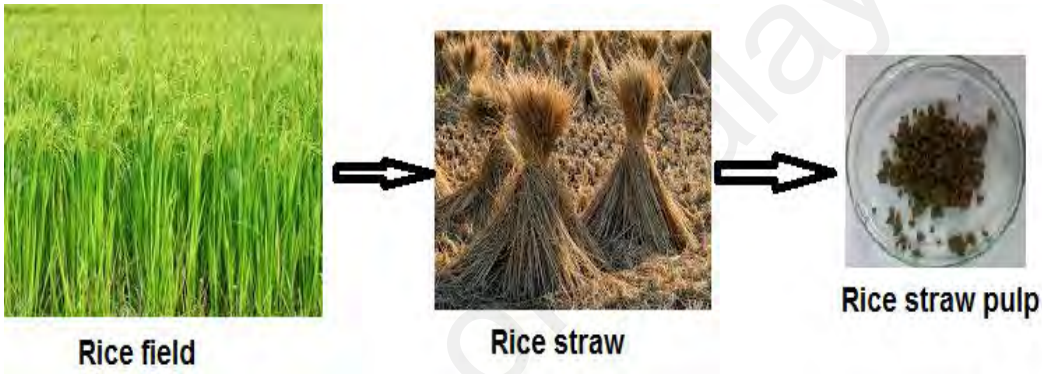

Figure 2.5: Rice starw pulp from rice field.

Rodríguez et al. (2010) evaluated the suitability of rice straw and sodaeanthraquinone (sodaeAQ) pulping process to produce pulp and paper. They concluded that nearly one half of the raw material can be efficiently converted into cellulose pulp and and the pulp can be used to obtain paper or board and recycled paper. (Navaee-Ardeh, Mohammadi-Rovshandeh, & Pourjoozi, 2004) studied the influence of independent variables (alcohol concentration, cooking time and temperature) in the catalytic soda–ethanol pulping of rice straw on various mechanical properties of papers obtained from each pulping process. They reported that short cooking time (150 min), high ethanol concentration (65%) and high temperature (210 °C) could be used to produce papers with suitable burst and tear index.

2.4 Pulp beating

A variety in pulp sources have made a demand for having a fundamental process for improvement of the fiber quality that can be applied on all types of pulps. One of the processes that is conducted in the stock preparation is so-called "pulp refining" or "beating". Pulp refining or beating could be described as a mechanical treatment of the pulp by using the special equipment (refiner). In beating process, the fibers are under compression and shear forces which are causing several changes in specifications of fibers. Dependent on the initial fiber properties, pulp consistency (weight in grams of oven-dry fiber in 100 grams of pulp-water mixture) and refiner specification, the changes in fiber result in higher bonding (Mohlin, Miller, Mohlin, & Miller, 1995).

Major effects of beating on fibers that result changes in fiber structure are categorized by many researchers (Loijas, 2010; Oksanen, Pere, Buchert, & Viikari, 1997; Page, 1989b; Rene, Ulrich, & Wolfgang, 2006). These are listed as: fibrillation (External fibrillation, internal fibrillation (swelling)), fines formation, fiber shortening and fiber straightening.

The first effect of beating on fiber layer is internal fibrillation. This is delamination of the P and S1 layers, caused by the cyclic compression action of forces inside the refiner (Haavisto, Koskenhely, & Paulapuro, 2008; Nugroho, 2012).

Internal fibrillation has been extensively studied, because it is believed by several investigators, to be the most important effect of beating (Ingmanson & Thode, 1959; Kang, 2007). Hardwood and softwood pulps swell inwardly and this behavior is confirmed by the decrease in the lumen size (Mossello, Harun, Shamsi, et al., 2010). A different behavior of swelling in bamboo pulp as a non-wood pulp, in comparison to wood pulp was reported by Wai, Nanko, and Murakami (1985). They claimed, the bamboo swells toward the outside of cell wall, and this is due to the small size of lumen in bamboo. Furthermore, they emphasized that the internal fibrillation dispreads rapidly

in bamboo than wood pulps. Internal fibrillation also makes the fiber more flexible or conformable (Genco, 1999). It can be speculated that the layers which are delaminated during beating are major restraints against swelling due to their hydrophobic nature and the high fibril angle of the S1 layer. Loosening of the fiber wall or reducing the bending stiffness of the fiber wall due to a decrease in the effective E-modulus (a tendency of the fiber, to be deformed elastically. Fiber with a high E-modulus show high tensile strength) occur in result of internal fibrillation.

Pilling off the fibrils from the fiber surface is associated with exposing of the S2 layer which is defined as an external fibrillation (Page, 1989b); this phenomenon can be observed in the microscopic images as the fibrils are still attached to the fiber wall. Sometimes these un-removed layers are sources of roughness enhancement (Fardim & Duran, 2003). The most significant effect of external fibrillation is increasing of the specific surface area of fibrils (Clark, 1969; Nugroho, 2012). During the fibrillation process, some hydrophilic compounds from the cell wall are released which produce the gel- like layers. These gelatinous layers improve the fiber-fiber bonding which can be appeared as a film after drying (Mou et al., 2013). However it is claimed that external fibrillation is the main reason for improving the bonding (Clark, 1969), the role of external fibrillation on pulp and paper properties is a controversial subject. In comparison with internal fibrillation, the external fibrillation has subjected to less interest because during beating it is associated with internal fibrillation and fine formation and these simultaneous changes made it difficult to judge the role of external fibrillation.

Beating increases the amount of fines. The fines consist of fragments of primary and secondary walls with size less than 0.3 mm (Heymer, 2009; Pattara, 2012). Usually a 200 mesh (75μm) screen of a classifier is used to remove fines (Ferreira, Matos, & Figueiredo, 1999). Fines have high surface area and can improve the fibers bonding, though, they have negative effect on drainage time (Wistara & Young, 1999). Increase

of beating time or shear rate means an increase of the amount of fines (González et al., 2012; Page, 1985a; Zeng et al., 2012).

Another change in fiber quality is a reduction in fiber length (Kerekes & Olson, 2003) which usually is an undesirable impact during the beating. It was described above that fines generation also occurs in beating because of excess force during external fibrillation. Since there is a relationship between fiber cutting and fine generation, so accurate measurement of the fiber length changes during beating is difficult (Batchelor, Kjell-Arve, & Ouellet, 1999). Practically, reduction of the fiber length was calculated based on the length weighted average before and after beating. It is notable that the changes in the length-weighted fiber length did not completely reflect the changes in the number of long fibers per unit mass, due to that the measured average fiber length is affected by the generation of fines during beating (Batchelor et al., 1999).

Chemical pulp fibers are initially curly and beating causes the fiber straightening (Mohlin & Alfredson, 1990; Page, 1985a). Curl affects the drainage resistance of most pulps. A reduction in curl index results in a reduction in freeness value (Page, 1985b). The average curl index for straight fiber and curly fiber is 0.1 and 0.2 respectively. Fiber straightening plays an important role in the paper properties. Straightening of fibers improves the load carrying ability as well as the stress distribution in the fiber network and mostly increase the elastic modulus and tensile strength of the paper (Gärd, 2002; Haavisto et al., 2008; Hartler, 1995).

In the study of beating influence on fiber morphology of soda pulp derived from oil palm empty fruit bunches, it has been stated that with the increase of the beating degree, the fiber curl index have the largest decrease among other fiber morphologies (Rushdan, 2003).

Change in the crystallinity during beating is another hypothesis that has been considered in some studies. Although the supermolecular structure of cellulose consists

of two domains; crystalline and amorphous regions, presence of long chains and large amount of hydrogen bonds formed between chains due to the hydroxyl groups, increase the cellulose tendency to have a crystalline structure. The ratio of crystalline to amorphous domains is so-called "degree of crystallinity" (Sixta, 2008). The degree of crystallinity of cellulose is one of the most important crystalline structure parameters. Generally, an increase in crystallinity brings about an increase in tensile strength and stiffness and a decrease in chemical reaction (Chen et al., 2012; Leitner, Seyfriedsberger, & Kandelbauer, 2013; Tschirner, Barsness, & Keeler, 2007; Yuan et al., 2013). Another parameter that has been affected by crystallinity is swelling. As the water dose not penetrate into the crystalline reign, the absorption of water by the cell wall will be decreased by an increase in crystallinity. In other words, an increase in the crystallinity results in a decrease in swelling of fiber (Kongdee, Bechtold, Burtscher, & Scheinecker, 2004; Wan, Yang, Ma, & Wang, 2011). It should be noted that crystallinity of pulps usually used in papermaking is approximately 60-70% (Kočar et al., 2004).

An increase in crystallinity in the prior stages of beating specially has been reported for unbleached pulps. Unbleached pulps contain lignin and hemicelluloses (amorphous structure). As a result of beating, these materials can be removed partly which result in an increase in crystallinity (Leitner et al., 2013). In Leinter's study, the data has been presented only after 2000 revolution PFI mill and there is no data available regarding the further beating for monitoring the trend of the crystallinity.

To sum up, it can be stated that crystallinity is sensitive to degree of beating, and increase or decrease in beating time or severity will change the results.

It is stated that beating can release and expose the chemical compositions existence in the fiber wall pores. This theory has been recently attracted some interests to investigate the effect of beating on surface chemical compositions. The results showed

that during beating, the functional groups have no strong change while the slight variations occur in the distribution of surface chemical compositions.

Numerous studies have been conducted on the effect of beating on electrokinetic properties of fibers (Bhardwaj, Duong, & Nguyen, 2004a; Bhardwaj, Kumar, & Bajpai, 2004b; Carrasco, Mutje, & Pelach, 1996; Herrington & Petzold, 1992; Horvath & Lindstrom, 2007; Penniman, 1992). Beating increases the surface charge while it has no considerable influence on the total charge.

It is widely known that charge groups affect the fiber swelling, fiber flexibility and conformability, wet-end chemistry, retention of cationic papermaking additives, flocculation and mechanical properties of the paper such as tensile index (Grignon & Scallan, 1980; Joutsimo, 2004; Laine, Buchert, Viikari, & Stenius, 1996; Lindström, 1989; Lyytikäinen, Saukkonen, Kajanto, & Kayhko, 2010; Zhang, Sjögren, Engstrand, & Htun, 1994), thus the measurement of the charges is a subject of interest. To obtain the charges, some methods based on titration are recommended, such as Polyelectrolyte titration, conductometric titration and potentiometric titration (Bhardwaj, Hoang, & Nguyen, 2007a; Cui, Pelton, & Ketelson, 2008; Horvath, 2006; Hubbe & Chen, 2004). In polyelectrolyte titration, use of a cationic polymer of high molecular weight is suggested. Using a polymer with low molecular mass is not recommended because the cellulosic fibers have a porous structure and the low molecular mass of the polymer can penetrate through the internal layer of fibers, thus losing much of its ability to affect the electrokinetic measurements. It is worth noting that the previous findings show that there is no significant difference between results obtained from conductometric titration and potentiometric titration (Bhardwaj, Duong, et al., 2004a; Fardim et al., 2002). Apart from the size and molecular weight of additives, the presence of fines could affect the charges. The magnitude of surface charge for fines is more than the fibers due to the

different accessibility level of charged groups in the fibers and fines (Lyytikäinen et al., 2010).

As explained earlier, there are two mechanisms occurring during the beating which contribute in changing the cationic demand. There is an interesting question on how these mechanisms can contribute during beating. The facile answer is that an increment in interactions between ionizable groups and cationic chemicals due to the fiber fibrillation during beating generally lead to the presence of ionic exchange as a first mechanism. In the next stage of beating, carboxylic groups get surrounded by water molecules, so their activity as well as ionic exchange decreases. With further beating, due to fibrillation and fines formation, the surface area increases. As a result of this development, adsorption as a second mechanism contributes to enhance the cationic demand of suspension (Carrasco et al., 1996). It is noticeable that during beating, change in the ionic exchange is not significant and is independent from beating degree (Mutjé et al., 2006). There is a difference of behavior between different types of pulps. This behavior could be explained by considering the amount of fines as well as magnitude of carboxyl group's density, in the pulps.

Monitoring of changes in the behavior of zeta potential has revealed that the refined pulps with no chemical cationic, result higher magnitude of zeta potential than unrefined pulps, and once cationic chemical is added, the refined pulp will show a very large cationic demand. Also, there is an almost linear correlation between zeta potential and cationic demand (Bhardwaj et al., 2004b; Miyanishi, 1995). Similar conclusions have been reported by Sarrazin et al. (2009). Bhardwaj et al. (2007a) also presented the linear relationship between the surface charge and freeness. They used the pine kraft pulp and two types of eucalyptus pulps and reported that in the same freeness, the surface charge for pine kraft pulp is higher than eucalyptus pulps; however, it has the lowest charge ratio. Furthermore, in another study, it has been found similar trend

between the fiber surface charge and beating level for various types of wood and non-wood fibers (Banavath, Bhardwaj, & Ray, 2011). The study showed bagasse has the highest change of surface charge based on the increase in the freeness while bamboo has the lowest change among the pulps.

By considering the research results, cited throughout this study, it can be concluded that beating can affect the fiber structure and its properties through some simultaneous changes. Although, these changes are not quite desirable and have either advantages or disadvantages in papermaking, the profitable gain from beating is more than its adverse effects. For example, fine formation improves the bonding while decreases the drainage time.

2.5 Freeness

One of the most commonly used methods to monitor the occurred changes during the stock preparation, is the measurement of the amount of water in a pulp suspension which could pass through a mesh screen, and is so called "Freeness".

Since the value of freeness is found to be a function of fiber fibrillation and fines formation (Polan, 1993), the freeness test can be used as an indicator of beating effects (Bhardwaj et al., 2007a). In other words, generally, the fiber and paper properties could be presented based on freeness (Helmerius et al., 2010).

Effect of beating on freeness can be described from relevant theories involved in water release during paper manufacturing. As mentioned, beating causes the swelling and hence the fibers become flexible. In this situation, fibers entangled firmly together and make a web during draining in the freeness test. Furthermore, beating creates the fines that are not attached to the fibers. These fines move freely and finally get stuck in the pores between fibers, which mean blocking the water flow path and slowing the drainage (Figure 2.6) (Hubbe & Heitmann, 2007; Paradis et al., 2002). Therefore, it is

concluded that beating reduces the drain ability (Beg & Pickering, 2008; Gao et al., 2009) which is not attractive in the paper making.

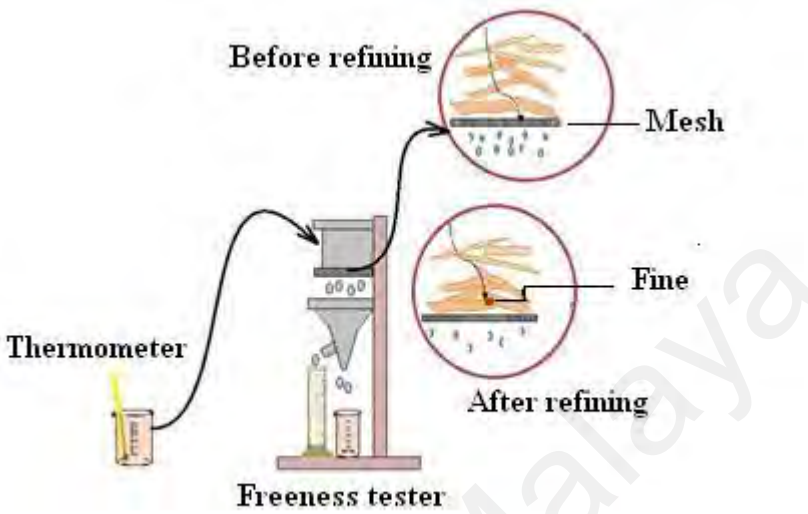

Figure 2.6: Schematic of measurement of the CSF value and the mechanisms affecting the freeness.

The widely used method to measure the freeness especially in the laboratory scale has been so-called Canadian Standard Freeness (CSF) [ml]. To carry out freeness test, a sample of suspension with disintegrated pulps (3 g of pulp in 1 L of water) is poured in the chamber and passes though the (funnel) mesh. The water is drained from the side and the bottom orifices where the collected discharged volume by side orifice is the freeness value. The higher CSF value means higher and faster draining. To eliminate the effect of chemical ions present in the water and to gain the accurate results it is recommended to use the distilled or de-ionized water during the test.

The CSF value measured in the laboratory can be correlated with the pulp consistency and temperature according to the tables presented in (TAPPI, 1999). It can be found from the TAPPI tables, for example, at 400 CSF; around 10% change in CSF value could be caused by the ± 5 ^{o}C change in temperature or by the consistency

variation of ± 0.06% in comparison to the reference temperature 20 ^{o}C and consistency 0.3%.

Usually the unrefined, unbleached softwood kraft pulps have the CSF values as high as 750 ml while after beating, the typical values of Freeness for kraft pulps drop down in the range of 600-250 ml which is strongly depended on the initial Freeness value (Genco, 1999; technology, 2001). Reduction in freeness for both wood and non wood pulps has been reported by different authors (Bhardwaj et al., 2007a; Lumiainen, 2000; Nugroho, 2012). For example, it has been reported that during beating of organosolv wheat straw, the freeness decreases disproportionately due to the presence of weak fiber which appears from the fiber dehydration (Tschirner et al., 2002). It has been reported that at the same beating revolution, the pulps with fewer Kappa number exhibit the lower freeness degree (Gulsoy & Tufek, 2013; Rosli, Mazlan, & Law, 2011).

2.6 Pulp suspension

No other non-Newtonian fluid is pumped in larger volumes than fiber suspensions, yet the flow behavior of fiber suspensions remains one of the most complex and least understood industrial flows.

Pulp concentration is the most important parameter for pulp suspension. (Kerekes, Soszynski, & Doo, 1985) categorized the ranges as follows: low consistency (*Cm*=0-5%) where the suspension is water-fiber suspension; medium consistency (*Cm*=5-20%) formed by mechanically pressing water from a medium consistency suspension and ultra-high consistency (*Cm*>40%). Duffy (2006) proposed the existence of four different particles in the pulp suspension. The Fibers/filament presented in the low concentration suspension are as the individual particles which can bend and absorb turbulent energy. Slightly increase in pulp concentration resulting to the limitation in fiber movements and existence of floccettes as the new particles. At the higher consistency these

floccettes can entangle to each other to form entities called " floc". The last term is called network resulted from fibers in locked status. Networks usually take the shape of the vessel or conduit at the lower flow rates.

As indicated above, the interface between fibers is the important parameter in suspension behavior. Kerekes and Schell (1992) proposed the crowding number N to explain the state of fiber interactions. It can be expressed as the number of fibers in a volume swept out by the length of a single fiber (Kerekes et al., 1985). The mass and volume forms of the N are presented in equation 2.1.

$$N = \frac{2}{3} C_v \left(\frac{L}{d}\right)^2 \cong 5 C_m \frac{L^2}{\omega} \qquad (2.1)$$

The equation 2.1, based on the mass, where L is the length-weighted average length of the pulp fibers ; C_m is the mass concentration (%), and ω is the fiber coarseness (mass per unit length, kg/m). For the equation based on volume, the C, L and d are the volumetric concentration, fiber length, and fiber diameter respectively.

Based on the N number, N=1 is a critical concentration where below than this the suspension is considered as a dilute suspensions. At crowding number between 1 and 60, the suspension is semi-concentrated and at the value higher than 60, the suspension is concentrated (Fällman, 2009; Karppinen, 2014). Martinez, Kiiskinen, Ahlman, and Kerekes (2003) introduced another critical crowding number, $N \sim 16$ named “gel crowding number”. It is notable that in commercial papermaking, pulp suspensions are formed into paper by filtration in the range $16 < N < 60$ to minimize both water usage and flocculation (Derakhshandeh, 2011). It is stated that even a small amount of fibers can change the suspension properties significantly.

2.7 Rheology of pulp suspension

Fibers in water change the rheological behavior of the water. The interactions between the fibers and hydrodynamic disturbance to the flow field results in an increase

in viscosity. It is notable that the behavior of the pulp suspension deviates from Newtonian behavior. The suspension can be shear thinning or shear thickening. Furthermore, there might be time effects when the interaction forces between the particles are adjusted, causing thixotropy (Karppinen, 2014).

A typical rheogram for a pulp suspension has presented in Figure 2.7. Two stresses can be distinguished in the diagram. The minimum stress which is required to overcome the network stress of the suspension for generating the initial flow, is known as yield stress. Another stress labeled as τ_D is the magnitude of stress needed to fully disrupt the system to obtain turbulent flow (Bousfield, 2008). Between these two stress, the yield stress is arguably the most important rheological property of fiber suspensions (Derakhshandeh, 2011) as it has application in various fields such as pulp pipe flow (Moller & Elmqvist, 1980) as well as pulp mixing operations (Sha et al., 2015).

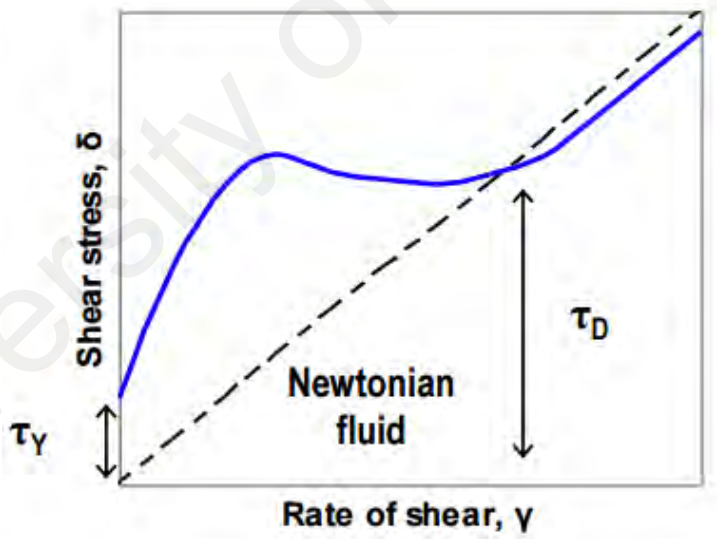

Figure 2.7 A typical rheogram for a pulp suspension.

It is stated that the yield stress to dependent on mass concentration according to the formula presented in equation 2.2.

$$\tau_y = aC_m^b \tag{2.2}$$

Where, τ_y is the yield stress (Pa), a and b are constants specific to the fiber type, and C_m is the mass concentration of the pulp suspension (%) (Kerekes et al., 1985).

Moreover, Bennington, Kerekes, and Grace (1990) reported ranges of a and b from 1.18 to 24.5 and 1.25 to 3.02 respectively for commercial wood pulp fibers using a vane rotor.

However, rheological characteristics are dependent mostly on pulp concentration, other factors such as fiber properties, fiber-fiber interaction, the presence of other components in the suspensions, temperature, shear forces, and shear history can change the reheology of pulp suspension as well (Derakhshandeh, 2011). Dalpke and Kerekes (2005) have investigated the effects of fiber properties on the pulp yield stress and have evaluated the yield stress for a range of pulps of differing species pulped by differing methods. They have reported that longer fibers resulting higher yield stress. Similar attempts have been done to correlate the yield stress with fiber length, concentration, and temperature. Ventura et al. (2007) reported that increase in consistency resulting an increase in air content in the pulp fiber suspensions where the gas congregates around the rotor of the rheometer, impeding momentum transfer into the suspension. According to the studies performed by Bennington et al. (1995), the yield stress was dependent on the fiber concentration and air content as correlated by equation 2.3.

$$\tau_y = aC_m^b(1-\rho)^c \qquad (2.3)$$

Where, φ is the volume fraction of air in the suspension (%) and a , b , and c are parameters related to the fiber properties (Sha et al., 2015).

2.8 Heat transfer and pressure drop of flow through tubes

An enormous amount of work has been carried out in the study of heat transfer and pressure drop in tubes for generating data that have later been used as a basis for designing heat exchanger and cooling systems in industry. But the research requirements of that arena are not over yet. The advancement of science and the rapid growth of problems emerging in industry have generated more avenues to continue

research in this field. Empirical correlations are usually of greatest practical value for design engineering purposes due to their simplicity. The Darcy–Weisbach equation (Equation 2.4) can be used to calculate the energy loss due to friction undergone by a Newtonian liquid flowing in a pipe:

$$\mathrm{H} = f\frac{L}{D}\frac{u^2}{2g} \tag{2.4}$$

Where f is Moody (f_M) which and simply calculated as follow:

$$f_M = \frac{D}{L}\frac{g.\mathrm{H}}{\frac{1}{2}u^2} = \frac{D}{L}\frac{\Delta P}{\frac{1}{2}\rho u^2} \tag{2.5}$$

Apart from the Moody factor, the Fanning friction factor can also be used, which is defined as follows:

$$f = \frac{\tau_w}{\frac{1}{2}\rho u^2} = \frac{1}{4}\frac{D}{L}\frac{\Delta P}{\frac{1}{2}\rho u^2} \tag{2.6}$$

It is well known that the friction factor depends on the Reynolds number (*Re*), and on the relative roughness of the pipe, ε/D. Based on this fact, variety of equations have been developed for different regimes and pipe roughness ranges. For laminar and turbulent flows, the friction factors are calculated through the Hagen–Poiseuille equation and Colebrook and White equation (Colebrook & White, 1937) as presented by equations 2.7 and 2.8 respectively.

$$f = \frac{64}{Re} = \frac{64\mu}{uD\rho} \tag{2.7}$$

$$\frac{1}{\sqrt{f}} = -2\,log\left(\frac{\varepsilon/D}{3.71} + \frac{2.52}{Re\sqrt{f}}\right) \tag{2.8}$$

The Colebrook–White equation is valid for *Re* ranging from 4000 to 10^8, and values of relative roughness ranging from 0 to 0.05.

For convective heat transfer, Petukhov (1970) and Gnielinski (1976) developed correlations (Equations 2.9 & 2.10) based on the Nusselt number for fully developed turbulent in a smooth circular duct and rough surface.

$$Nu = \frac{\left(\frac{f}{8}\right) Re\ Pr}{1.07+12.7\left(\frac{f}{8}\right)^{0.5}\left(Pr^{\frac{2}{3}}-1\right)} \qquad \begin{cases} 0.5 < Pr < 10^6 \\ 4000 < Re < 5 \times 10^6 \\ \text{where } f = (0.79\ lnRe - 1.64)^{-2} \end{cases}$$

(2.9)

$$Nu = \frac{\left(\frac{f}{8}\right)(Re-1000)Pr}{1+12.7\left(\frac{f}{8}\right)^{0.5}\left(Pr^{\frac{2}{3}}-1\right)} \qquad \begin{cases} 0.5 < Pr < 2000 \\ 2300 < \text{Re} < 5 \times 10^6 \end{cases} \tag{2.10}$$

Martinelli (1947) proposed equation 2.11 as a correlation for fully-developed turbulent flow in the fully-rough flow regime of a circular duct.

$$Nu = \frac{Re\ \text{Pr}\sqrt{\left(\frac{f}{8}\right)}}{5(Pr+\ln(1+5\ Pr)+0.5\ln(Re\sqrt{\frac{f}{8}}/60))} \tag{2.11}$$

2.9 Pressure study of fiber suspension flow

Pipe flow is a typical example of a fully developed flow used in papermaking processes. Due to the simple axi-symmetric geometry of a pipe flow, most experimental research has focused on this type of flow (Moayed, 1999). The earliest works on flow mechanisms of pulp suspension in pipes were presented by (Daily & Bugliarello, 1958; Forgacs, 1957) in which the flow behavior can divided in three different regimes: Plug, mixed, and turbulent. Further developments into this behaviour are given by (Duffy & Titchener, 1975; Duffy, Titchener, Lee, and Moller (1976)).

Duffy's outlines (Duffy, 1972) proposed for various regimes for chemically cooked pulps in terms of head loss-velocity curve for a consistency are shown in Figure 2.8. The letters used refer to points on the friction loss curve in Figure 2.8.

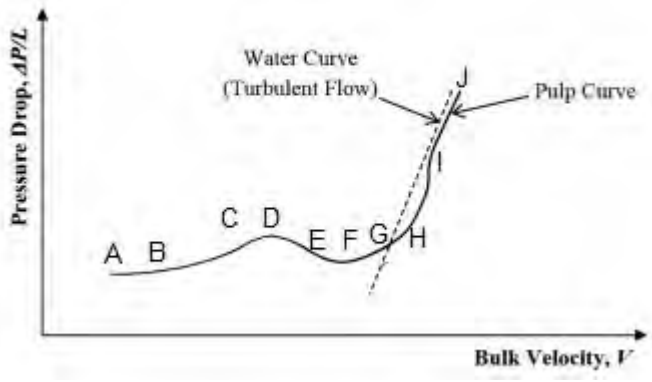

Figure 2.8: Typical friction loss curves for pulp suspension.

Regime A to H

Region AH containing several sub- regime attributed to the plug flow. In the region AB a fiber network is presented in the region with no shearing motion. The weak shear stress due to low Reynolds number could not disrupts the fiber network, and therefore the suspension has pulg structure (Duffy, 1972). In this process, the turbulent energy of fibers is partly captured as the elastic energy of the network. This elastic energy manifests itself as an elastic force that pushes fibers towards the pipe wall. In this regime of low flow velocity, the elastic force is, however, large enough to keep the fiber plug in a contact with the wall. With the increasing of velocity, a water layer would have developed near the pipe wall (BC). In this region an increment in velocity results in an increase in friction head loss. At point C, the laminar water annulus is formed.

Region DF corresponds to the plug flow with water annulus in laminar shear. This region characterized by the change in the head loss curve slop from positive to negative. Slightly before F, the point E is the onset of turbulence annulus.

FG region is attributed to the plug regime with water annulus in turbulent shear which is indicated as a change in the head loss curve slop from negative to positive. Point G is a unique point where the friction head loss of the suspension is same as water and corresponds to the onset of drag reduction. This phenomenon is discussed more in section 4.5.

Regime H to I

This region is known as mixed or transition regime. Point H, is the onset of plug flow disruption. The shear stress is bigger than yield stress and the fiber plug is only formed at the core and a turbulent annulus remains in proximity of the pipe wall. Moayed (1999) showed that the thickness of plug in this region is equal to the proportion of yield stress to shear stress times to pipe diameter.

Regime I to J

Region I to J corresponds to the fully developed turbulence where the fibers are homogeneously dispersed in the suspension. In this region, the friction head loss curves are still below water curve. The transition from mixed flow regime into fully turbulent regime is gradual.

Jäsberg (2007) presented an schematic (Figure 2.9) of flow behavior in the straight pipe according to the mechanisms described above and his new experiments were carried out to obtain more details of flow behavior of chemically released pine or birch pulps with consistency 0.52.0% by weight in a flow loop with pipe diameter of 40 mm. He presented more features of the plug flow by measuring the thickness of a lubrication layer based on the intensity of laser light reflected by fibers and showed that the thickness of the layer reduces with increasing the pulp concentration.

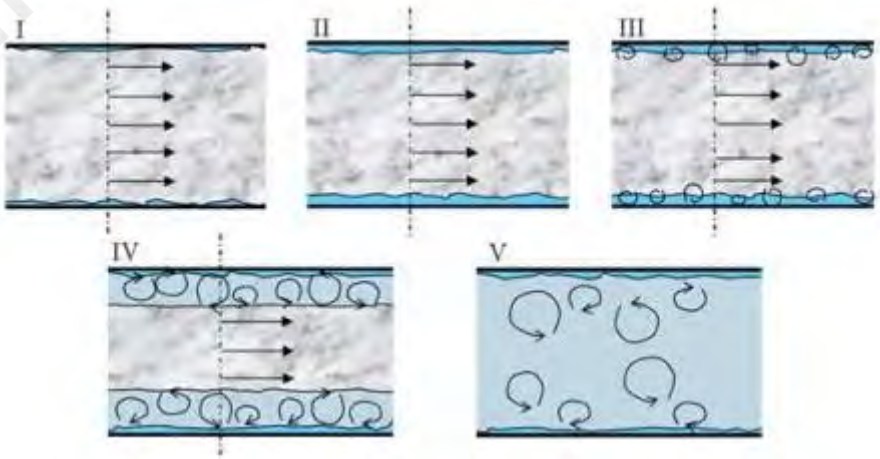

Figure 2.9: The main regimes of fully developed flow of fiber suspension. (I) Plug flow regim with direct fiber-wall contact, (II) Plug flow regime with lubrication layer, (III) Plug flow with a smearing annulus, (IV) Mixed flow and (V) fully turbulent flow.

Based on the results, it is proposed that the flow may be divided into five different regimes according to flow rate, namely plug flow with wall contact, plug flow with a lubrication layer, plug flow with a smearing annulus, mixed flow, and fully turbulent flow.

2.9.1 Drag reduction

The drag reduction occurs when the pressure drop of a solvent–additive system is lower than the pressure drop of the pure solvent flowing at a similar flow rate (Duffy, 1972). Drag reduction phenomena can be described as any modification to a turbulent fluid flow system which results in a reduction in the normal rate of frictional energy loss and which leaves the resulting flow turbulent (a reduction in the wall friction where the shear in the boundary layer redistributed). This effect alters the nature and strength of the vortices formed, resulting in near - wall structural modification of the turbulent boundary layer (MacKenzie, Martinez, & Olson, 2014). A drag-reducing fluid has a value of D_R smaller than 1 (Duffy et al., 2000).

$$D_R = \left[\frac{\left(\frac{\Delta P}{L}\right)_{solvent-additive}}{\left(\frac{\Delta P}{L}\right)_{solvent}}\right] \qquad \text{at v=constant} \qquad (2.12)$$

2.9.2 Fiber- induced drag reduction

pulp slurries are one of the most consistent solid–liquid suspensions in which the drag reduction phenomena has been observed (Kazi, Duffy, & Chen, 1999). Fundamentally, it is important to investigate the drag reduction in the fiber slurry to gain insight into pulp suspension turbulence. Studies of the drag reduction behavior of pulp slurries have been revealed that the existence of fibers and flocs results in turbulence damping (Amin, Abdel-Aziz, & El-Ashtoukhy, 2014; Luettgen, Lindsay, & Stratton, 1991). Addition of fiber to the suspension increases the pseudo-viscosity of

slurry resulting more transport of the momentum without Reynolds stresses and consequently more drag. In fact, during transition from plug flow to fully developed turbulent flow, the momentum transfer is enhanced by interlocking fibers in the network core, which behaves like a solid continuum, on the other hand, momentum transfer is reduced by fibers and flocs that have a damping effect on turbulence, thereby decreasing transfer rate. Momentum transfer enhancement will thus be dominating at low flow rates, while fiber damping will dominate at higher flow rates (Fällman, 2009). The competition between these two mechanisms result in maximum level of drag reduction at intermediate flow rates as was found by e.g. Duffy & Lee (1978). It has been stated that the changes in turbulence mechanisms induced by fibers occur in the turbulent core, not at or near the wall as fibers tend to migrate away from the wall and are not generally present there (Lee & Duffy, 1976b; Vaseleski & Metzner, 1974). To obtain a net reduction of drag, fibers must reduce turbulent momentum transfer without increasing other forms of momentum transfer (MacKenzie et al., 2014).

Moller and Duffy (1978) have proposed an empirical correlation (Equation 2.13) for the fractional drag reduction where it is applicable in a region between the onset of drag reduction and the maximum level of drag reduction.

$$\tau_w' = \frac{\tau_w^3}{(1-\Lambda)\tau_w^2+\Lambda\,\tau_D^2} \tag{2.13}$$

Where, τ_w, τ_w' and $\tau_D$are the wall shear stresses for the pulp suspension and for water for a given flow rate, and the wall shear stress at the onset of drag reduction respectively. Λ is the maximum fractional drag reduction (Jäsberg, 2007).

It has been reported that the drag reduction can be obtained by adding the enough amount of fibers with aspect ratio (fiber length / fiber diameter) >30. Several researchers (Lee & Duffy, 1976a; Vaezi, Katta, & Kumar, 2014) have observed the drag reduction increases with a decrease in fiber diameter for the fibers with same aspect ratio (Bobkowicz & Gauvin, 1965).

Kazi et al. (2014b) experimentally studied the drag reduction of fiber suspension over a range of velocities, concentration, fiber properties (flexibility) and some processes involving the pulping and paper making (e.g., bleaching and beating). They conducted the experiments based on the four different concentrations of bleached kraft pulp for pipe flow (0.05, 0.1, 0.3 and 0.4%) and a velocity range from 0.26 to 1.3 m/s. Results showed the drag ratio of 0.92 for 0.4% pulp consistency at the velocities higher than 1 m/s. Results stated that more drag reduction is achievable with fibers having more Coarseness. Moreover, they postulated that fiber flexibility and population are delicate fibre properties which affect turbulent eddy interactions and hence affect the frictional pressure drop characteristics of fibre suspensions.

2.9.3 Polymer- induced drag reduction

The drag reduction in turbulent flow caused by the Polymer was reported by Toms (1948). Till now, many studies have been done related to the effect of polymers on the behavior of the fluid (Kamel & Shah, 2009; Luettgen et al., 1991). Concentration, polarity, salinity and molecular weight of polymers are important factors affecting the extent of drag reduction phenomena in the fluid. Kamel and Shah (2009) used 2% KCl brine and synthetic sea water to investigate the effect of salinity on drag reduction of ASP-700 and ASP-820. Moreover to study the effect of temperature, they conducted the test at temperature 72, 100 and 130 °F and observed the drag reduction is in range of 30–80% by using the mentioned polymers.

This suggests that a polymer solution flowing in a pipe requires a lower pressure gradient to maintain the same flow rate (Kim et al., 2009). Actually interaction between eddies and pipe wall leads to friction and pressure drop of the flow, so adding a small concentration of such additives to the fluid reduces the friction of the fluid and increases the flow capacity of the pipeline (Karami & Mowla, 2012).

The effect of concentration and molecular weight of the polymer on the pressure loss has been reported by several authors. In early work, Hirose and Oka (1971) studied the friction factor of suspension containing C.M.C. solutions in the fully developed turbulent flow. They have investigated and reported the friction factors of the flow in smooth 13, 25 and 35 mm-dia pipes at different Reynolds numbers and C.M.C. concentrations. They got 64% reduction in friction factor by using 0.3 wt% of C.M.C solution at a Reynolds number of 2×10^3.

Kim et al. (2009) also examined the effect of 4 molecular weights (2×105, 4×105, 9×105 and, 4×106) and 4 concentrations (1, 5, 10 and, 20 ppm) of polyethylene oxides in the Reynolds number range of 30,000 to 60,000 on the drag reduction level. The results demonstrated that drag reduction increases with the increase of molecular weight and Reynolds number. A maximum drag reduction of 50% was obtained at a molecular weight and concentration of 4×10^6 and 20 ppm, respectively. 60-70% amount of drag reduction has been reported by the (Ptasinski, Nieuwstadt, Van Den Brule, & Hulsen, 2001) who conducted the experiments on the flow of a solution containing three different concentrations of partially hydrolyzed polyacrylamide and water, in the pipe flow at the Reynolds number 10000.

Extensive studies have been conducted on the mechanisms related to polymer-induced drag reduction (Jovanović et al., 2006; Min, Yul Yoo, Choi, & Joseph, 2003; Roy & Larson, 2005; Sreenivasan & White, 2000) and two mechanisms have been proposed. The first mechanisms has been based on the viscous effect of the polymer proposed by Lumley (1969) where stretching polymers resulting the viscosity enhancement near the wall where damping the small vortices causes the drag reduction. There is an argue on this mechanism as if the drag reduction in dilute polymer solutions only came from viscous effects, drag should be reduced regardless the polymer concentration (Fällman, 2009). Therefore, the second theory has been suggested by

various researchers (De Gennes (1990); Joseph, Riccius, and Arney (1986)) who studied the role of elastic properties of polymers. They stated that the major effect of polymer on the drag reduction arises only when the elastic energy stored by the partially stretched polymers becomes comparable to the turbulent energy. It is generally agreed that the mechanism for polymer based drag reduction is based on the ability of polymers to stretch and relax. Specifically, the polymers are believed to absorb turbulence while in a stretched state, and then subsequently dissipate that energy through polymer relaxation (MacKenzie et al., 2014).

Sasaki (1991) has measured the effectiveness of drag reduction of various polymers with several types of solvents and stated that the drag-reducing ability of polymer slurry tends to decrease when the polymers become more flexible. Den Toonder, Hulsen, Kuiken, and Nieuwstadt (1997) have both numerically and experimentally studied the effect of polymer on the drag reduction in the turbulent flow. They propose that the viscous anisotropic stresses introduced by extended polymers play a key role in the mechanism of drag reduction by polymer additives. Unlike the fiber-induced drag reduction, the mechanism of drag reduction through the polymers occurs near the wall.

2.9.4 Fiber/polymer - induced drag reduction

Water-soluble polymers having molecular mass greater than about 4 million grams per mole as the retention agents are commonly used additives in papermaking (Hubbe, Nanko, & McNeal, 2009; Hubbe & Wang, 2002). They tend to flocculate the fine materials in fiber suspensions which improve the retention and dewatering on the wire section of the paper machine (Page, 1989c). It is widely known that the polymer addition in fiber flows causes the significant changes in the flow mechanism and rheological properties. Cationic polymer can increase the size of the flocs and the

number of fiber–fiber contact points and the shear strength of the flocs in dilute fiber suspensions.

Cationic polyacrylamide (CPAM) is the most widely used retention aid product in the papermaking (Charani et al., 2013; Horn & Linhart, 1996) where it typically adsorbed by loops and tails and flocculate pulp by bridging (Karppinen, 2014).Wågberg and Lindström (1987) have shown that the flocculation following the addition of polyelectrolyte is a very rapid process irrespective of charge density of the polymer, pH, level of polymer addition, concentration of fibers, concentration of simple electrolytes or type of fibers. CPAM was found strongly has effect on the yield stress of cellulose suspensions; low doses of CPAM increased the yield stress, but at higher concentrations the yield stress has declined. The data suggest that CPAM modifies the interaction between cellulose surfaces via several mechanisms, with electrostatic interactions in the form of charge neutralization and charged patch formation dominating; polymer bridging and steric repulsion also has influence on the overall balance of forces between interacting cellulose fibers (Mosse, Boger, Simon, & Garnier, 2012). The subject of CPAM addition in the fiber flow has been addressed in several reports. A distinct rheological difference is seen at low bulk flow rates, where in dilute suspensions without polymer, a loose and continuous network entraps all the solvent and moves as a plug. With the addition of polymer, denser flocs form with a fluid phase containing few fibers. MacKenzie et al. (2014) studied the influence of softwood kraft pulp fibers and synthetic polymer additives e.g., CPAM and anionic polyacrylamide (APAM) on turbulent drag reduction in a hydrocyclone. They reported a slight increase in DR with an increase in polymer concentration from 100 to 500 ppm APAM/CPAM. They showed that fluid energy losses can be reduced through the addition of polymer additives with and without a suspension containing cellulose fibers (MacKenzie et al., 2014).

2.10 Heat transfer study

Pressure loss behavior of fiber suspensions have been studied extensively by many researchers. However a few works have focused on the heat transfer characteristics of the pulp slurries. One of the earliest works have been done by Middis, Muller-Steinhagen, and Duffy (1994) who studied heat transfer properties of fiber suspensions containing the wood fibers and nylon filaments with different degrees of stiffness and aspect ratios flowing in the 25.3mm ID horizontal brass pipe with constant ΔT. They had given their main attention to fiber concentrations of more than 2% where fibers entangle and form network structures. The heat transfer ratio (heat transfer coefficient of fiber/heat transfer coefficient of water) for short fibers increased with velocity up to 3.5m/s and then remained constant at higher velocities. At low velocities the heat transfer ratio tends towards unity. Some heat transfer enhancement was seen for the long-fiber runs at low velocities and high concentrations. They stated that the Nylon fibers do not form a strong plug due to their low network strength and thus the fiber wall interaction was small. The trends for the heat transfer and pressure drop ratios were similar although the magnitude of the heat transfer ratio was generally slightly less. At low velocities heat transfer reduction of up to 40% was observed. The crossover from heat transfer enhancement to reduction appeared to correspond to the point at which a water annulus formed around the fiber plug. This can be seen from the wood pulp fiber data as a local maximum in the pressure drop ratio results. They observed that the wood pulp fiber data showed regions of both heat transfer enhancement and reduction. The heat transfer ratio for Nylon fibers almost always lay below unity over the range of velocities, 2-10m/s.

The heat transfer reduction for the nylon fibers was much less than those for the pulp when $u > 1$m/s. They concluded that the nylon fibers have a thermal conductivity about two/three times greater than that of wood pulp fibers. The higher conductivity may

offset some of the heat transfer reduction as a result of the increased thermal conduction within the fibers themselves. They reported that at low fiber concentration (0.03%) and high bulk velocities (3-10m/s) some heat transfer enhancement for suspensions which had the same pressure drop as water. They stated that for Nylon fibers at low aspect ratios r < 60 the pressure drop and heat transfer coefficients of the suspensions were similar to those for water. The differences are due to the turbulence damping effect of the fibers. They reported that the frictional pressure drop ratio (suspension/water) and heat transfer coefficient ratio curves (suspension/water) were shifted to higher values with the increase of velocities at increased concentrations. This effect shows similar trends both in nylon and wood pulp fibers.

Momentum transfer and heat transfer are interrelated in conventional fluid flow and it would be expected that fiber suspensions would alter both the mechanisms and rates of transfer. It is observed that the various mechanisms causing changes in momentum transfer also affect heat transfer. The h values are altered with the variation of flow velocity, concentration of fiber (population), length, flexibility, coarseness (mass per unit length), surface topography and the amount of fibrillar fines present in the suspension (Kazi, Duffy, & Chen, 2015).

The extensive works on the heat transfer of low concentration pulp slurries (< 0.4) have been done experimentally in both pipe and annular pipes by Kazi et al. (1999) who stated that the measurements of pressure drop and heat transfer coefficient are closely related. They conducted a series of experiments on the pulp slurries containing the fibers obtained from different sources (different parts of the same tree) and different processes (chemical treatments, mechanical refining at different levels, thermomechanical treatment, bleaching etc.) with variable fiber characteristics (length, flexibility etc.). Their observations are stated in the following paragraphs. Kazi, Duffy, and Chen (2014a) had studied the effect of entrance length of the closed conduit flow on

the heat transfer to pulp suspensions which is defined by the length of the conduit from the entry to the point where the fully developed flow begins. The results showed that change in entrance length does not have any significant effect on the heat transfer coefficient of the fiber suspension (Kazi et al., 2014a).

Fiber suspensions flow at low consistency provides data with little variation whereas at higher consistency heat transfer coefficient data provides some variations but the trend remains similar for both short and long entrance lengths in the test section. At a specific velocity of 0.3 m/s, 0.4% fiber produced 52% higher h_c than water and 44% higher than fiber suspension at low concentration (0.2%). However at velocity 0.3 m/s and concentration (0.2%) h values are 5.8% higher than that of water. At 0.2 m/s water, Pinus radiata high coarseness fiber of 0.2 and 0.4% concentrations show 1.765, 2.471 and 3.177kW/m2K h values (Kazi et al., 2014a). It was found that the magnitude of the heat transfer coefficient was above water at equivalent experimental conditions at very low fiber concentrations, but progressively decreased until it was below water at slightly higher concentrations. It should be noted that the results reported by (Kazi, 2001) are related to turbulent flow only. For the laminar flow, Middies et. al., reported that fiber suspensions exhibit a higher heat transfer coefficient than water alone at low flow rates where plug flow exists. The fibers in the thin annular layer around the plug are now modifying the heat transfer rate and consequently the magnitude of the heat transfer coefficient. Thus the region of heat transfer enhancement corresponds to the plug flow in hydraulic transportation in a pipe. At elevated velocities the heat transfer coefficient for pulp suspensions is lower than that of water at the same flow. They said that the suspension at higher velocities behaves more like a continuum whereas at low velocities the various factors causing a deviation in ratio are due to the plug-like nature of the fiber suspension. In general at each velocity point the highest value of h occurs when the fiber concentration is the lowest. It is noted that fibers in suspension at very low

concentrations enhance heat transfer coefficient to a significant value and the h_c values gradually approach the water value as the concentration of fiber increases. At higher concentrations the h_c values of suspensions are below the water data. Similar results were obtained by previous researchers (Kazi et al., 2015).

Heat transfer to fiber suspensions decreases with increase of fiber flexibility and decrease of freeness degree. The heat transfer coefficient of 80% and 81% of water has been reported for softwood fiber suspensions with two level of freeness (200 and 500 CSF) at 0.4 m/s velocity respectively. In the same freeness degree, the decrease in heat transfer was more sensible where the suspension was containing the more flexible fibers (thermomechanical fibers) (Kazi et al., 2015). Increases in flexibility and decrease in freeness are the results of beating process, so it is logic to expect that beating results in a heat transfer coefficient reduction. It has been reported that for the three medium density fibre board (MDF), there is a progressive lowering of the coefficient where more refining energy is used to make the MDF fibers more flexible. It is observed that at 0.4 m/s velocity the lowering of heat transfer coefficient for MDF (Low), MDF (Medium) and MDF (High) are 3.3, 19.9 and 25.1% of water respectively. With the increase of velocity the h_c values of the suspensions are increased keeping the same trend (Kazi et al., 2015).

There is a hypothesis that h_c can be correlated with the fiber and paper properties and the heat transfer to fiber suspensions can be used as a means for the characterization of the papermaking pulps (Duffy et al., 2000). Once a value of h_c is linked to the acceptable paper product qualities, then this could be used as a pulp quality parameter or indicator. However, this question remains that to what extent the diversity in the properties of fibers used in industries resulted from different pulp sources and pulping processes, could affect the characterizations and correlations.

In the case of fiber length, the general trend is that decrease in fiber length causes a decrease in h_c. Fiber length can be presented (based on the shape of the fiber cross section) by the aspect ratio (L/D) or equivalent aspect ratio (L/(2*(W+T)). Equivalent aspect ratio is used for the fibers with rectangular cross section where W and T are the fiber width and fiber wall thickness.

The data reported for fiber stiffness (inverse fiber flexibility) versus heat transfer coefficient stated that the fiber stiffness plays an important role in modifying h_c. moreover there is a general behavior that heat transfer coefficient increases with the increase of coarseness (in addition to fiber length) (Kazi et al., 2015).

Various fibers result in the papers with different properties. Kazi et al. (2014b) used the heat transfer coefficient to correlate the quality of the papers with sheet density of 700 kg/m^3. The results presented as the paper specifications (e.g., tensile index, tear index, burst index, stretch, scattering coefficient and formation index) versus heat transfer coefficient of the fiber suspensions and an almost linear relationship obtained based on the graphs.

2.11 Nanocrystalline cellulose

The crystalline region of cellulose can be extracted by using the acid hydrolysis method which would result a stable suspension containing the rod-shape nanocrystalline cellulose (NCC) (Rånby, 1951). A commonly used method to make the NCCs is a hydrolysis using the Sulphuric acid which introduces the anionic sulfur ester groups on the surfaces and makes the suspension stable (Brinchi, Cotana, Fortunati, & Kenny, 2013; Shafiei Sabet, 2013).

Depending on the fiber sources and hydrolysis condition, different sizes of NCCs (2-20 in width and 100 nm to several micrometers) can be produced (Elazzouzi-Hafraoui et al., 2007; Lu & Hsieh, 2010; Xu et al., 2013). A broad range of sources which have

been used to prepare the NCC is including the bacterial cellulose (Roman & Winter, 2004), softwood and hardwood fibers e.g., black spruce and bleached kraft eucalyptus (Beck-Candanedo, Roman, & Gray, 2005; Hamad & Hu, 2010), cotton (Fan & Li, 2012), Corn husk (de Carvalho Mendes, Ferreira, Furtado, & de Sousa, 2015) microcrystalline cellulose (Bondeson, Mathew, & Oksman, 2006) and cellulose nanofibers (Li et al., 2015) (see Table 2.1). The crystallinity of the microfibers affect the NCC size where the microfibrills with high crystallinity yield longer nanocrystals.

Table 2.1: Different sources of cellulose nanocrystals (Adopted from (Jonoobi et al., 2015))

Source	Process	References
Ramie	H_2SO_4 hydrolysis	(Habibi, Lucia, & Rojas, 2010)
Industrial bioresidue	H_2SO_4 hydrolysis	(Oksman, Etang, Mathew, & Jonoobi, 2011)
Grass fiber	H_2SO_4 hydrolysis	(Pandey et al., 2009)
Cotton linter	HCl hydrolysis	(Braun, Dorgan, & Chandler, 2008)
Wood pulp	TEMPO-oxidation followed by HCl hydrolysis	(Neto, Silvério, Dantas, & Pasquini, 2013)
Cotton linters	Enzymatic treatment + H_2SO_4 hydrolysis	(Beltramino et al., 2015)
Curaua fibers	H_2SO_4, H_2SO_4/HCl, HCl hydrolysis	(Correa, de Morais Teixeira, Pessan, & Mattoso, 2010)

Generally the NCC preparation process is consisted of mixing, heating, stirring and sonication which refer to acid/ fiber ratio, temperature reaction, time of reaction and sonication time and energy.

Dong, Revol, and Gray (1998) carried out a series of tests in order to find the optimal hydrolysis conditions for experimental phase separation studies and reported that the formation of chiral nematic phase strongly dependent on the particle size of nano crystals.

Beck-Candanedo et al. (2005) studied the properties of nanocrystal suspensions made from different hydrolysis conditions. Different acid to pulp ratios and reaction times

have been selected for hydrolysis of black spruce acid sulfite pulp. The results showed that with the increase in time the nanocrystals become shorter and less polydisperes. Li et al. (2015) also reported a reduction in aspect ratio with increasing the hydrolysis time where results in higher critical transition concentration for the formation of anisotropic phase. A reduction in nanocrystal dimension and an increment in critical concentration have been reported by increase in acid to pulp ratio. Increase in temperature resulted de-esterification of the sulfate groups on the surface of the crystals. Moreover a reduction in chiral nematic pitch reported by an increase in cellulose concentration as well as a reduction in nanocrystal length.

Apart from the NCC, there are other types of cellulose nanomaterials such as microfibrillated cellulose (MFC) and nanofibrilated cellulose (NFC). MFC is produced through the mechanical treatment using the high pressure homogenizer and the isolation of NFC is achieved by a combination of enzymatic and mechanical treatment (Eyholzer et al., 2010; Jonoobi et al., 2015; Kalia, Boufi, Celli, & Kango, 2014). MFC and NFC samples are more flexible than NCC due to less crystallinity. MFC and CNF suspensions consist of interconnected cellulose fibrils and form a gel like, highly viscous network at very low concentrations (i.e. 2 wt.% aqueous suspensions) (Shafiei Sabet, 2013).

2.11.1 NCC properties and its applications

NCCs have attracted a lot of attention not only because of sustainability and abundance of their sources but due to their unique properties. Rod like species exhibit nematic liquid crystalline alignment. Revol et al. (1992) reported that suspensions of acid-hydrolyzed cellulose crystallites can also form an ordered phase displaying chiral nematic (cholesteric) orientation. As in the nematic phase, the fibrils align parallel to each other along a director (n), however, with each subsequent plane of crystallites the

director twists through an angle perpendicular to the director, shown in Figure 2.10. The cholesteric pitch is defined as the distance in the cholesteric axis of a 360 degree rotation of the director (Holt, Stoyanov, Pelan, & Paunov, 2010; Orts, Godbout, Marchessault, & Revol, 1998; Revol et al., 1992). The suspensions made from collagen or DNA fragments can formed the chiral nematic phase.

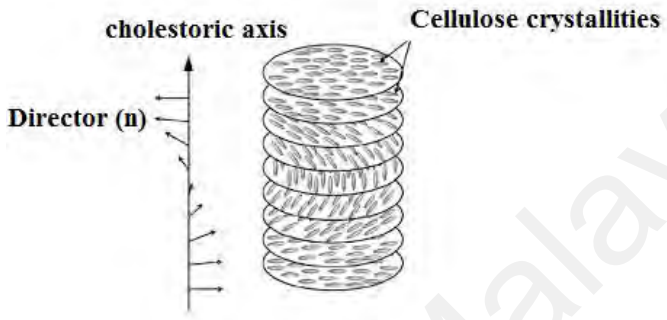

Figure 2.10: Schematic representation of the chiral nematic order displayed by cellulose crystallites. The director is shown to rotate along the cholesteric axis between consecutive planes of parallel cellulose crystals (Holt et al., 2010).

For suspensions of acid hydrolyzed cellulose microfibrils , the chiral nematic phase forms above a critical concentration (greater than 1.5% (w/w)) where the samples exhibit a fingerprint texture. A birefringent gel can be obtained at even higher concentrations (Araki, Wada, Kuga, & Okano, 2000; Orts et al., 1998; Shafeiei-Sabet, Hamad, & Hatzikiriakos, 2013). The helical organization of a chiral nematic liquid crystal causes angle-dependent selective reflection of circularly polarized light, which results in iridescence when the helical pitch is of the order of the wavelength of visible light. For this reason, chiral nematic liquid crystals have been extensively studied for their photonic properties and used for applications such as polarizing mirrors, reflective displays and lasers (Shopsowitz, Qi, Hamad, & MacLachlan, 2010; Yang, West, Chien, & Doane, 1994). By casting films from CNC suspensions (Kim & Song, 2015), cellulose films with the optical properties of chiral nematic liquid crystals can be prepared. These films can have important applications, such as security paper, including

bank notes, passports, and certificates (Shafiei Sabet, 2013). These solid films, in addition to allowing fundamental studies of their striking behavior, have numerous potential applications such as coating materials for decorative materials and security papers (because the optical properties cannot be reproduced by printing or photocopying (Habibi et al., 2010).

Apart from the optical properties of NCC solutions, they attracted many of interests due to their mechanical properties. They are stronger than metal and very light. Šturcová, Davies, and Eichhorn (2005) reported an elastic modulus of 143 Gpa for tunicate cellulose whiskers using a Raman spectroscopic technique. Cellulose crystals can be added to the base material and act as the reinforcement agents. El Miri et al. (2016) used a combination of NCC and graphene oxide to enhance the tensile properties of Poly(vinyl alcohol). Ma et al. (2011) reported the preparation of green all-cellulose composites by adding cellulose nanocrystals to the cellulose ionic liquid solution. Nagalakshmaiah, Mortha, and Dufresne (2016) extracted the nanocrystalls from chili leftover. They reported an increase in the tensile strength and modulus values of commercial latex/NCC composite. Moreover, NCC can be used as an additive in bio-nanocomposites (Benhamou et al., 2015; Habibi et al., 2010; Ye et al., 2016).

In pulp and paper industries, several reports are available regarding the utilizing the nano and micro fibrillated cellulose and NCC in papermaking. Zimmermann, Bordeanu, and Strub (2010) prepared CNF from five wood and wheat straw sources and examined their reinforcement potentials. Recently, there is a great interest in utilizing of NCC to increase the strength and quality of the paper and paper boards. In papermaking process, it is important that the papermakers are able to effectively retain mineral fillers and fiber fines while simultaneously improving dewatering rate. Xu et al. (2013) reported the NCC isolated from bleached aspen kraft pulp and used the NCC as an additive in the deinked pulp. They got the papers with improved properties. Strength properties of hand

sheets were improved due to presence of NCC in the fiber suspension which increased the hydrogen bonding between pulp. Moreover, breaking length and tear index were improved. However, the drainage rate was negatively affected to some extent. NCC couldbeusedinthe microparticle retention systemas the organic anionic particle, due to its nano rangediameter and surface charge density.

Since using the NCC in paper making process is going to be applicable, study on the flow of NCC suspension in the pipe is inevitable. Shafiei-Sabet, Hamad, and Hatzikiriakos (2012) had an extensive work on the rheological properties of NCC suspension. Their results shown the suspension up to 3 wt.% shows isotropic phase. The NCC samples with higher concentrations show the anisotropic phase with fingerprint texture and liquid crystal behavior. Further increase in concentration results in a gel form of NCC. They found that ultrasound energy and temperature has great influence on rheological and viscosity behavior of NCC suspensions. The NCC aqueous suspension remained isotropic in a wide NCC concentration range in which the suspension underwent transition from dilute solution to gel (Lu, Hemraz, Khalili, & Boluk, 2014). Gonzalez-Labrada and Gray (2012) measured the viscosity of dilute aqueous suspensions of cellulose nanocrystals using a rolling ball viscometer and evaluated the non-Newtonian character of NCC suspensions at increasing concentrations.

However various studies carried on the rheological properties of MFC and NCC suspensions, there is no any information about the pressure loss data of the suspension containing NCC in the pipe flow. Even the pressure loss data for MFC flow suspension is rare. Haavisto et al. (2011) reported the pressure loss data versus mean velocity of commercial MFC at consistencies from 0.2% to 1.5% using a laboratory-scale novel pipe rheometer. In general, the loss for MFC was strongly dependent on consistency. At low flow rates, the loss for MFC is considerably higher than that for water in all cases. For the suspension with consistency of 0.2%, the pressure loss approaches exactly that

of water at high flow rates (>1 m/s). Increase in concentration to 0.3% yield pressure drop data blow than water data. Moreover, in comparison to the Brich cellulose (1.5wt% concentration), MFC suspension showed higher pressure drop in the tested velocity range (Haavisto et al., 2011).

2.12 Summery

chapter 2 presented the literature review which covers the fibers structures, properties of fibers and papers, definition of beating as a mechanical action in paper making process and its effect on fiber and paper properties, and heat transfer and pressure loss studies of fiber suspensions. According to the literatures the fiber flexibility and population are delicate fibre properties which affect turbulent eddy interactions and hence affect the frictional pressure drop and heat transfer characteristics of fibre suspensions. The h values can be altered with the variation of flow velocity, concentration of fiber (population), length, flexibility, coarseness (mass per unit length), surface topography and the amount of fibrillar fines present in the suspension. The efforts which have been made by others to investigate the effect of additives on pressure drop of fiber suspensions were presented in this chapter. Moreover, studies on preparation of NCC and its properties as a new generation of additives were reviewed.

CHAPTER 3 METHODOLOGY

3.1 Pipe line flow loop

A detailed overview of the test rig and the measuring equipment are presented in this section. The experimental set-up is shown in Figure 3.1(a and b). The main parts of the setup consists of a tank with volume of 100 L, variable speed pump, magnetic flow meter, pressure transducer across the test section, heated pipe section, chiller for cooling suspension inside the tank, and a recycle piping system. The specifications of the equipment used in test rig are presented in Table 3.1. Moreover the photos of some devices which have been installed on the rig are shown in Figure 3.2 (a-f).

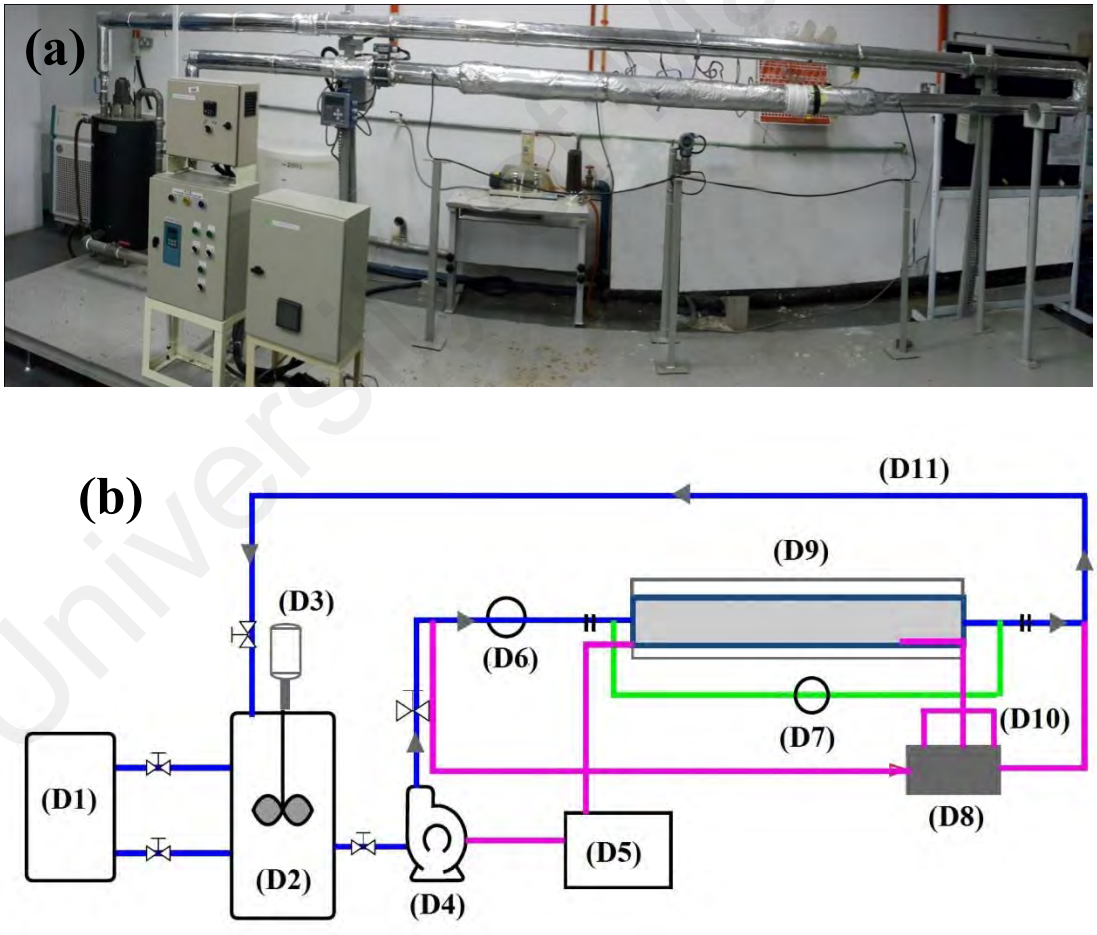

Figure 3.1: (a) Photograph and (b) schematic diagram of the test rig.

Table 3.1: The specifications of the equipment

Name	Specification	Tag number
Chiller	HX-45H (JEIO TECH),Cooling capacity: 4.7 KW @ 20^{o}C Working Temperature Range: 3-40 ^{o}C	D1
Tank	100 Liter, SS	D2
Stirrer Blade	15x100 mm	D3
Pump	COM500/22/A (LOWARA), Power: 2.71 KW Speed: 2795 RPM	D4
Inverter	60 Hz	D5
Flow meter	8000 A SERIES (FOXBORO), Magnetic flow meter	D6
D/P cell transmitter	Model: Model IDP10 (FOXBORO), Sensor temperature limits:-46-121 oC	D7
Data Logger	GRAPHTEC GL220	D8
Test section	Aluminum, (See Figure 3.2)	D9
Thermocouple	K- Type ((Omega), Temp. range 20-150℃	D10
Return line	Stainless steel	D11

The fluid was pumped from the tank by the centrifugal pump. The suspension was then passed through a magnetic flow transmitter and the test section. The fluid was then returned to the stock tank through the return line. Fluid in the jacketed tank was then cooled to the desired tank temperature by the chiller. The flow loop piping except the test section is of stainless steel material.

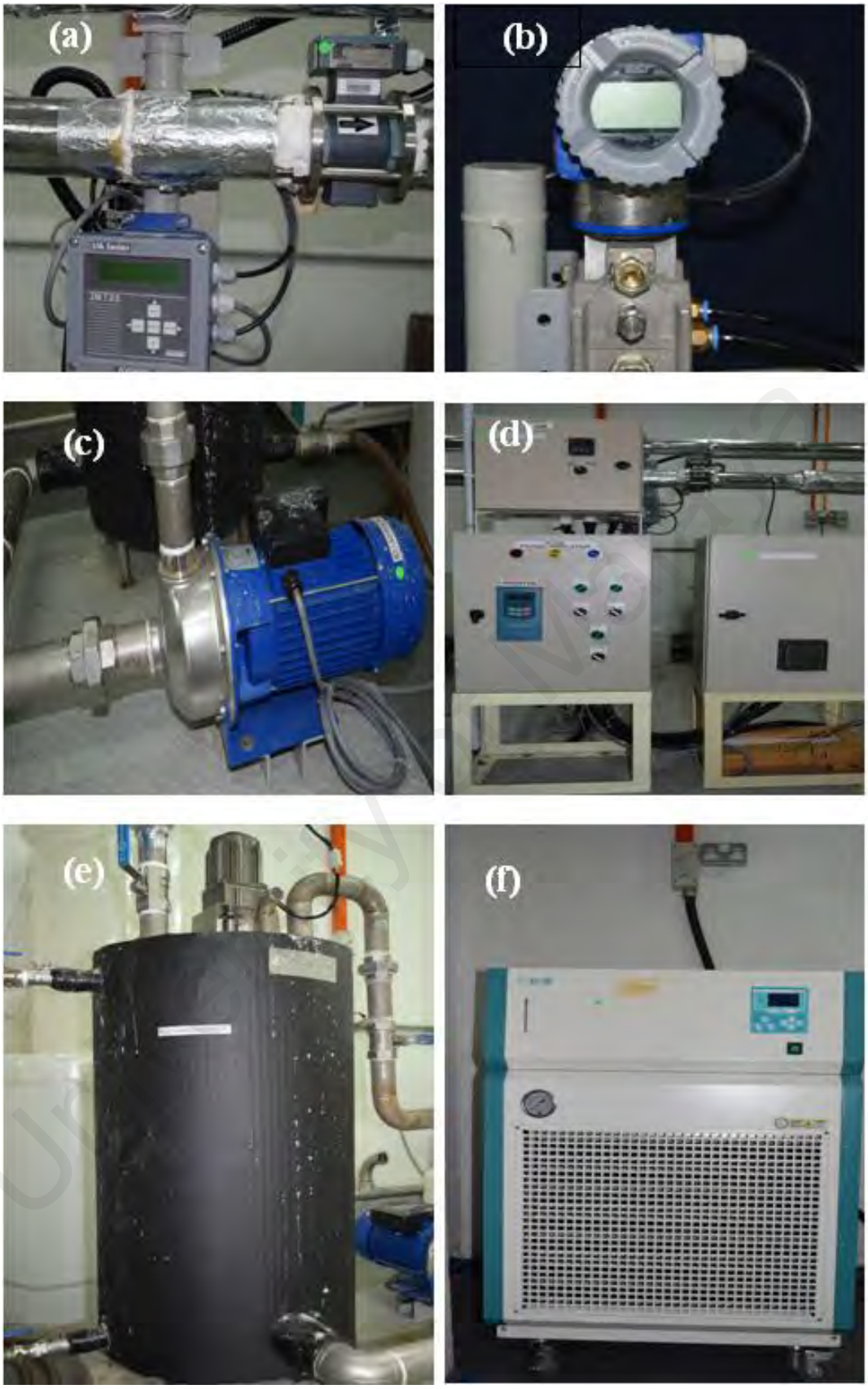

Figure 3.2: Photo of (a) flow meter, (b) D/P cell transmitter, (c) pump, (d) PLC box, (e) tank and (f) chiller.

The test section is made from Aluminum. The whole test rig is insulated in order to avoid heat loss to the atmosphere. Inlet and outlet fluid temperatures were measured by type-K thermocouples located in the center of the flow. The Thermocouples were inserted facing downstream in the elbows before and after the test section to reduce fiber stapling. The test section is installed far away from the flow meter at discharge section of the loop to avoid disturbance and obtain steady state at the point of measurement. Frictional pressure loss across the test section and on the Al straight piping were measured by pre calibrated pressure transducers. The heat transfer test section was designed and constructed at the University of Malaya. The sectional view of the experimental test section is presented in Figure 3.3.

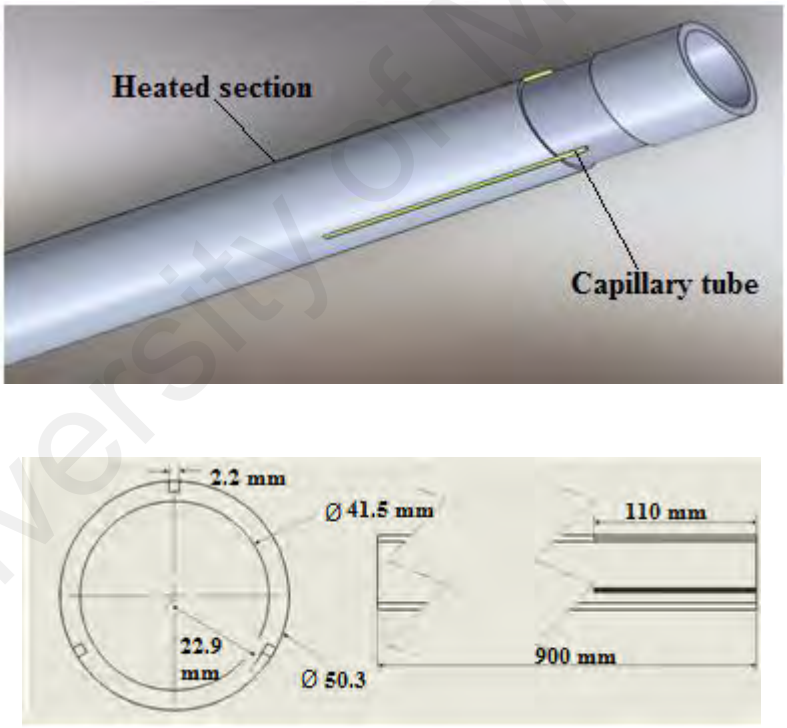

Figure 3.3: View of the experimental test section.

The heat transfer test section is a 900 mm length of 41.5 mm internal diameter Aluminum pipe. Three grooves were cut along the section that was to be heated starting from the discharge end of the heated section and proceeding up to 110 mm inside along the section. These longitudinal grooves were used to house the thermocouples. The

grooves were cut as deep as possible while ensuring that the inside surface of the pipe was not disturbed. The distance between groove surface and inner surface of the tube was maintained at 2.25 mm. Then to keep the thermocouple in location three stainless steel 1.5 mm diameter thermo-wells were installed. Stainless-steel capillary tube thermo-wells were laid in the grooves downstream from the heated section with one end exiting outside the pipe wall. The grooves were filled with high temperature resistance paste to fix the thermo-wells in location. Three Omega type–K thermocouples were inserted up to the end of the capillary tubes to obtain the wall temperature at a point approximately 110 mm from the discharge end of the heated section. One set of pressure tapping, across the test section was connected to differential pressure transducer to obtain friction loss measurements. The test section was heated by ten flat coil heaters each with wattage of 900 W. The heaters were clamped on the outside of surface of the test section.

3.2 Data acquisition

Data for the inlet and outlet temperatures and wall temperatures are logged using a data logger (Graphtec, midi logger GL220). The current and voltage were measured by 1000 A true RMS clamp meter (Agilent) to calculate the heater power. All measurements were taken after the heat transfer loop had reached steady-state conditions at the chosen velocity, bulk temperature and heat flux. The velocity was systematically increased, the heat flux was adjusted to achieve desired amount.

The thermocouples were calibrated to measure the surface temperature according to equation 3.1.

$$T_w = T_t - \frac{\dot{q}}{\lambda/x} \tag{3.1}$$

Where the heat flux ($\dot{q}$) was the amount of total heat supplied through the phase angle power controller to the heaters divided by the heated area. The actual wall

temperature (T_w) was calculated from the temperature measured in the test section (T_t) with a correction to account for the distance of the thermocouple below the heating surface to the inner wall of the pipe in fluid contact. The wall resistance for each thermocouple (λ/x) was determined by calibrating the test rig with water as presented in Appendix B.

The local heat transfer coefficient h_c was calculated from equation 3.2.

$$h_c = \frac{\dot{q}}{(T_w - T_b)} \tag{3.2}$$

The bulk temperature T_b was a position-weighted average of the inlet and outlet temperatures (T_i and T_o respectively). Equation 3.3 presents bulk temperature as a function of inlet and outlet temperatures. This was based on the assumption that the fluid temperature increased linearly over the heated section and remained constant in the unheated sections of the rig. This is reasonable because the temperature rise between inlet and outlet thermocouples was normally less than 1°C.

$$T_b = T_i + \frac{X_1}{X_2}(T_o - T_i) \tag{3.3}$$

Where, X_1 and X_2 representing the distance of thermocouples tip along the flow direction and heated length respectively.

3.3 Experimental procedure

The preparation and characterizations of fibers and handsheets along with experimental conditions to conduct the heat transfer and pressure loss test is presented in this section.

3.3.1 Material

Three non-wood pulp samples including Rice straw which was prepared by the mechanical process, EFB (soda process) and two-stage soda Kenaf in lap form were used as the pulp sources. Bleached commercial softwood (Acacia mangium) pulp was

used as a source of NCC. All pulp sources have been provided by Forest Research Institute of Malaysia (FRIM). CPAM (provided by FRIM) and potato starch (soluble in water from Sigma Aldrich) was used as the additives. Sulfuric acid (95–98%) for hydrolysis was purchased from Sigma Aldrich Company.

3.3.2 Preparation of fiber suspension

The experimental study consisted of several sets of runs to achieve the defined objectives. Pulp fiber suspensions were prepared from three non-wood pulp samples: EFB, Rice straw and two stages soda Kenaf. For a known concentration the required calculated amount of the sample, based on the moisture content was disintegrated. The specimen was added to 2000 mL tap water (1.2% consistency) at 20 ± 2°C and was disintegrated at 3000 rpm until all fiber bundles were dispersed. The disintegration process was done according to the TAPPI standard where the revolutions were not more than 50,000 (TAPPI, 2002). The required revolutions for EFB, Rice straw and Kenaf were set on 9000, 9000 and 21000 respectively. Since Kenaf samples were provided in lap form, a 24 hours soaking process before disintegration, and more revolutions were needed to rehydrate and disperse the samples. After disintegration, the pulp suspension was added to the tank and dispersed by the agitator homogenously. The concentration of the slurry was adjusted to the desired value. To measure the pulp consistency, the standard provided by TAPPI was followed (TAPPI, 1993). In the case of beating study the Kenaf fibers were beaten (before adding to the tank) by the PFI mill refining machine with two beaten degree of 2000 and 4000.

3.3.3 Preparation of hand sheets

A flowchart of papermaking process is presented in Figure 3.4.

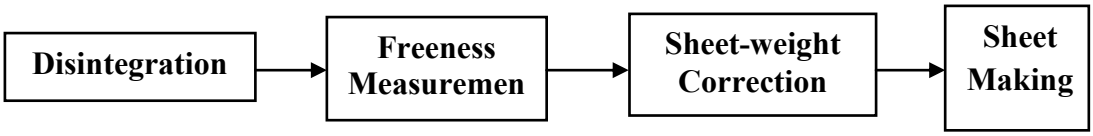

Figure 3.4: Flowchart of sheet making process.

Hand sheets of all three fibers were made according to the flowchart presented in Figure 3.3 and the TAPPI standard T-205 (TAPPI, 2002). The procedure is as below:

1. Add 24 g oven dry pulp into the 2 liter of distilled water. Then, disintegrate in the standard disintegrator at 2000 revolution per minutes (RPM).

2. Pour the sample in the stock divider and reach the level of suspension to 8 liters in the stock divider. Open the air inside the tank and wait for several minutes.

3. Do the freeness test. Take out 2 samples from stock divider into special cup which is around 1000 ml. Take the temperature reading of the sample using thermometer. After that, pour the samples into the freeness tester and measure the volume of drained water in the side orifice. Wash the remaining fiber in the freeness tester and use that for papermaking (hand sheet)

4. Open the sheet machine and turn on the water and gently rub the surface of the wire with the finger to clear away any adhering fibers. Close the machine and pour the amount of stock needed for one sheet into sheet machine. Fill it with water until the depth level reach a line inside of the cylinder. Then, fully open the drain of the machine with a rapid movement and let the water be drained through the sheet suction from the water leg.

5. Open the sheet machine. Place two pieces of blotting paper centrally on the drained sheet. Lay the flat couch on the blotters and place couch roll gently on the middle of the plate. Rotate the roll backward and forward for five times. After that, remove the couch plate and set it aside. Lift the blotters and the sheet should be found to

the underside of the lower couch. Discard the sheet from blotters and put it into the oven.

6. For second round, adjust the level of suspension to 14 liters by adding water into the stock divider. Then, take two samples from the stock divider and do the papermaking for sheet -weight correction. The weight of each paper should be around 1.22 g. Adjust the concentration of the stock suspension if is needed. If the concentration is high add water based on below calculation:

$$Amount\ of\ water\ (ml) = \left(\frac{Average\ weigth\ of\ two\ samples}{1.22} \times 12000\right) - 12000 \qquad (3.4)$$

7. Take the samples and do papermaking.

8. Then, apply the press to the samples by using press machine. The pressure of the press machine is 45 lb/in^2. The press should be done twice.

9. Discard the press blotters from each test sheet. Fit each plate with its attached test sheet into drying ring. Place a heavy weight which is around 20 kg on the top of stack of the rings. After drying period, remove the plates from the drying rings and peel the test sheet from the plates. At the end the handsheets can be characterized using the standard methods.

3.3.4 Characterization of fibers and hand sheets

The pulp samples were boiled in water in separate beakers to remove air from the fibers and then placed in separate test tubes containing an equal amount of glacial acetic acid and 35% hydrogen peroxide. For this study, fiber length (*L*), fiber width (*W*) and lumen diameter (*d*) were measured based on an average of 50 measurements by using a Quantimeter Image Analyzer equipped with a Lecia microscope and Hipad digitizer (from Quantimet 520, Cambridge Instruments). Three derived values: slenderness ratio (*L*/ *W*) and flexibility coefficient (100 × *d*/ *D*) were calculated using the measured data. (Mossello, Harun, Resalati, et al., 2010).

The microscopic images (Appendix A, Figures A.1-A.5) of fibers were taken using the scanning electron microscope (SEM). Physical properties of hand sheets were examined using different devices and according to TAPPI procedure (Table 3.2). The paper divisions for physical testing were shown in Figure 3.5.

Determine the average mass per unit area of five conditioned sheets by weighing them together on a balance sensitive to 0.001 g. The grammage is ten times the weight of the five sheets. Tensile index, burst index and tear index were measured using tensile tester, bursting tester and tear tester respectively. Brightness was determined by opacimeter. No. of fold, was obtained using MIT folding tester.

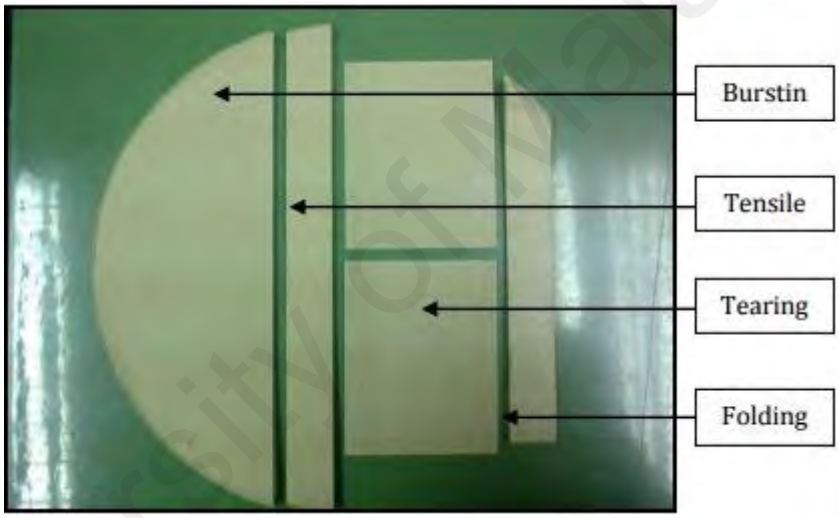

Figure 3.5: Division of paper for testing

Table 3.2: TAPPI standards for paper testing

Type of test	TAPPI standard
Grammage	TAPPI T410-om-98
Tensile index	TAPPI T494 om-96
Tear index	TAPPI T414 om-98
Burst index	TAPPI T403 om-91
Folding endurance	TAPPI T511 om-02
Brightness	TAPPI T452 om-98

3.3.5 Preparation of CPAM and potato starch

CPAM was provided from the FRIM in the solution form with mass concentration of 20.5%. To use in experiments the CPAM solution was diluted to 2% and stirred for 1 hour gently. Then the CPAM solution was added to the Kenaf pulp in the tank where the concentration of CPAM was set on 70 and 150 ppm. The mixture of pulp and CPAM was slowly stirred inside the tank for 2-3 hours and then circulated through the loop. Kenaf pulp concentration in the mixture of pulp and CPAM was kept at 0.6 wt%.

The potato starch powder was purchased from the Sigma Aldrich Company. It was prepared by adding certain amount of potato starch to the 100 ml distilled water and was heated to 80 °C while it was stirred and then kept at the 80 °C for 25 min. Finally, the solution was diluted with 100 ml distilled water and used freshly. The potato starch solution was added to the pulp slurry and stirred for 2-3 hours before being pumped through the test rig.

3.3.6 Preparation of NCC sample

Concentrated sulfuric acid was diluted to 64 wt.% by adding the acid to the cold deionized water under vigorous stirring. Pulp (30 g based on oven dry weight) was added to the 262.5 ml of preheated diluted acid at 45 °C (ratio of acid to pulp was set on 8.75 ml/g) in an Erlenmeyer flask. The mixture was stirred for 25 min at constant temperature of 45 °C (Beck-Candanedo et al., 2005; Lu & Hsieh, 2010). The hydrolysis process was stopped by diluting the suspension with 10 fold cold water. A whitish cloudy layer at bottom and a clear layer at the top of the suspension were formed where the suspension was allowed to settle overnight (Hamad & Hu, 2010). The cloudy layer was centrifuged at 6000 RPM for 10 min, the settled layer was mixed with DI water and then centrifuged again. After repeating the procedure for 2-3 times the setteled layer was placed in the dialysis tube (with a molecular weight cut off of 12000–14000). The

dialysis process was carried out against DI for 3-4 days until the pH of the DI become constant for a specific period of time (Shafiei-Sabet et al., 2012). The suspension was dispersed by an ultrasound treatment for 15 min at 65% power and followed by filtration. The pH of NCC suspension was adjusted to 7 using the 0.1 M NaOH and finally freeze-dried. It is notable that the fresh NCC samples were used for pressure loss studies and the freezed-dried one was used for some of the characterizations.

3.3.7 Characterization of NCC sample

The microscopic morphology of the prepared sample was observed using a high-resolution FEI Quanta 200F field emission scanning electron microscope (FESEM) and a transmission electron microscope (TEM, Zeiss Libra 120). The samples were prepared for TEM characterization by deposition of a drop of diluted suspension of NCC on a carboncoated grid (aqueous dispersions), and the sample was stained with a 2 wt% solution of uranyl acetate. X-ray diffraction (XRD) of the NCC powder was performed using a PANalytical's Empyrean XRD with mono-chromated Cu-Kα- radiation (λ = 1.54056 Å), operated at 45 kV, 40 mA, a step size of 0.026° and a scanning rate of 0.1° s^{-1} over a 2θ range from 20° to 60°. For polarized light microscopy, small amount of sample was transferred to 1.0 x 10 mm rectangular cross-section glass micro-slide and images were captured from a Leica DMRXP polarizing light microscope and analyzed with Leica QWin software. The zeta potential of the NCC sample was determined by dynamic light scattering (DLS) Malvern particle size analyzer, Model Nano ZS (Worcestershire, UK). The rheology of NCC suspension was studied using a *Bohlin C-VOR* rheometer with plate and plate (40mm) at temperature of 23 °C. Before starting the actual measurements, a 15 min pre-shear interval at 300 s was applied on the sample. The intensive pre-shear period was implemented to break down the flocculated NCC network structure. Then the sample was left to rest for at least 10 min. Oscillation

measurements were performed after the pre-shear and rest periods. Frequency sweep was measured from 0.02 to 100 Rad/s at 0.5% strain.

3.3.8 Experimental runs for heat transfer study of pulp suspension

The experiments were set on different concentrations. For each concentration the run consisted of a series of measurements of temperature differential as a function of suspension bulk velocity with constant bulk temperature and heat flux. In all experiments, the bulk velocity was varied from 0.4 to 2.8 m/s for heat transfer data in increments of approximately 0.4 m/s. The heat flux was manually adjusted with the power controller to give a constant power of 3400W. Once this condition was satisfied at steady state, measurements were recorded to determine the heat transfer coefficient. A summary of experimental conditions is given in Table 3.3.

3.3.9 Experimental runs for pressure loss study of pulp suspension

The procedures conducted for pressure loss study consisted of several set of runs. The effects of temperature and additives on pressure loss were investigated. For pure pulp suspensions the experimental settings were almost same as the heat transfer with the difference in bulk velocity where the range is between 0.4 m/s to 3.6 m/s. In order to study the effect of temperature on pressure loss the experiments were conducted at two bulk temperatures of 23 °C and 30 °C for 0.6 % SK pulp suspension.

3.3.10 Experimental runs for pressure loss study of pulp/additive suspension

The effect of additives on pressure loss data were examined by adding different concentrations of CPAM, potato starch and NCC to the Kenaf pulp. The experiments were done at velocity range of 0.4 m/s to 3.6 m/s and bulk temperature of 23 °C. Summary of experiments is presented in table 3.2.

Table 3.3: A summary of experimental conditions for heat transfer and pressure loss studies

Parameter	Heat transfer study	Pressure loss study
Pulp type	Empty fruit bunch (EFB) Rice straw Kenaf Kenaf beaten at 2000 and 4000 degree	Empty fruit bunch (EFB) Rice straw Kenaf Kenaf beaten at 2000 and 4000 degree Kenaf + CPAM Kenaf + potato starch Kenaf + NCC
Pulp concentration	For unbeaten samples:0.2, 0.4, 0.6 For beaten samples: 0.6	For unbeaten samples:0.2, 0.4, 0.6 For beaten samples: 0.6 For pulp + additives samples: 0.6
Additive concentration	-	70 ppm and 150 ppm
Velocity range	0.4-2.8 m/s	0.4-3.6 m/s
Bulk Temperature	30 °C	23 °C for pulp + additives samples and 30 °C for other samples
Power	3400 W	For bulk temperature 30 °C: 3400W For bulk temperature 23 °C: no heat

3.4 Summary

The materials, preparation and characterization methods and experimental procedures related to the heat transfer and pressure loss studies were presented in the chapter 3. The test rig and specifications of devices which have been used for experiments and data acquisition are explained in detail. Materials are introduced and synthesis process of NCC, pulp suspension making, and procedures for fiber and paper characterizations are explained. Moreover, the standards used for paper characterizations were tabulated in Table 3.2. Three non-wood pulp samples including Rice straw, EFB (soda process) and two-stage soda Kenaf in lap form were used as the pulp sources. In heat transfer experiments, the bulk velocity was varied from 0.4 to 2.8 m/s for heat transfer data in increments of approximately 0.4 m/s. For pure pulp

suspensions the experimental settings were almost same as the heat transfer with the difference in bulk velocity where the range was between 0.4 m/s to 3.6 m/s. Details of experimental conditions and procedures were presented in Table 3.3.

CHAPTER 4 RESULTS AND DISCUSSION

4.1 Water run results

Experimental water run data were reduced and analyzed by calculating the Nusselt number and comparing with the existence correlations (Figures 4.1 and 4.2). The results highlight (Figure 4.1) there is relatively small difference between the current measurement and the existing well-known correlations which ensures high confidence on the acquired data. The lowest average deviation of Nu is obtained from comparison of the experimental results with Dittus-Boetler (Figure 4.2) which is 2.6%. Gnielinski equation shows more deviation from experimental values over the velocity range.

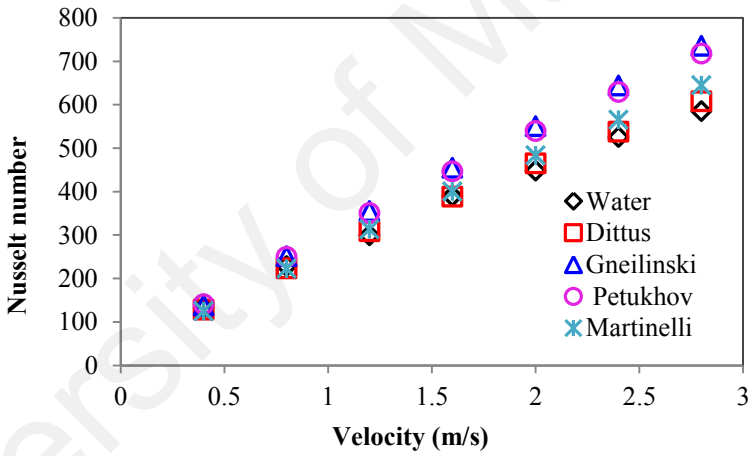

Figure 4.1: Comparison of Nusselt number as a function of velocity obtained from the experimental data and the standard correlations.

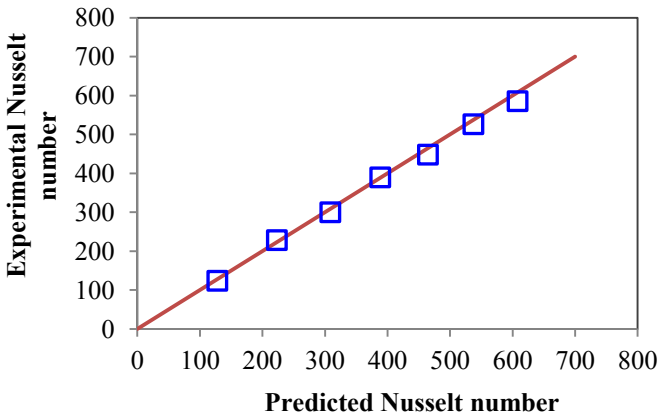

Figure 4.2: Comparison of Nusselt numbers at increasing velocities between present measurements and Dittus-Boelter correlation.

The experimental and empirical equations friction factor plots for the water run are presented in Figure 4.3. The results show excellent agreement between the experimental data with the existence correlations. The average errors of 2.5%, 3.15% and 3.88% were recorded for comparison of experimental pressure loss data with the results from Blassius, Pethukov and Colebrook respectively. It can be seen form Figure 4.3 that the deviation of experimental results from correlations are decreased with the increase of velocity.

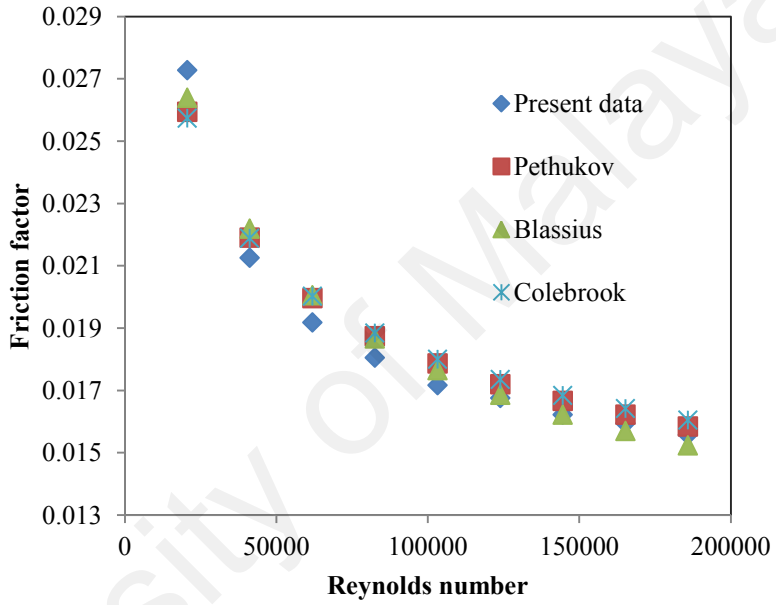

Figure 4.3: Plot of friction factor against Reynolds number for water and its comparison with the data from the existing correlations.

Further, the uncertainty analysis was conducted based on the method described in Appendix C. Uncertainty analysis is necessary to ensure the reliability of both raw and derived data as well as to determine the range where the true value of each acquired and calculated properties is likely to exist (Zubir, 2015). The list of uncertainty for different parameters governing the present heat transfer and pressure loss experiments is presented in Table 4.1.

Table 4.1: list of uncertainty for different parameters governing the present heat transfer and pressure loss experiments

Parameter	Uncertainty (%)
Heat flux	2.06
Heat transfer coefficient	2.10
Nusselt Number	2.12
Velocity	0.57
Reynolds Number	1.39
Friction factor	2.38

Pressure drop data at different bulk temperatures for water flow are presented in Figure 4.4. The results obtained at two different temperatures of 23 °C and 30 °C, and the velocity range is 0.4 m/s to 3.6 m/s. As can be seen in Figure 4.4 a reduction in temperature resulting an increment in pressure drop. However the trend of pressure drop versus velocity is same at both the temperatures, for each velocity point, the pressure drop at 23 °C is higher than that at 30 °C.

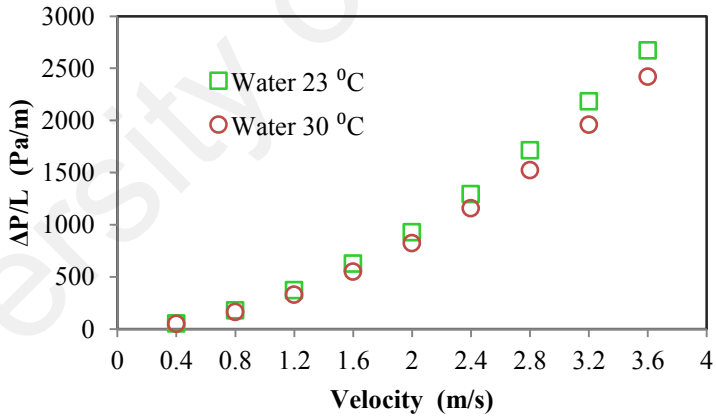

Figure 4.4: Frictional pressure drop as a function of velocity for water at bulk temperatures of 23 °C and 30 °C.

4.2 Heat transfer to fiber suspensions

Heat transfer to fiber suspension can be studied by considering the effect of fiber concentration and fiber beating degree. Three different concentration 0.2, 0.4 and 0.6 wt.% and two degrees of beating (2000 and 4000) were considered for heat transfer studies.

4.2.1 Effect of fiber concentration

In order to examine the effect of fiber concentration on heat transfer to fiber suspension a series of experiments were conducted by using different samples. The heat transfer to pulp suspensions was studied at different suspension concentrations and velocities. Figures 4.5- 4.7 display heat transfer coefficient as a function of velocity for samples with three different concentrations of 0.2, 0.4 and 0.6 wt.% at bulk temperature of 30 °C and velocity range from 0.4 to 2.8 m/s.

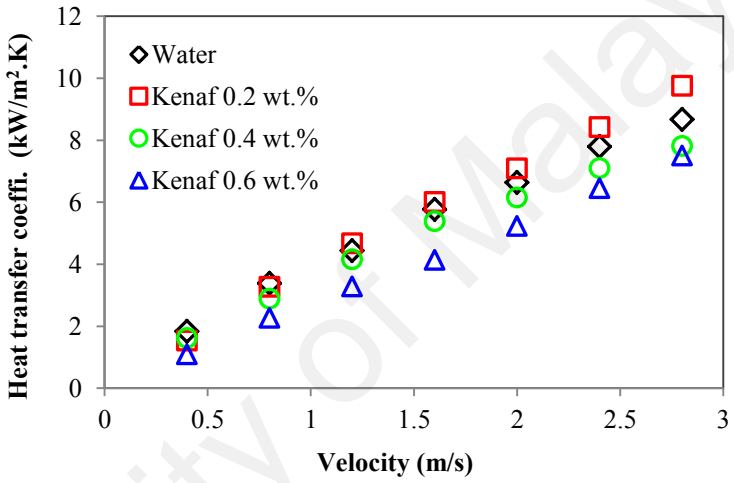

Figure 4.5: Heat transfer coefficient as a function of flow velocity for water and different concentrations of Kenaf pulp fiber suspensions. The heat transfer data were obtained at bulk temperature of 30 °C.

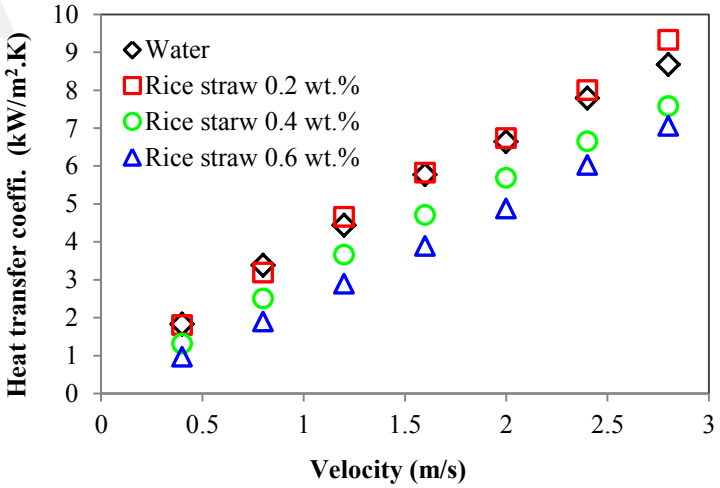

Figure 4.6: Heat transfer coefficient as a function of flow velocity for water and different concentrations of Rice straw pulp fiber suspensions. The heat transfer data were obtained at bulk temperature of 30 °C.

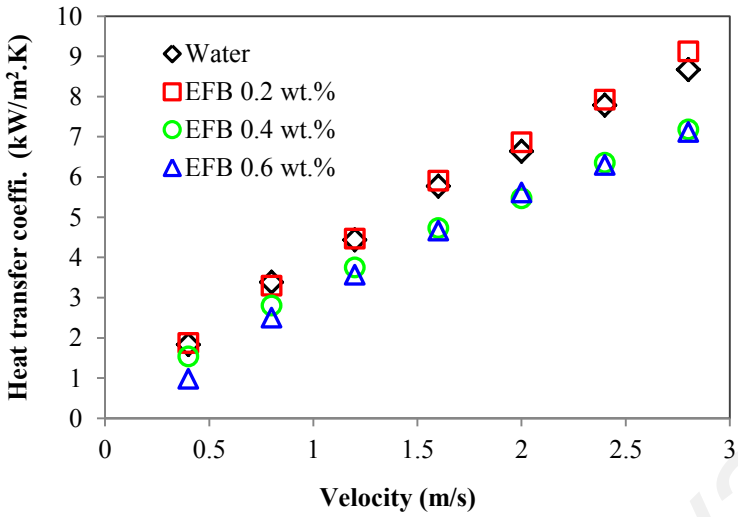

Figure 4.7: Heat transfer coefficient as a function of flow velocity for water and different concentrations of EFB pulp fiber suspensions. The heat transfer data were obtained at bulk temperature of 30 °C.

All three samples are showing similar trend. The velocity range can be divided into three ranges. Low range (velocity < 1 m/s), middle range (1 m/s ≤ velocity ≤ 2 m/s) and high range (velocity < 2 m/s). Comparing the results obtained from water run and the three concentrations of all the samples reveal that flow of fiber suspension at velocities lower than 1 m/s results in a lower heat transfer coefficient than water. The effect of concentrations on heat transfer coefficient is more highlighted when the velocity increases. At the middle and high ranges of velocities the suspension with the lowest concentration (0.2 wt.%) tends to show the heat transfer coefficient higher than water. However thermal conductivity of fiber suspension is lower than that of water, the contribution of fibers in enhancement of h_c is through the modifying the turbulent eddies. This trend is more pronounced for Kenaf sample at maximum velocity of 2.8 m/s. Comparing the h_c value of water with the enhancement of h_c for Kenaf, Rice straw and EFB suspensions at 0.2 wt.% are 12.4%, 7.5% and 4.0%. In order to confirm the h_c values obtained from Kenaf sample the experiment was repeated and same results were obtained (see section 4.8).

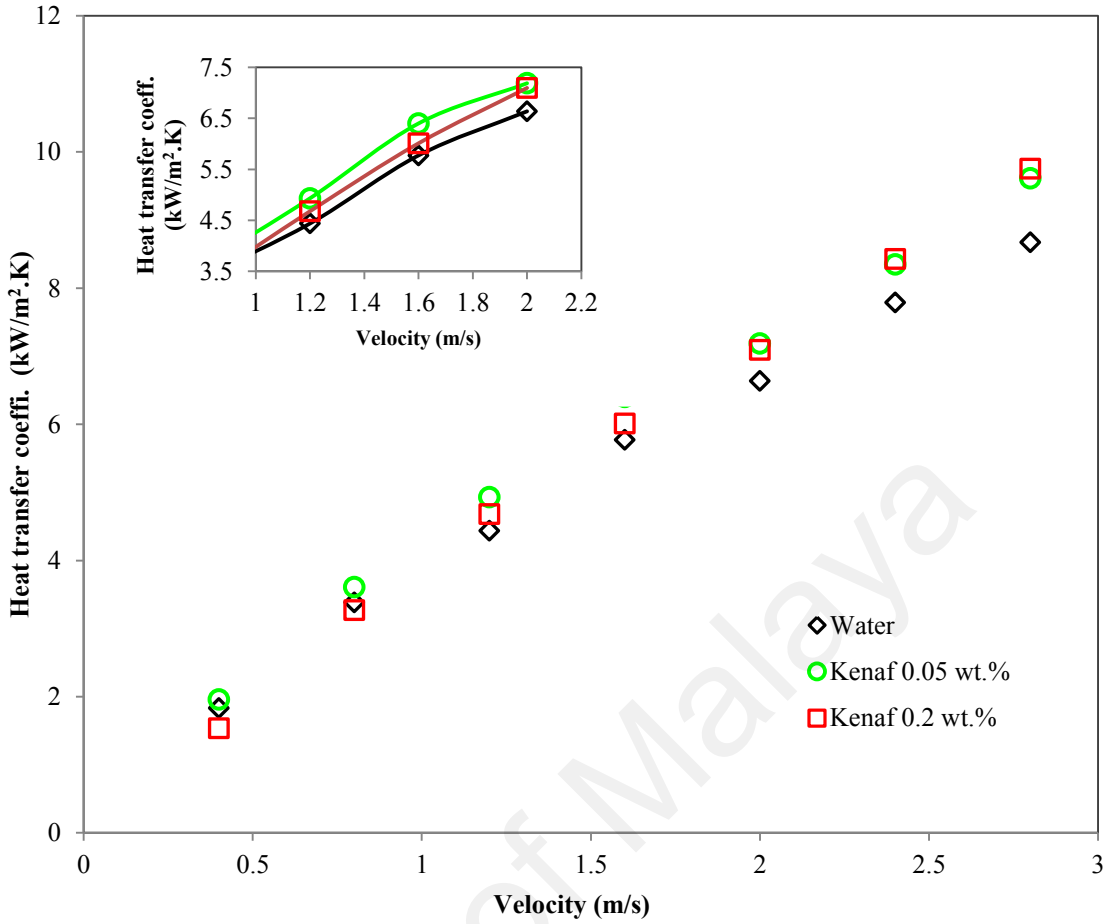

Figure 4.8: Heat transfer coefficient as a function of flow velocity for water and Kenaf samples with concentrations of 0.05 wt.% and 0.2 wt.% at the bulk temperature of 30 °C.

Moreover a very low concentration of 0.05 wt.% was selected to see whether there is such enhancement in suspensions of concentration lower than 0.2 wt.%. The results are presented in Figure 4.8 for Kenaf suspension of 0.05 wt.%.

The h_c trend of suspension at 0.2 wt.% concentration is more similar to that of water. The inset figure (Figure 4.8) shows that there is a slight peak in velocity of 1.6 m/s for both water and Kenaf suspension with 0.05 wt.% whereas this peak does not appear in the suspension with 0.2 wt.%. The suspension with concentration of 0.05 wt.% also shows an enhancement of h_c. The h_c values are slightly higher than that for suspension of 0.2 wt.% in low and middle velocity ranges. Further increase in velocity causes a decreasing trend of h_c where at 2.4 and 2.8 m/s the h_c values for Kenaf suspension with 0.05 wt.% are 0.9% and 1.4% lower than that for Kenaf suspension with 0.2 wt.%.

Unlike the suspension with 0.2 wt.% concentration, two others suspensions (0.4 wt.% and 0.6 wt.%) show lower h_c value compared to that of water. The h_c values obtained from suspensions with 0.4 wt.% concentration are more close to the water throughout the velocity range while the 0.6 wt.% suspensions show lowest heat transfers coefficient values. The h_c values of suspensions with 0.4 wt.% and 0.6 wt.% are more close together at velocities greater than 2 m/s.

Variations of h_c values obtained for samples can be distinctly observed by the heat transfer coefficient ratio defined as h_c value of pulp suspension sample to h_c value of water. The heat transfer ratio of water was set on unity. Figures 4.9 to 4.11 represent the heat transfer ratio of slurries versus velocity range of 0.4 m/s to 2.8 m/s. In the presented figures the differences between data are more highlighted.

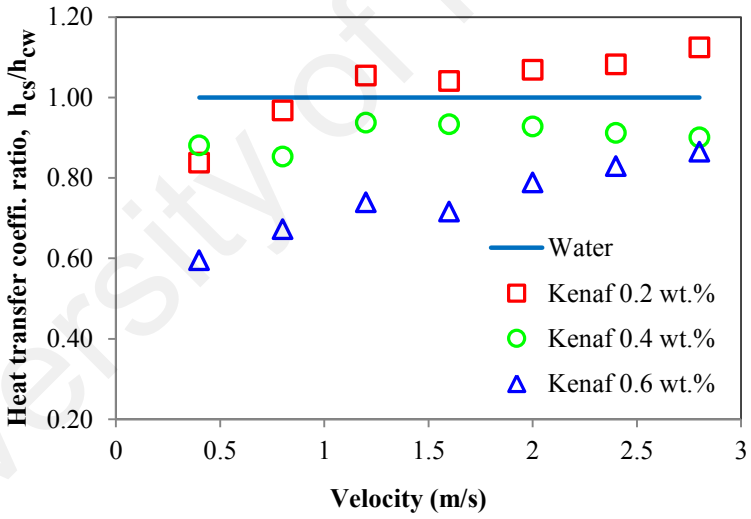

Figure 4.9: Heat transfer coefficient ratio as a function of flow velocity for water and different concentrations of Kenaf pulp fiber suspensions. The heat transfer data were obtained at bulk temperature of 30 °C.

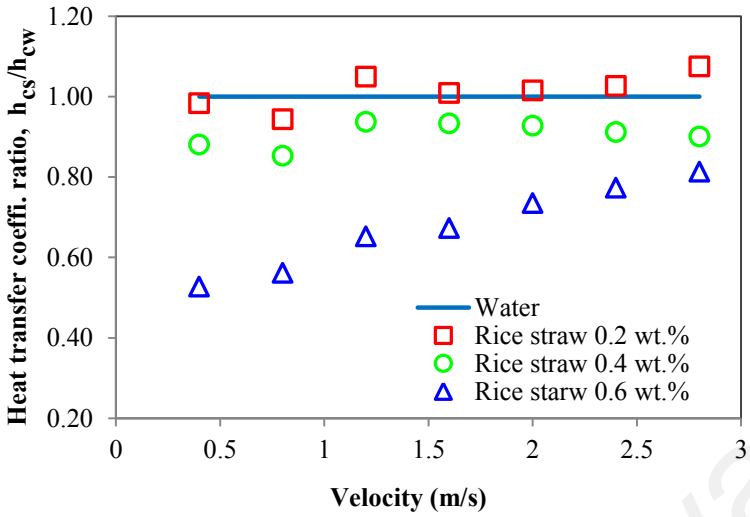

Figure 4.10: Heat transfer coefficient ratio as a function of flow velocity for water and different concentrations of Rice straw pulp fiber suspensions. The heat transfer data were obtained at bulk temperature of 30 °C.

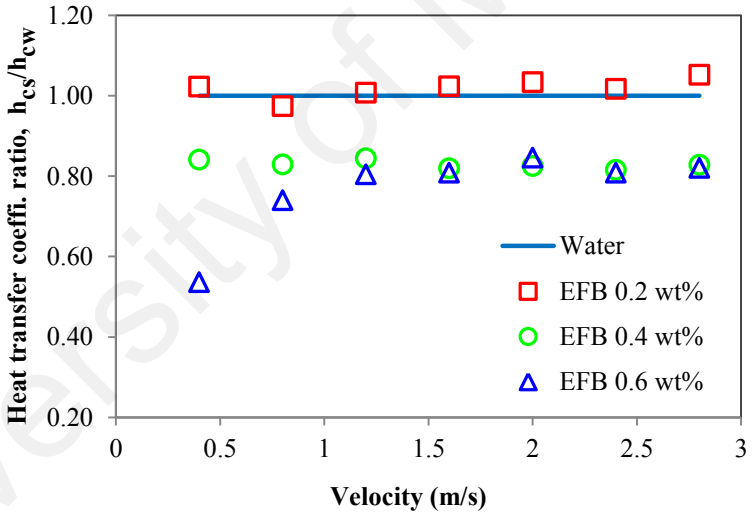

Figure 4.11: Heat transfer coefficient ratio as a function of flow velocity for water and different concentrations of EFB pulp fiber suspensions. The heat transfer data were obtained at bulk temperature of 30 °C.

For suspensions with 0.4 wt.%, the h_{cs}/h_{cw} values of Rice straw and Kenaf slurries are more close to water than that for EFB sample. All samples with concentration of 0.6 wt.% show maximum heat transfer coefficient ratio at maximum velocity.

Table 4.2 shows the h_{cs}/h_{cw} values for all samples at maximum velocity of 2.8 m/s extracted from Figures 4.9 to 4.11.

Table 4.2: The h_{cs}/h_{cw} values for samples at velocity of 2.8 m/s and bulk temperature of 30 °C.

Sample	Heat transfer coefficient ratio		
	0.2 wt.%	0.4 wt.%	0.6 wt.%
Kenaf	1.12	0.90	0.86
Rice straw	1.08	0.87	0.81
EFB	1.04	0.83	0.82

More graphs were presented in Appendix D to study the effect of fiber sources on h_c values.

4.2.2 Effect of pulp beating

The requirement for high quality fibers which are widely used in paper industries has increased the demand for pulp beating (refining) process. Pulp beating is a promising approach to improve the pulp quality by changing the fiber characteristics (Gharehkhani, Sadeghinezhad, et al., 2015).

Figure 4.12 represents heat transfer coefficient as a function of velocity for Kenaf fibers with two different beating degrees of 2000 and 4000. These two degrees of beating were selected based on the type of sample as non- wood fibers needs low degree of beating and sever beating results in shorter fibers with negative effect on drainage and paper properties. The suspension bulk temperature was maintained at 30 °C and the suspension concentration as 0.6 wt.%.

Low degree of beating has no significant effect on the heat transfer coefficient at low velocities. Further beating decreases h_c value of suspension. Reduction in h_c is due to an increase in fiber flexibility and fines content. Generally it is observed that the heat transfer coefficient decreases slightly with the increase of beating degree (Figure 4.13).

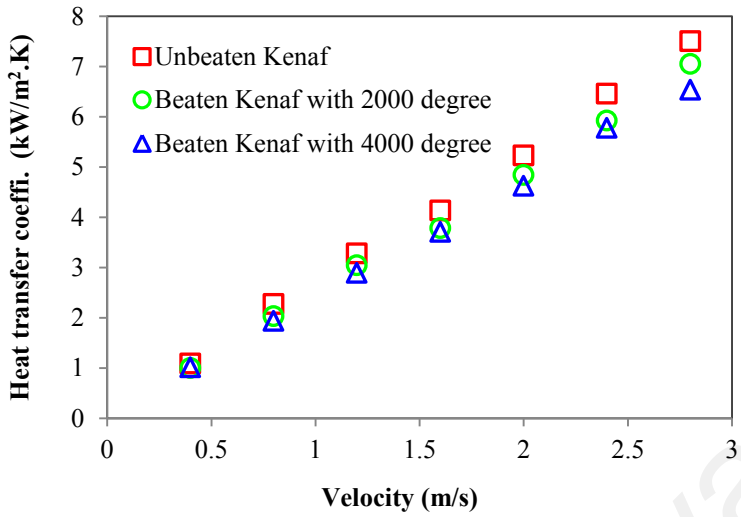

Figure 4.12: Heat transfer coefficient as a function of velocity for water and refined (two different degree of beating 2000 and 4000) fiber suspensions. The experiments were performed at bulk temperature of 30 °C and concentration of 0.6wt.%.

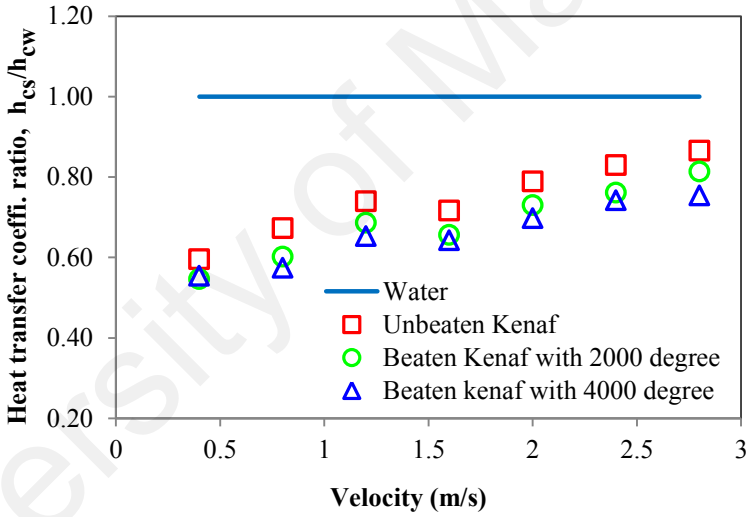

Figure 4.13: Heat transfer coefficient ratio as a function of velocity for unbeaten and beaten (two different degree of beating 2000 and 4000) fiber suspensions. The experiments were performed at bulk temperature of 30 °C and concentration of 0.6wt.%.

The heat transfer coefficient ratio values for unbeaten and two different Kenaf samples beaten at 2000 and 4000 degrees are 0.86, 0.81 and 0.75 at velocity of 2.8 m/s. The lowering in heat transfer coefficient could be due to a reduction in coarseness and fiber length or due to an increase in relative fiber number and longitudinal flexibility (due to reduction in cell wall thickness) or a combination of these. Kazi (2001) stated that individual fiber suspension behavior in heat transfer is clearly dominated by

flexibility. With the increase of flexibility of fibers in suspension the h_c value decreases due to more energy absorption from fiber-eddy collision and also from more interaction. The data obtained from beaten suspensions were used to correlate the fiber properties with h_c values in following section.

4.3 Heat transfer and fiber physical properties

A few studies had been carried out previously to determine how various fiber properties would modify turbulence. The studies aimed to find a relationship between the fiber/paper properties and heat/momentum transfer data to provide a means of measuring and monitoring fiber characteristics and pulp quality. It had been found in pipe flow that specific fiber characteristics and some fiber and paper properties could be assessed by both heat transfer measurements and friction loss determination (Kazi et al., 2014b). Following those studies there was a need to evaluate heat and momentum transfer measurements or both h and $\Delta P/L$ values of non-wood fibers over a range of flow conditions which is covered in the following section and sections 4.4, 4.6 and 4.7.

Paper properties are strongly affected by fiber properties. The well-known physical properties of fibers are fiber length, fiber width and lumen size. There is diversity in fiber properties based on the source of the fibers. Physical characteristics of fibers used in this study were presented in Table 4.3.

The length of Kenaf sample is the longest among all the examined samples where Rice straw and EFB have almost same length. Rice straw sample has lowest width and lumen size. In the case of beaten samples, the results show that length of the samples decrease with increase in beating degree. Beating with fibrillation and fiber shortening decreased the slenderness ratio but increased the flexibility coefficient of pulp fibers. These results are similar to the previous reports (Main et al., 2015; Mossello, Harun, Resalati, et al., 2010).

Table 4.3: Properties of Kraft fibers used in the experimental investigation

Fiber type	Length, L (mm)	Width, W (mm)	Lumen (mm)	Flexibility ratio (Lumen/W)	Slender ratio (L/W)
Kenaf	2.322	0.0408	0.0246	60.29	56.86
Beaten Kenaf with 2000 degree	2.240	0.0420	0.0276	65.71	53.33
Beaten Kenaf with 4000 degree	2.131	0.0438	0.030	68.49	48.63
Rice straw	0.920	0.006	0.003	50	153.33
EFB	0.922	0.016	0.009	56.25	57.62

Figures 4.14 to 4.16 presents the effect of various fiber dimensions and fiber properties on the magnitude of heat transfer coefficient for the same fiber concentration and flow velocity (0.6 wt.% and 1.2 m/s). The heat transfer data were obtained at bulk temperature of 30°C.

Three different samples of Kenaf pulp (0 degree, 2000 degree and 4000 degree of beatings) and another two samples (Rice straw and EFB) were considered to study the relationship between fiber properties and heat transfer coefficient values. However with different species of pulp samples the result may not be statistically significant (see Appendix D). Some of the fiber properties are interactive as seen by the fact that other pulp species tested were not on the same regression line. The situation is complex as there are actually distributions in fiber properties rather than true mean values. From a logical standpoint it makes sense to select one species of pulp with different physical properties which can be obtained by different degree of beating. First attempt was started using the fiber length as a variable. Fiber length is the most common parameter which is used to describe the paper sheet properties (Jahan et al., 2010). Beating the fibers is a way to tailor the fiber length. A long fiber can have more fiber joints and

therefore create a stronger network compared to a shorter fiber. It is not always clear, how the long fibers are affecting the paper strength. The longer fibers have the tendency to form more or bigger flocs compared to shorter fibers. The flocculation leads to a more uneven sheet, which may affect the paper properties. This can be avoided by lowering the fiber concentration of the long fiber stock during forming and by improving the dewatering elements on the wire (Johansson, 2011).

Variation of heat transfer coefficient based on different fiber length for Kenaf samples are presented in Figure 4.14. A clear trend is that a decrease in fiber length causes a decrease in h_c.

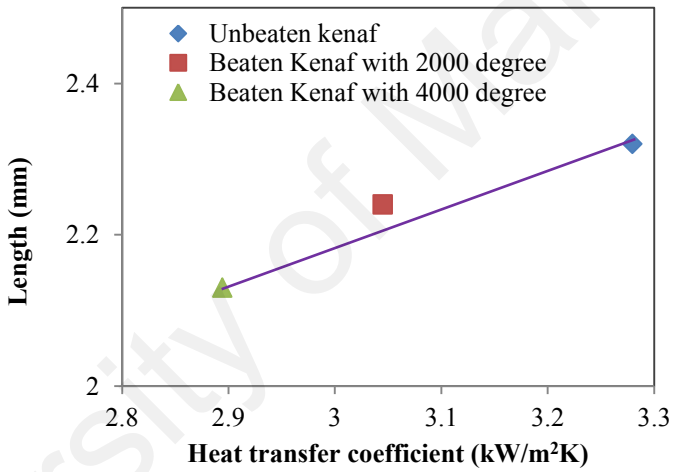

Figure 4.14: Fiber length as a function of heat transfer coefficient for Kenaf with no beating, Kenaf with 2000 and 4000 degree of beating.

Figure 4.15 represents the fiber length to fiber width (L/W) versus h_c. L/W can be ascribed to slender ratio. Figure 4.15 shows the changes in h_c by slender ratio for three different Kenaf samples. Data are obtained at concentration of 0.6 wt.%, bulk temperature of 30 °C and at the velocity 1.2 m/s.

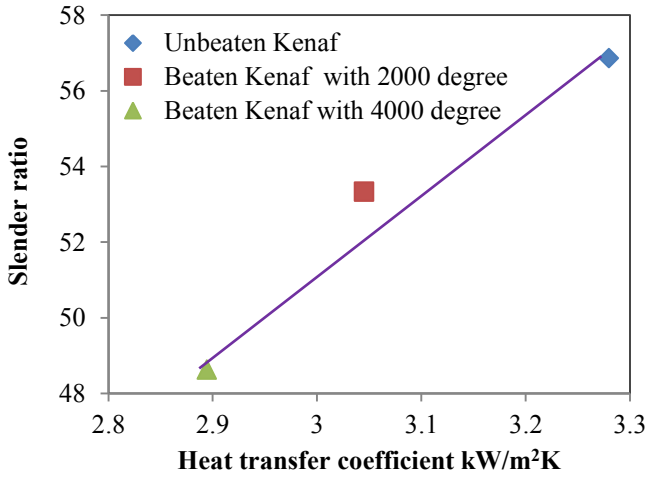

Figure 4.15: Slender ratio (L/W) as a function of heat transfer coefficient for Kenaf with no beating and with 2000 and 4000 degree of beating.

h_c data versus slender ratio present similar changes as observed in case of h_c as function of fiber length. The samples with higher slender ratio produce higher value of h_c. Fiber characteristic studies could be followed by plotting the flexibility ratio against h_c where deviation from the linear trend is much less pronounced than the previous graphs (Figure 4.16).

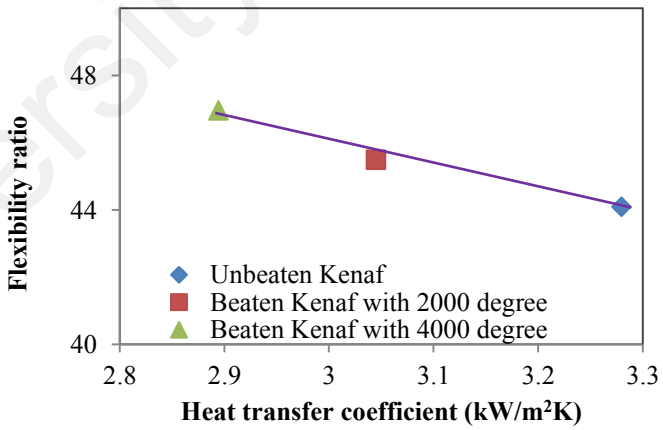

Figure 4.16: Flexibility ratio (Lumen/W) as a function of heat transfer coefficient for Kenaf with no beating, Kenaf with 2000 and 4000 degree of beating.

Comparison of the data of Kenaf sample with no beating and beating shows an increase of 3.1% and 6.4% in flexibility ratio due to beating with 2000 and 4000 degrees respectively which ultimately results a decrease of 7.1% and 11.7% in h_c. The results show that h_c can be correlated well with flexibility.

4.4 Heat transfer and paper properties

Paper properties such as tensile index, burst index and tear index are the most important parameters in paper making considerations. Some paper properties of the samples are presented in Table 4.4.

Table 4.4: Paper properties of the samples

Fiber type	Tensile index	Burst index	Tear index	Folding endurance	Brightness
Kenaf	42.04	2.81	14.78	25.5	37.45
Beaten Kenaf with 2000 degree	71.05	4.87	10.013	246	35.4
Beaten Kenaf with 4000 degree	78.02	5.1	8.9	635	34.3
Rice straw	48.57	2.78	4.7	29.25	23.3
EFB	22.57	1.7	6.42	9.33	45.7

Increasing beating revolutions resulted in high fiber flexibility and fiber swelling due to fibrillation and the presence of more fine fiber content, promoted better interfiber bonding within the paper formation and thus led to an increase in burst and tensile strength values (Main et al., 2015; Nayeri et al., 2013). The tensile index, burst index and stretch-to-break are improved when fines are added, especially when adding secondary fines (Johansson, 2011).

Figure 4.17 indicates the tensile index of Kenaf samples versus h_c. The h_c increases with a decrease in tensile index which corresponds to the results obtained for flexibility ratio vs. h_c. Previous researchers have obtained similar results (Kazi, 2001).

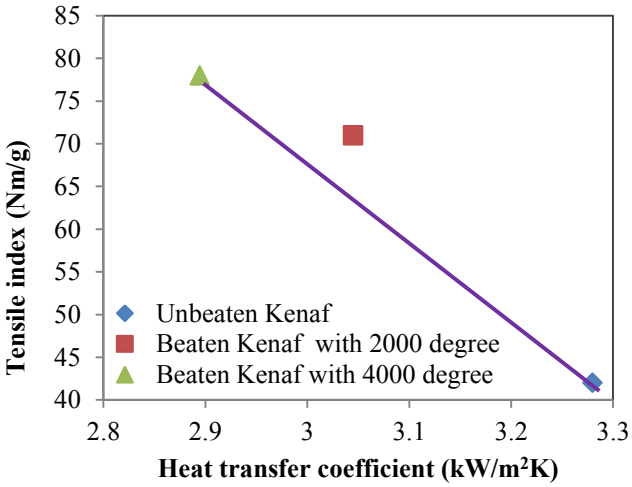

Figure 4.17: Tensile index as a function of heat transfer coefficient for Kenaf with no beating, with 2000 and 4000 degrees of beating.

Bursting strength measures the paper resistance to being burst when hydraulic pressure was applied to the paper (Hassan, Suhaimi, & Rushdan, 2013). Figure 4.18 shows heat transfer coefficient of the fiber suspensions as a function of paper sheet burst index for the no beaten and beaten Kenaf samples. The bulk temperature of the fiber suspensions was maintained at 30 °C. There is a clear trend in the relationship between paper sheet burst strength and heat transfer coefficient showing that the longer Kenaf sample (no beaten) provides the highest h_c value and produces papers with the lowest burst strength followed by Kenaf sample beaten at 2000 and 4000 degrees in an orderly manner.

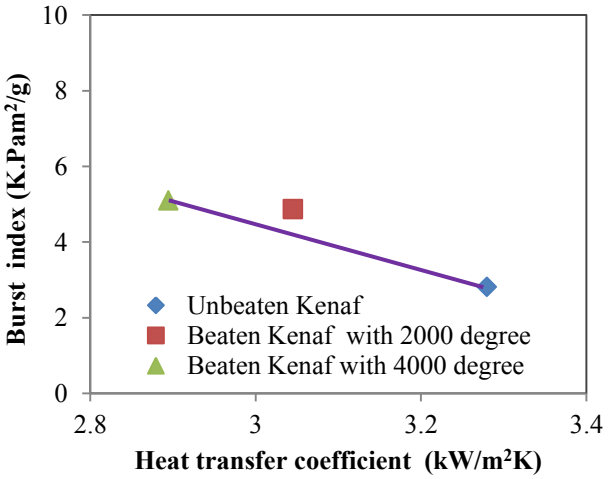

Figure 4.18: Burst index as a function of heat transfer coefficient for Kenaf with no beating, with 2000 and 4000 degrees of beating.

The relationship between tear index and h_c is presented in Figure 4.19. Beating decreased tear index of pulps. This can be explained, since under the condition of tightly bonded fibers, more fibers are ruptured through the initial cut, and fiber rupture requires less energy than pulling fibers out from network, so tear strength is reduced (Mossello, Harun, Resalati, et al., 2010). Tear index followed a different trend from tensile and burst index. Samples with less tear index were produced less h_c.

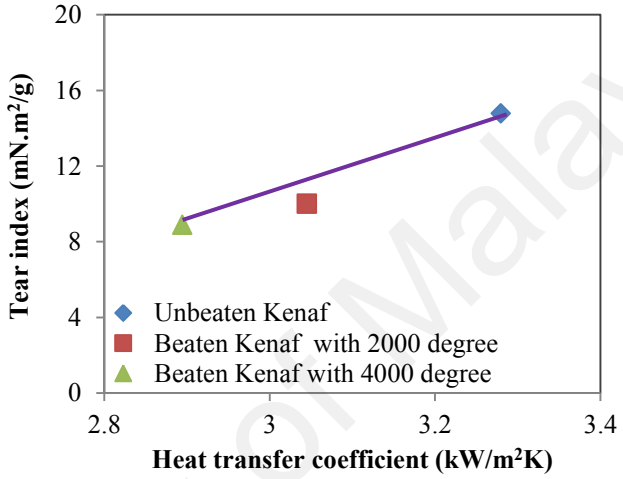

Figure 4.19: Tear index as a function of heat transfer coefficient for Kenaf with no beating, with 2000 and 4000 degrees of beating.

Folding endurance tests have been used to estimate the ability of paper to withstand repeated bending, folding, and creasing (TAPPI, 2006). The paper was folded backwards and fronts repeatedly between two rollers that rolling at 120 double folds per minute (Hassan, Muhammed, & Ibrahim, 2014). Increase in folding endurance would reduce the heat transfer coefficient (Figure 4.20).

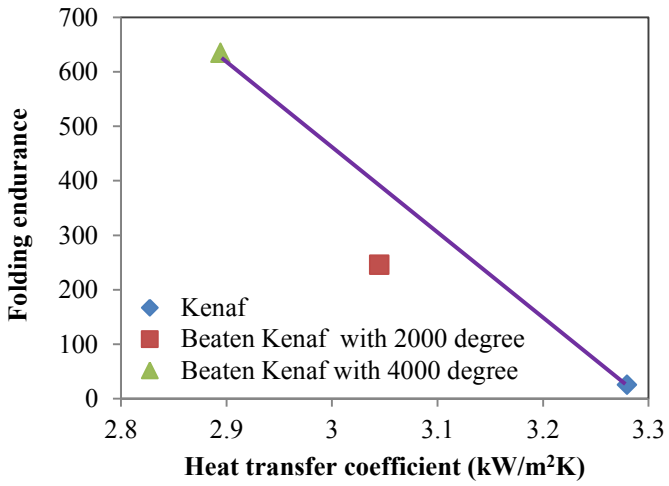

Figure 4.20: Folding endurance as a function of heat transfer coefficient for Kenaf with no beating, with 2000 and 4000 degree of beating.

All the strength properties except tear index will increase during beating. This happens because the tear strength depends on the individual strength of the fibers and the other properties rely on the fiber joints. Moreover, the increase of fiber joints will lead to a decrease of the light scattering coefficient. The bulk, opacity and porosity are other properties decreased by the beating (Johansson, 2011).

Beating degree has slight effect on fiber brightness. Brightness of Kenaf papers formed by different degrees of beating was studied and compared with h_c values obtained by their suspension flow to correlate the results.

Figure 4.21 represents heat transfer coefficient to fiber suspensions as a function of brightness (%) for the Kenaf samples. It is observed that unbeaten Kenaf shows the highest brightness corresponding to suspension heat transfer coefficient of 3.27 kW/m^{2}K whereas the Kenaf sample with 4000 degree of beating indicates the lowest brightness and lowest h_c.

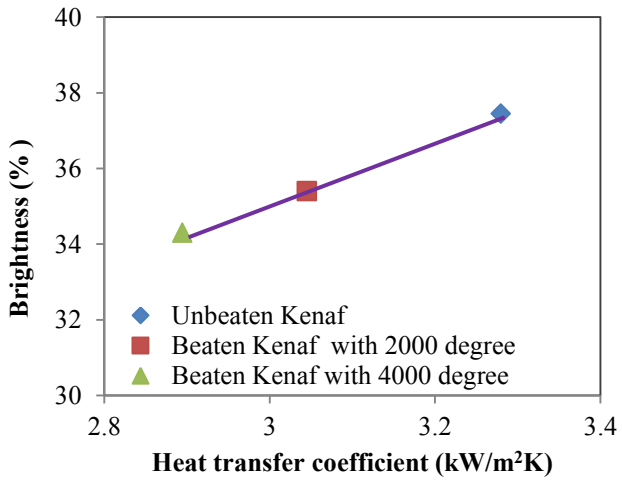

Figure 4.21: Brightness (%) as a function of heat transfer coefficient for Kenaf with no beating, with 2000 and 4000 degrees of beating.

4.5 Pressure drop of fiber suspension

The effect of fiber concentration and beating degree on the pressure drop data of fiber suspensions is presented in the following section.

4.5.1 Effect of fiber concentration

Figures 4.22 and 4.23 present the pressure drop versus velocity and the friction factor versus water Reynolds number for water and different concentrations of Kenaf suspension at bulk temperature of 30 °C. Data are presented in logarithm scale.

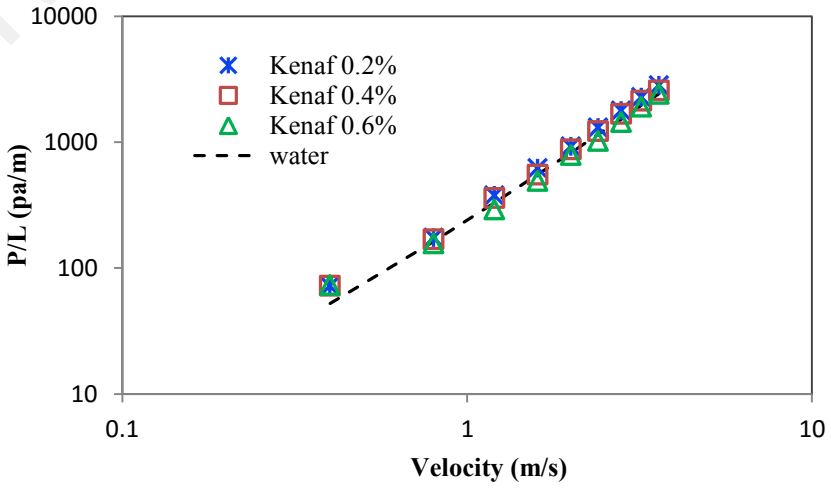

Figure 4.22: Pressure drop versus velocity for water and Kenaf suspensions with different concentrations.

The trends of data obtained for water and pulp suspension are similar to the typical diagram presented by Duffy (1972). At lowest velocity the data for Kenaf suspensions are higher than water data. Increase in velocity drops down the pressure loss data to below water data and further increase in velocity slightly increases the pressure drop near to the water data.

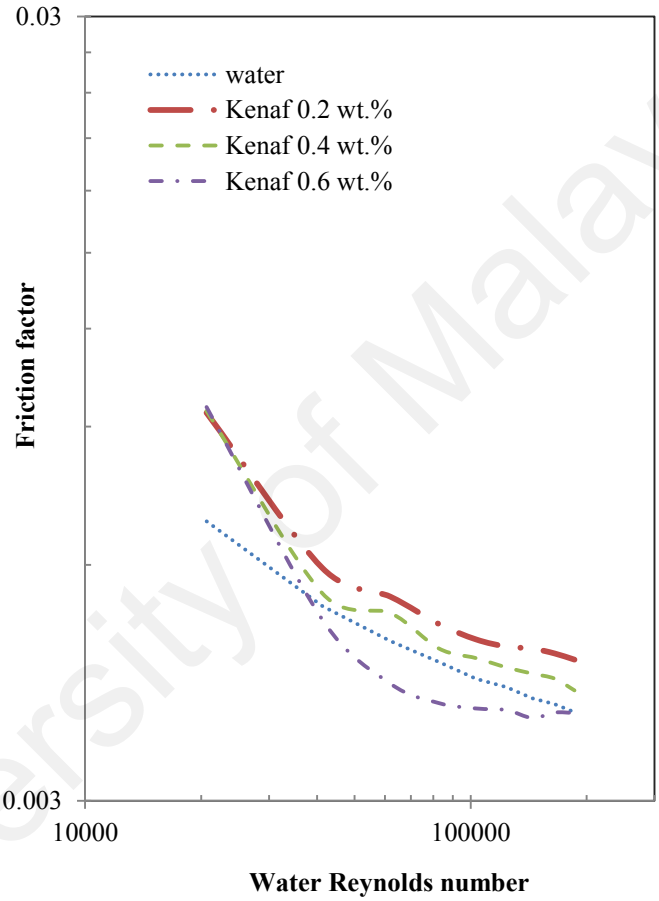

Figure 4.23: Friction factor versus water Reynolds number for water and Kenaf suspension with different concentrations.

In order to study the drag reduction behavior of the pulp suspension the pressure drop data are presented as the drag ratio data.

Figures 4.24 to 4.26 present frictional pressure drop as a drag ratio versus velocity for water Kenaf, Rice straw and EFB samples of different concentrations at bulk temperature of 30 °C. It should be mentioned that the pressure drop data obtained from the pulp suspensions are reliable (see Appendix D).

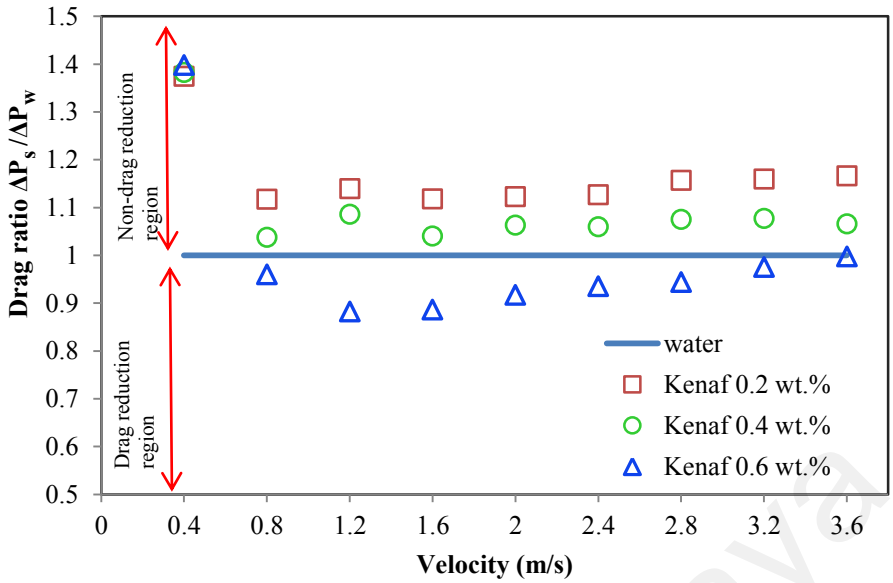

Figure 4.24: Drag ratio for Kenaf pulp suspensions of different concentrations as a function of velocity.

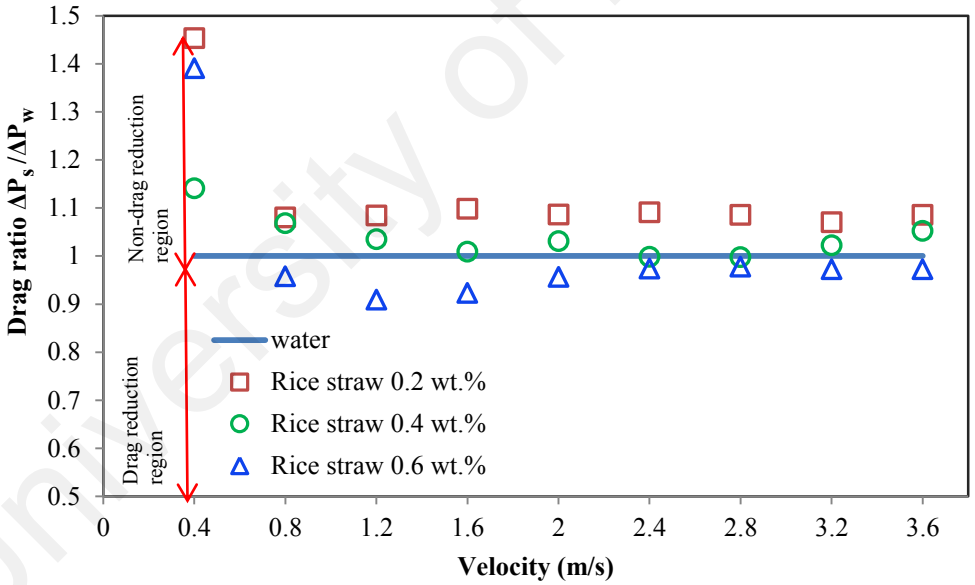

Figure 4.25: Drag ratio for Rice straw pulp suspensions of different concentrations as a function of velocity.

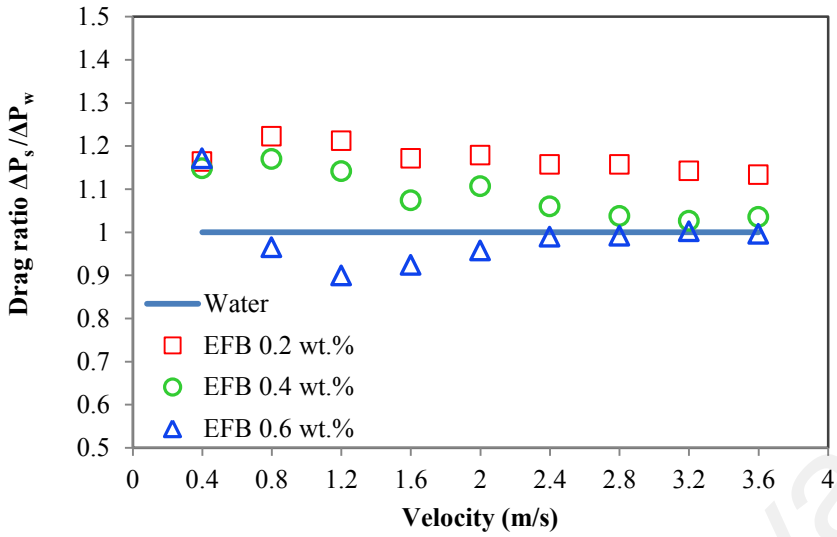

Figure 4.26: Drag ratio for EFB pulp suspensions of different concentrations as a function of velocity.

Water data were set as a unity. At lowest velocity value (0.4 m/s) the data are higher than water means no drag reduction. It is logic as usually floc formation occurs in such low velocity, so the drag ratio of fiber suspension is higher than water. From 0.8 m/s up to the 3.6 m/s the data are more close to the water data. By considering the water data as a border for drag reduction and non-drag reduction regions, it can be stated that there is a strong dependency between the concentration and obtaining the drag reduction. For suspensions at concentration of 0.2 and 0.4 wt.% the drag ratio data are higher than the water line in the low and middle velocity range while the 0.6 wt.% sample has lower drag ratio than 1 in the whole range except in 0.4 m/s. In general, the presence of very low amounts of fibers in slurries enhances the pressure drop. A critical concentration can be defined where the data are still higher than unity in the most velocities and further increase in fiber concentration results in reduction in pressure drop and drag ratio values to lower than water.

In the non-reduction region, the drag ratio data obtained from the suspensions of 0.4 wt.% concentration are more close to the water data compared to the suspensions of 0.2 wt.% concentration. Increasing the concentration up to 0.6 wt.% the data are moved

below water line where there is a drag reduction region. The magnitude of drag ratio decreases and increases at velocity range of 0.4 to 2 m/s where a maximum drag reduction occurs in this region. In the high range of velocity the drag ratio data increase close to water line. Figure 4.27 shows the drag ratio versus velocity for water, Kenaf, Rice straw and EFB samples of concentration 0.6 wt.%.

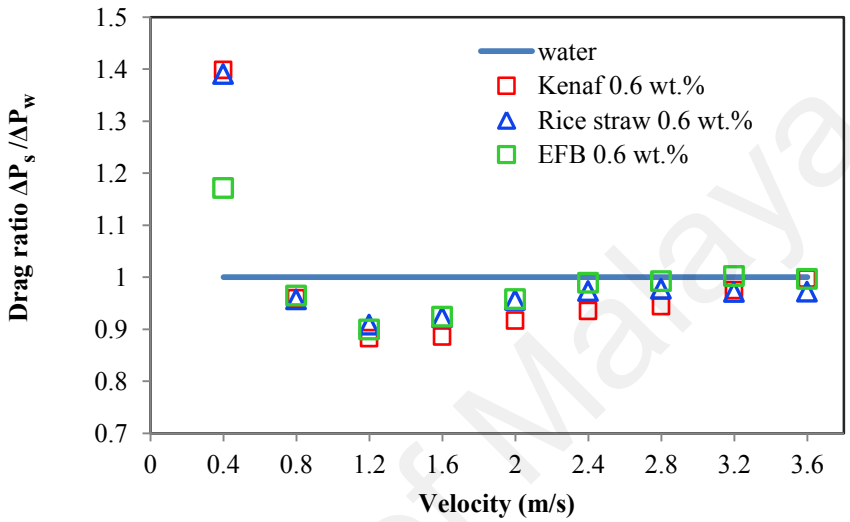

Figure 4.27: Drag ratio as a function of velocity for different pulp suspensions of concentration 0.6 wt.% .

The results show that Kenaf would produce higher amount of drag reduction among other samples. The momentum transfer behavior of all samples is almost same where a maximum drag reduction followed by increment in drag ratio. As it can be seen the maximum drag reduction occurred in the middle range of velocity. The values of drag ratio data for Rice straw and EFB are almost same and higher than that for Kenaf sample. It means Kenaf suspension poses more drag reduction. The maximum drag reduction of Kenaf, Rice straw and EFB samples are 11.7%, 9.1% and 10.05%.

4.5.2 Effect of pulp beating

Figure 4.28 presents the data of pressure drop as a function of velocity for unbeaten and beaten Kenaf fibers suspensions at concentration of 0.6 wt.%, velocity range of 0.4

to 3.6 m/s and bulk temperature 30 °C. The results show that the pressure drop values of sample with low degree of beating are close to the one with no beating. In other words, the suspension with 2000 degree of beating behave more or less same behavior as unbeaten fiber suspension. Around 0.8 m/s is the onset of plug disruption and with further increase in velocity noticeable reduction of ΔP/L occurred.

Increase in beating degree reduces the pressure drop of the suspension. The reduction in P/L with the flow of beaten Kenaf with 4000 degree is due to beating effect on fiber surface roughens by formation of fibrils which affects fiber-fiber and fiber-liquid interactions. Further beating increases fiber flexibility and fines content and the ΔP/L is lowered. The findings are in agreement with previous study done by (Kazi et al., 2014b).

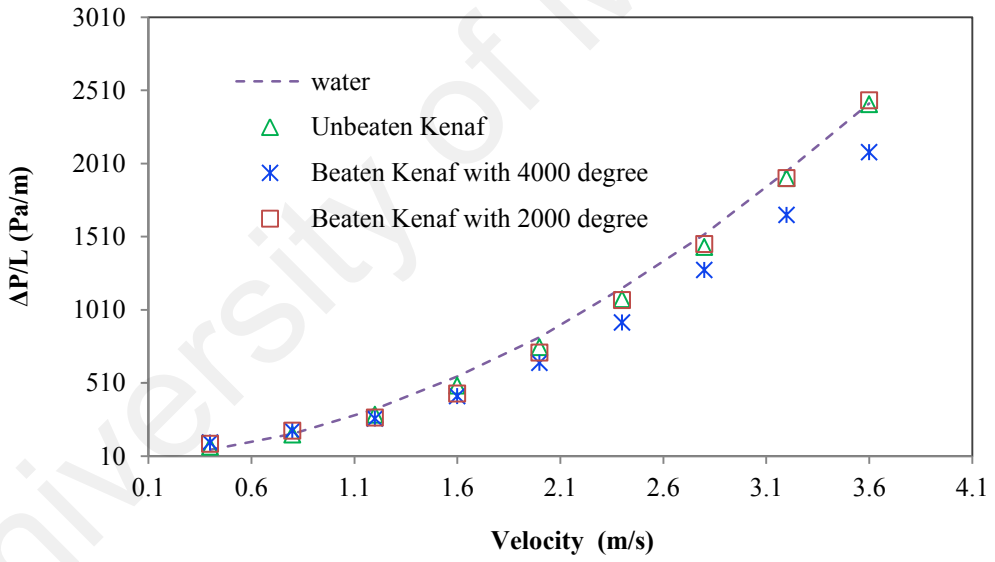

Figure 4.28: Pressure drop versus velocity for water, Unbeaten Kenaf and beaten Kenaf samples with two different beating degrees.

Figures 4.29 presents the data of drag ratio as a function of velocity for unbeaten and beaten Kenaf fibers suspension at concentration of 0.6 wt.%, velocity range of 0.4 to 3.6 m/s and bulk temperature of 30 °C. However in case of drag ratio, there is insignificant difference between the unbeaten Kenaf and beaten Kenaf with 2000 degree, further beating to 4000 degree results in lower drag ratio where the maximum drag reduction of 24% occurred at 1.6 m/s velocity.

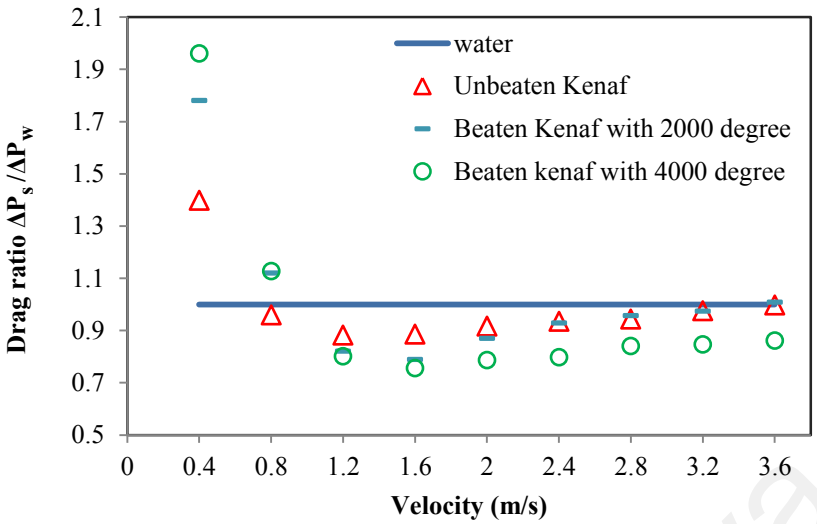

Figure 4.29: Drag ratio versus velocity for water, unbeaten and beaten Kenaf samples with two different beating degrees.

Detailed study of drag ratio data reveals that beating degree of 4000 slightly delayed the drag reduction phenomena. It can be claimed that beaten sample can produce lower drag ratio than unbeaten sample.

4.6 Pressure drop and fiber properties

Like heat transfer study, there is a hypothesis regarding the relationship between pressure drop and fiber properties. Figure 4.30 shows variation of pressure drop data versus fiber length. Different properties of fibers were obtained using the different degrees of beating. A decrease in fiber length due to beating would reduce the pressure drop values. Comparing to the Kenaf sample with no beating, a decrease of 3.5% and 8.9% in fiber length results in a decrease of 3.4% and 10.16% pressure drop. Same trend is presented in Figure 4.31 for variations of pressure drop versus slender ratio.

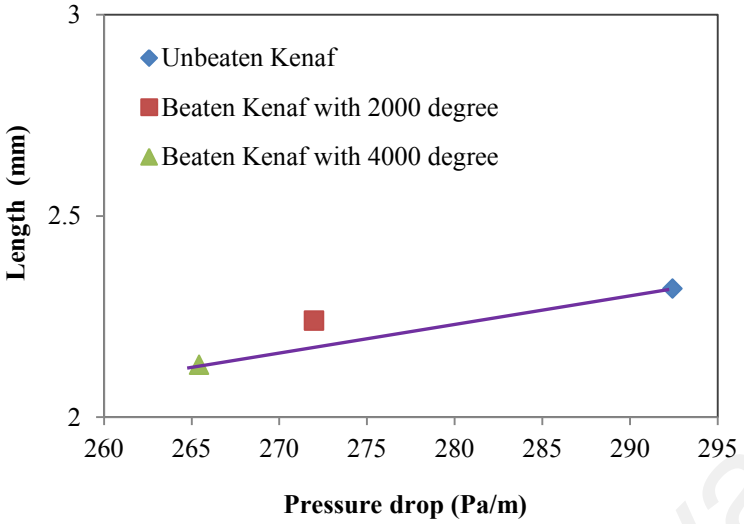

Figure 4.30: Fiber length as a function of pressure drop for Kenaf with no beating, with 2000 and 4000 degrees of beating.

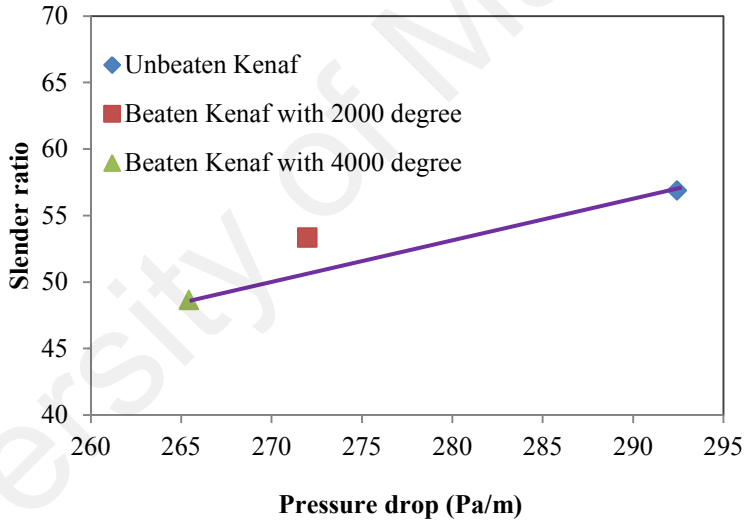

Figure 4.31: Slender ratio as a function of pressure drop for Kenaf with no beating, with 2000 and 4000 degrees of beating.

Figure 4.32 shows the changes of pressure drop versus flexibility ratio. A decrement in linear trend of pressure drop can be seen with increment of flexibility ratio.

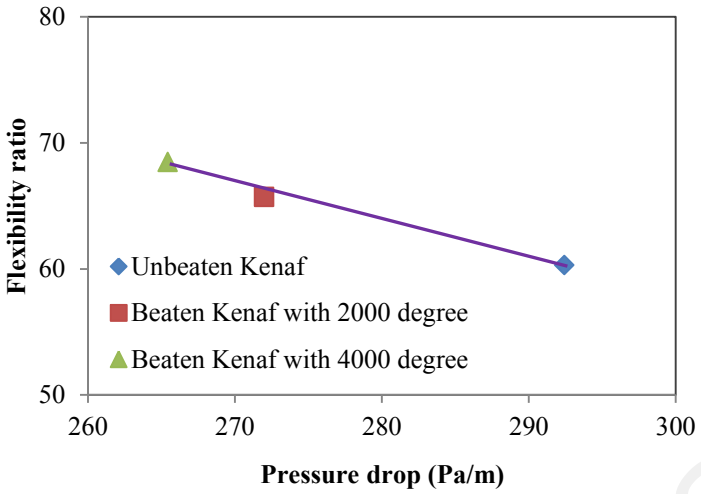

Figure 4.32: Flexibility ratio as a function of pressure drop for Kenaf with no beating, with 2000 and 4000 degrees of beating.

In conclusion, the trend of variations of pressure drop data with fiber properties is similar to those of variation of heat transfer coefficient data with fiber properties. However the variations of pressure drop data are correlated with fiber properties more linearly.

4.7 Pressure drop and paper properties

Frictional pressure drop measurement of fiber suspensions were used to correlate ΔP/L data with the properties of paper sheets made from the same type of fibers. Paper properties were obtained from laboratory-made hand sheets prepared from the same pulp fibers. Some of the data are presented in graphical form in Figures 4.33 to 4.37.

Approximate linear relationship is found for paper tensile index versus pressure drop at the velocity of 1.2 m/s and temperature of 30 °C (Figure 4.33). The hand sheets used for tests were at the same grammage. The decrement order of tensile index remains according to the degree of beating, such as unbeaten, beaten with 2000 and 4000 degrees respectively.

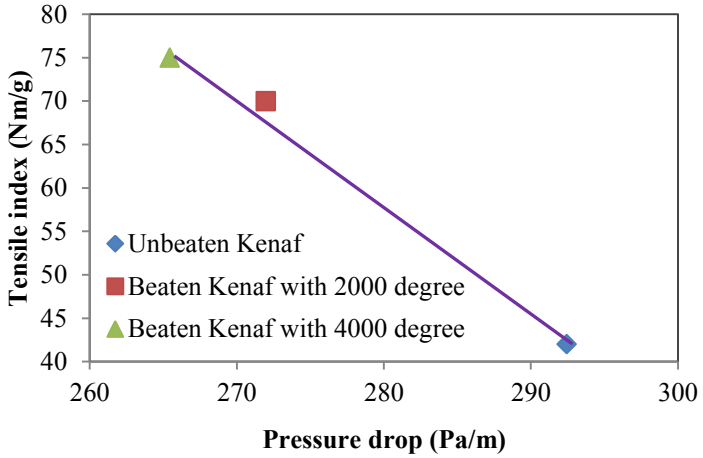

Figure 4.33: Tensile index as a function of pressure drop for Kenaf with no beating, with 2000 and 4000 degrees of beating.

The trend remains similar for burst index versus pressure drop (Figure 4.34). Burst index increases with the decreases of pressure drop of fiber suspensions.

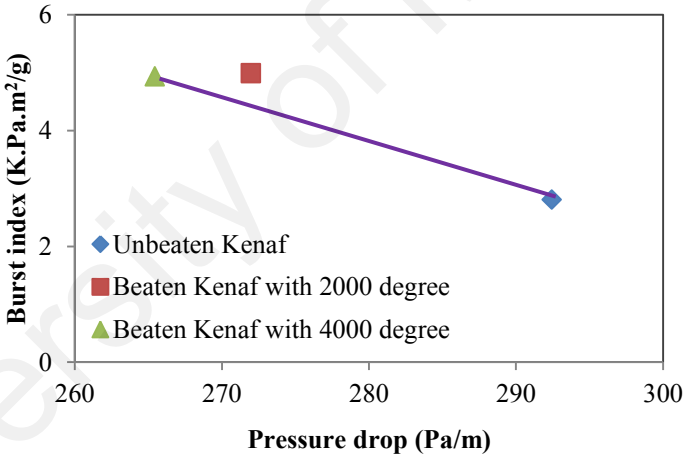

Figure 4.34: Burst index as a function of pressure drop for Kenaf with no beating, with 2000 and 4000 degrees of beating.

Figure 4.35 depicts increase of tear index with the enhancement of frictional pressure drop. The tear strength of the fibers contradicted the tensile strength, whereby the tearing value decreased with increase of beating degree.

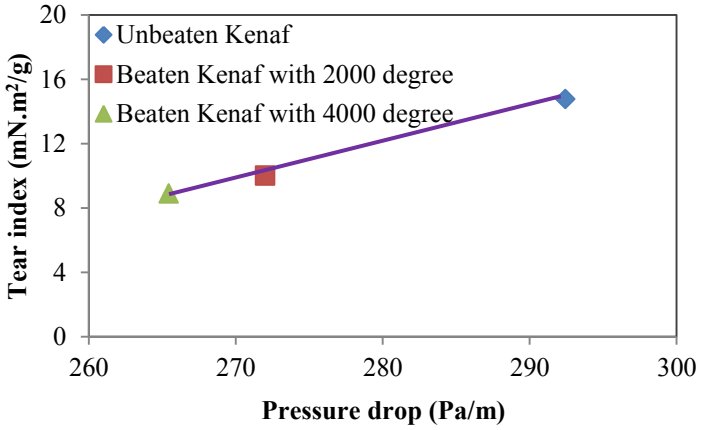

Figure 4.35: Tear index as a function of pressure drop for Kenaf with no beating, with 2000 and 4000 degrees of beating.

The tear test is very sensitive to the physical properties of the fiber (Main et al., 2015). The beating process resulted in changes to the fiber dimension such as shorter fibers, hence contributing to the decrease in tear strength. It is noticeable that sometimes decrease in tear index resulted from beating process is not significant. Main et al. (2015) reported only 0.4% decrement of tear index for coconut coir fibers at 2000 revolutions to 8000 revolutions. Figure 4.36 represents paper folding endurance as a function of pressure drop of suspensions of the unbeaten and beaten fibers. Although folding endurance increases with decrease of pressure drop, the relationship is not as good as tensile, burst and tear indices.

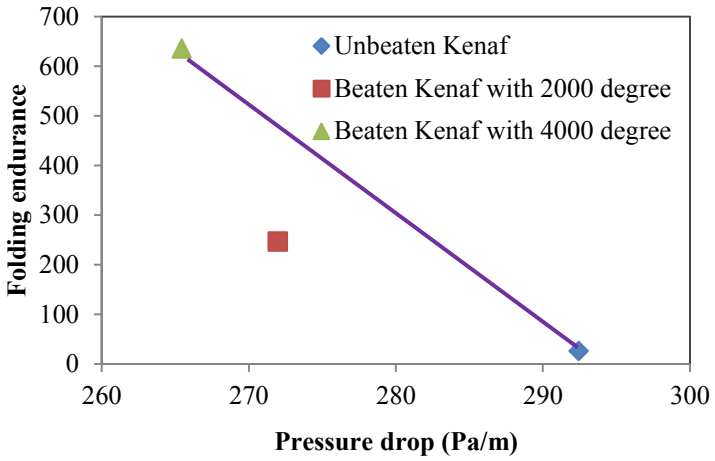

Figure 4.36: Folding endurance as a function of pressure drop for Kenaf with no beating, with 2000 and 4000 degrees of beating.

Figure 4.37 shows that paper brightness correlate well with frictional pressure drop for fiber suspensions of beaten and unbeaten Kenaf pulps. The brightness increases with increase in pressure drop.

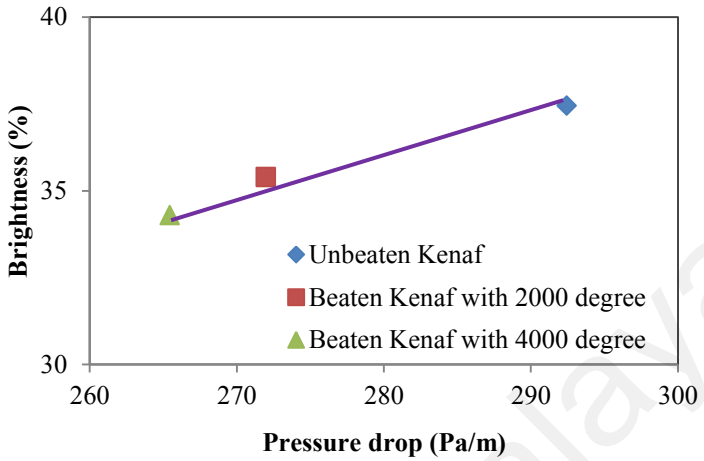

Figure 4.37: Brightness as a function of pressure drop for Kenaf with no beating, with 2000 and 4000 degrees of beating.

4.8 Pressure loss study of pulp suspension with additives

The suspensions of cellulose fibers used in papermaking are often treated by a range of polymers as additives: strength additives are used to increase the strength of finished paper, while retention aids are employed to flocculate fine particles, such as clays, used as filler in the paper (Mosse et al., 2012). Most previous studies on pulp suspension containing additives typically focused on rheological properties not on the pressure loss studies.

The effect of CPAM and potato starch as the conventional additives and NCC as the new generation of additives will be discussed in the following section. No study on the effect of NCC on pressure drop of pulp suspension has been reported before.

4.8.1 Effect of conventional additives

Fibers develop a negative surface charge when suspended in water (Aloulou, Boufi, Belgacem, & Gandini, 2004; Bhardwaj, Kumar, & Bajpai, 2004a; Sarrazin et al., 2009). The level of anionic charge on the pulp supplied from the pulp mill is typically –20 to–25 mV depending on the level of carboxyl acid groups present in the pulp which is dependent on the source of fibers, and some chemical treatments applied in the pulping process (Banavath et al., 2011; Genco, 1999). Therefore it is logical to select the positively charged polymers as the retention aids.

CPAM is one of the mostly used retention aid in paper making and it has been used to address the effect of cationic polymer on pressure drop of non-wood pulp fibers suspension. The experiments were conducted at room temperature 23 °C to eliminate the effect of temperature and decrease the experimental run times, which consequently retarded the polymer degradation. In general, high levels of hydrodynamic shear are understood to be the main cause of polymer degradation (Krochak, Ankerfors, Holm, & Lindstrom, 2011).

Figure 4.38 and 4.39 represents the effect on pressure loss from the addition of a small amount of CPAM to the suspension containing 0.6 wt.% Kenaf fiber. The drag ratio as a function of velocity was plotted for water, Kenaf suspension alone and with 70 ppm and 150 ppm CPAM. Little changes were sensed in drag ratio after adding the CPAM solution at 70 ppm concentration. For both the samples there is enhancement in drag reduction with the increase of velocity up to the highest level, then further increase in velocity results in a decrease in drag reduction.

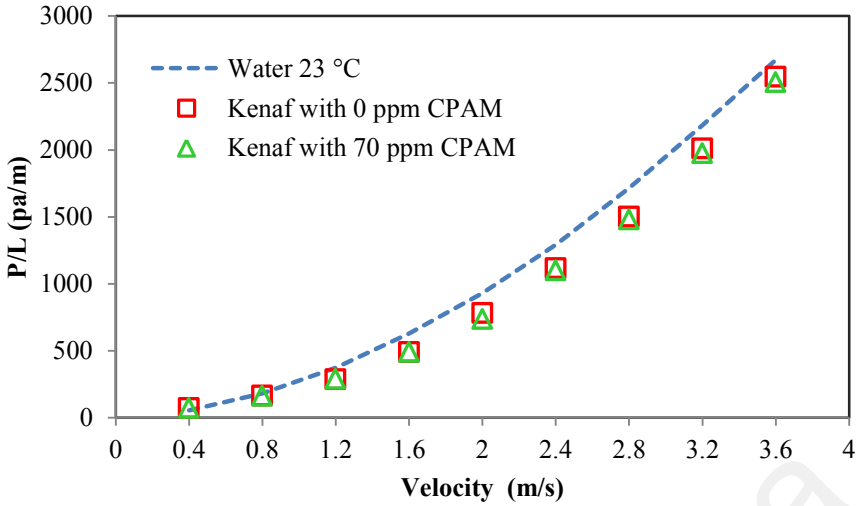

Figure 4.38: Pressure drop as a function of velocity for water, Kenaf suspension, and Kenaf suspension with 70 ppm CPAM.

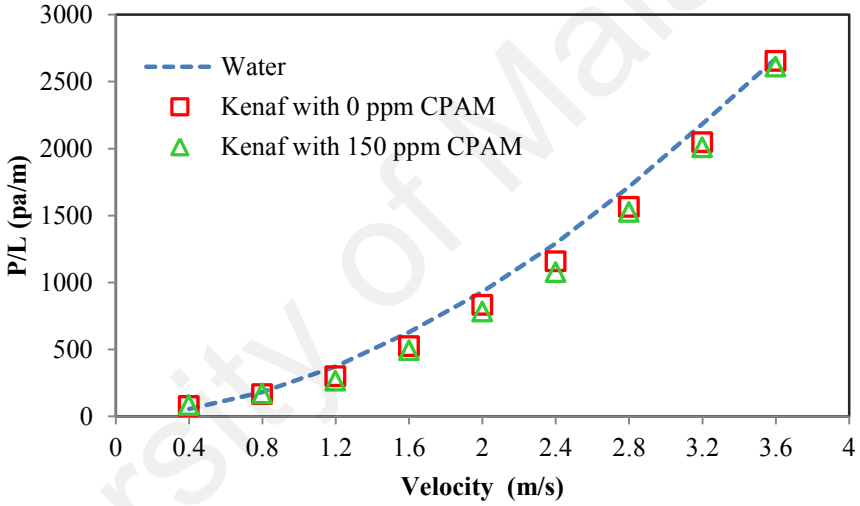

Figure 4.39: Pressure drop as a function of velocity for water, Kenaf suspension, and Kenaf suspension with 150 ppm CPAM.

Behavior patterns of drag ratio of fiber suspension alone and with CPAM are shown in Figure 4.40 and 4.41 where the effect of polymer concentration can be seen more clearly.

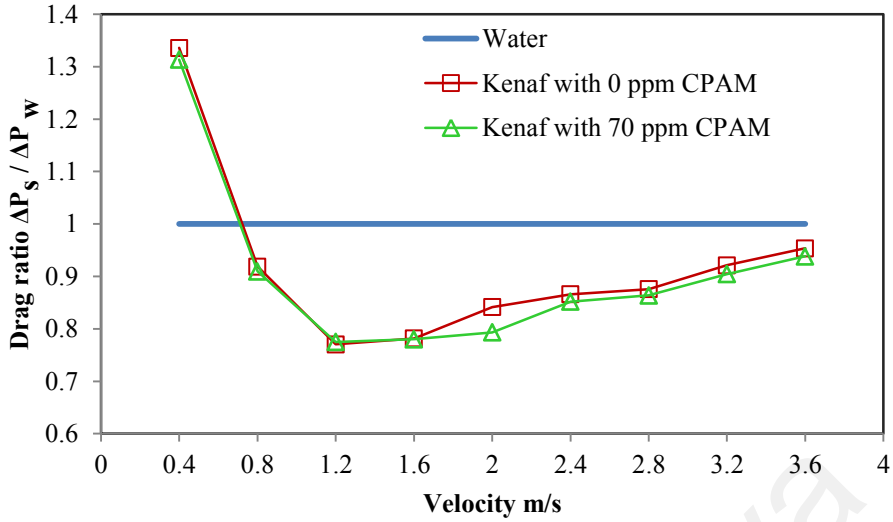

Figure 4.40: Drag ratio versus velocity for water, Kenaf suspension, and Kenaf suspension with 70 ppm CPAM.

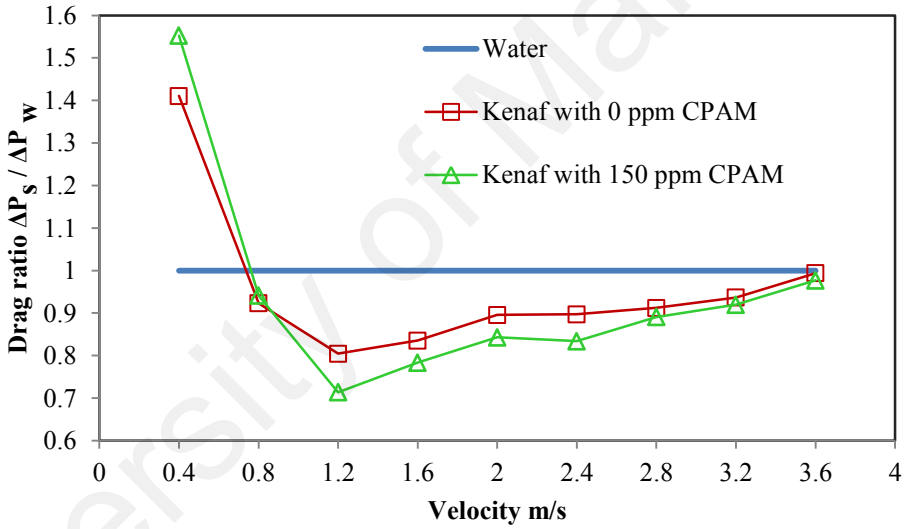

Figure 4.41: Drag ratio versus velocity for water, Kenaf suspension, and Kenaf suspension with 150 ppm CPAM.

The drag ratio of fiber suspension has decreased with the increase of CPAM concentration. This agrees well with the previous studies describing effect of polymer concentration on drag reduction which increased with the enhancement of polymer concentration up to an optimum dosage. Further increase in polymer concentration did not alter the friction factor (Ptasinski et al., 2001). Drag ratio of suspension with 70 ppm polymer changed after increase of velocity 1.6 m/s while suspension containing 150 ppm CPAM reduces the drag ratio from the lower range of velocity. Over the range of

velocities, the maximum reductions in drag ratio for suspension with 70 and 150 ppm were found to be 5.7 % and 11.2 % respectively above the pulp suspension alone. MacKenzie et al. (2014) stated that the change in drag reduction by different dosages of polymer depends on the level of surface polymer adsorption in dilute fiber suspension.

In the second part of this section, pressure drop measurements were taken to monitor the drag reduction of pulp suspensions containing 70 and 150 ppm of potato starch.

Figure 4.42 shows an increase in drag ratio of Kenaf suspension containing 70 ppm potato starch in comparison to Kenaf suspension alone. Adding small amount of potato starch (70 ppm) decreased the drag reduction percentage in the whole range of velocity except at velocity of 2 m/s which has experienced a slight reduction in drag ratio (0.5% reduction comparing the Kenaf suspension alone). It seems such a small amount of starch could not affect the hydrodynamic behavior of pulp suspension. During investigation, to keep the concentration of all suspensions at 0.6 wt.%, a known amount of fibers was replaced by the same amount of starch in the suspension. The negative effect of decrease of fiber concentration on drag reduction dominated the positive influence of starch added to the suspension. Therefore the economic aspect should be considered before recommendation is given on use of polymer in drag reduction

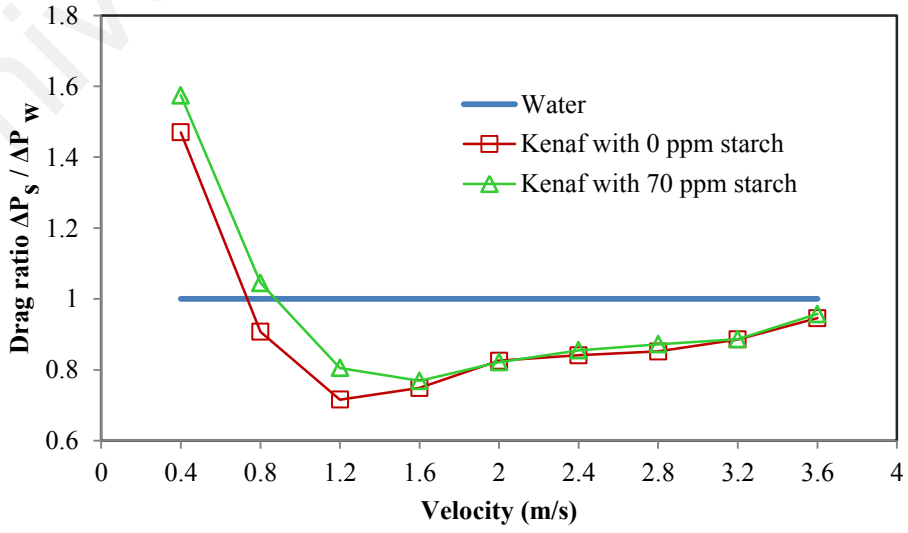

Figure 4.42: Drag ratio versus velocity for water, Kenaf suspension, and Kenaf suspension with 70 ppm starch.

Increase in starch dosage to 150 ppm shows increase in drag reduction at middle and high velocity ranges (Figure 4.43).

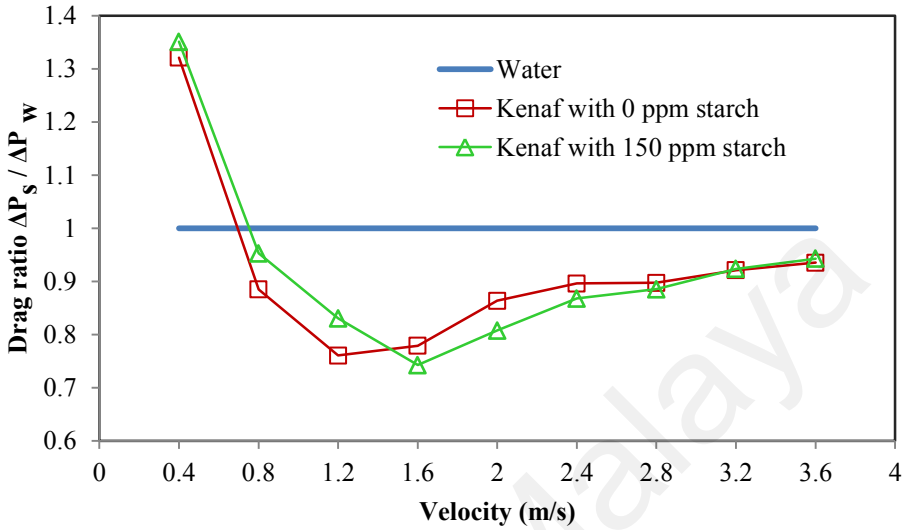

Figure 4.43: Drag ratio versus velocity for water, Kenaf suspension, and Kenaf suspension with 150 ppm starch.

At low velocities below 1.6 m/s drag reduction has reduced as being experienced in case of suspension containing 70 ppm starch. Further increase in velocity increases the drag reduction compared to Kenaf suspension alone. Maximum increment in drag reduction of 6.4% was occurred at velocity 2 m/s comparing to Kenaf suspension alone while maximum drag reduction was seen at velocity of 1.6 m/s.

Figures 4.40 to 4.43 have demonstrated that at the high velocity range the drag ratio data of pulp suspensions containing CPAM or potato starch are much closer to the data of pulp suspension alone. This is due to the polymer degradation caused by high level of shear as the retention aid polymers are shear sensitive, i.e., they undergo chain cleavage accompanied by a reduction in molecular mass and loss of functionality when exposed to too high levels of hydrodynamic shear.

4.8.2 Effect of NCC (a new generation of additives)

NCC has been attractive in many interests in different areas, its utilization in papermaking field is still under investigation. It has been reported that NCC can be used as an additive in papermaking (Xu et al., 2013). Therefore, study on flow behavior of pulp suspensions containing the NCC could shed some lights on the use of NCC in pulp and paper industries.

As mentioned in chapter 3, NCC was synthesized through acid hydrolysis of the Acacia mangium in the controlled condition. The prepared NCC was characterized through several methods. Prior to discuss about the effect of adding NCC to the pulp suspension on pressure lossin the present section, the properties of NCC are introduced here.

Figure 4.44 shows a FESEM image of freeze-deride NCC sample. The needle like nano crystals can be seen in the image. Moreover, in order to characterize the NCC in the colloide, the TEM image of NCC is presented in Figure 4.45. The dimensions of elongated nanoparticles prepared by sulfuric acid hydrolysis are indicated of 39±3 ×2± 1nm.

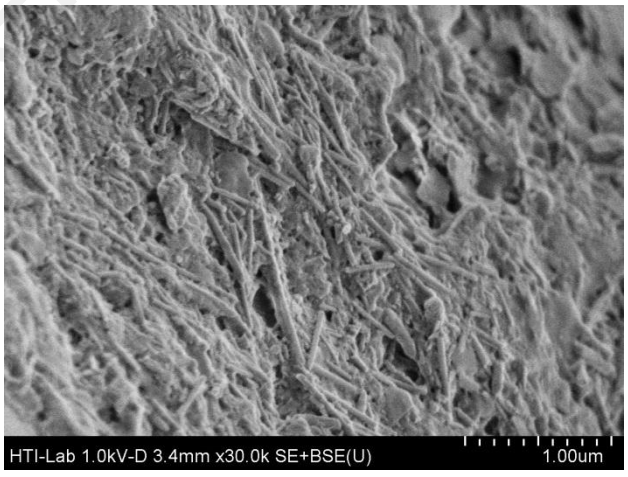

Figure 4.44: FESEM image from freeze-dried NCC sample.

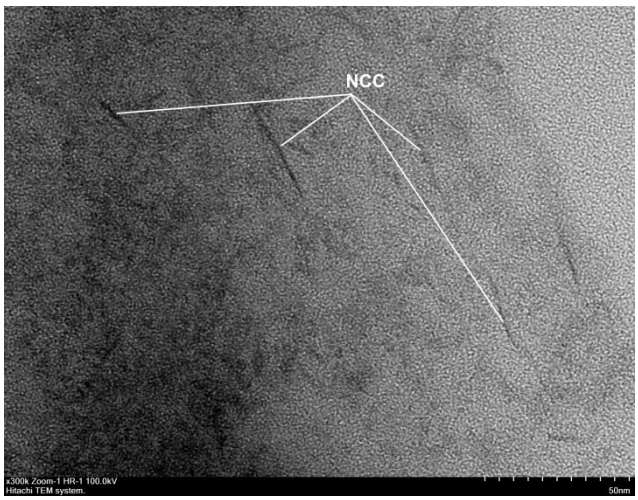

Figure 4.45: TEM micrograph of CNC suspension.

Due to smaller size and very high specific surface area, NCC has a tendency to form aggregates in various systems (Zaman et al. 2012). Sulfuric acid hydrolyzed cellulose nanocrystals have negatively charged sulfate ester groups on its surface that provide electrostatic stabilization. In this study the magnitudes of ζ-potential for NCC suspension was -31.1 mV which results in a stable suspension.

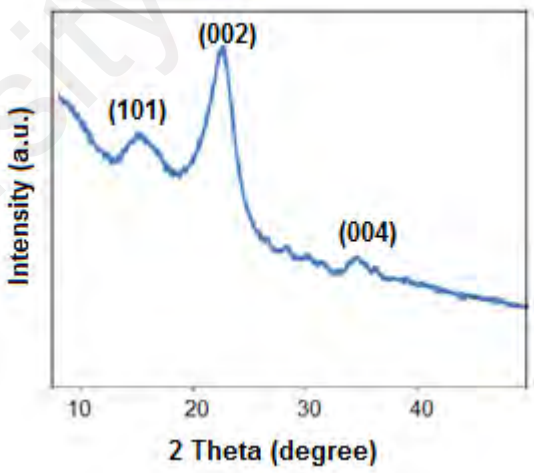

Figure 4.46: XRD patterns of NCC.

The XRD pattern of freeze-dried nanocrystals in Figure 4.46 exhibits the peaks around 2θ= 15.7°, 22.5° and 34.5°. The cellulose crystals exhibit characteristic assignments of 101, 002, and 004 planes, respectively (Kumar, Negi, Choudhary, & Bhardwaj, 2014). The internal cohesion was being established by the transition of the long cellulose chain molecules to nanofibrils inside the elementary fibrils. The

nanofibrils were parallely arranged into crystallites and crystallite strands caused by secondary valence hydrogen bonds formed by the hydroxyl groups (Liu et al., 2011).

Ordering the chiral nematic phase of NCC (see Appendix E) depends on the suspension concentration. Regardless of the NCC phase, the prepared NCCs could be used as an additive to increase the tensile properties of matrix. It should be noted that suspensions with isotropic order were used for pressure loss studies in the present work.

However the study of rheological properties of samples is not in the scope of present thesis, to get more information about NCC sample the rheology of NCC suspension with concentration of 1.9 wt.% (initial concentration of sample used for pressure loss study) was investigated by using the rheometer with plate and plate configuration. The three- region can be seen in the graph (Figure 4.47). First shear thinning region in the low shear rate, second a transition region at intermediate shear rates and third another shear thinning region at high shear rates.

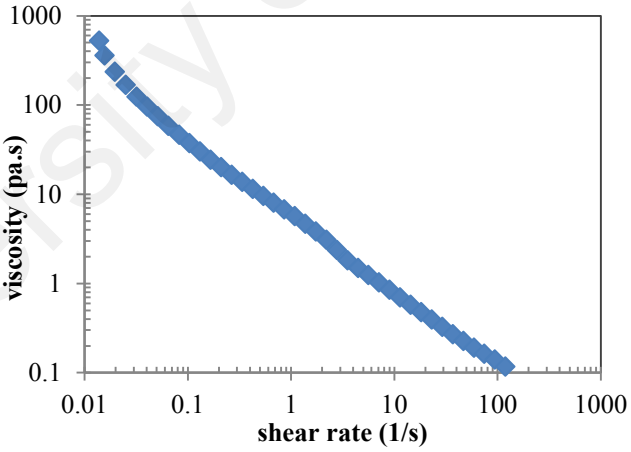

Figure 4.47: Viscosity as a function of shear rate for the NCC colloid.

The results of frequency sweep measurements are shown in Figure 4.48. The results indicate a viscoelastic liquid-like material structure where the storage modulus (G') is lower than loss modulus (G"). The storage modulus represents the ability of the suspension to restore energy, and therefore, it is regarded as the gel strength of the suspensions.

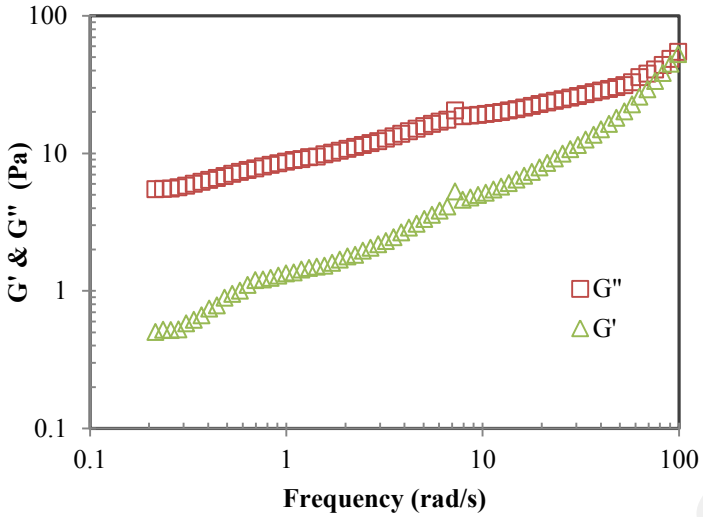

Figure 4.48: Storage modulus (G') and loss modulus (G") as a function of frequency for the NCC colloid.

NCC was diluted to a concentration of 1 wt.% and was added to the pulp suspension with two different amounts (70 ppm and 150 ppm corresponding to 1% and 2.5% of oven dry pulp weight). The final concentration of suspension containing pulp and NCC was kept at 0.6 wt%. The experimental conditions for suspension containing NCC were similar to those loaded with CPAM and potato starch.

Figure 4.49 shows the pressure loss versus velocity at temperature of 23°C. The trend follows the common behavior of pulp suspension.

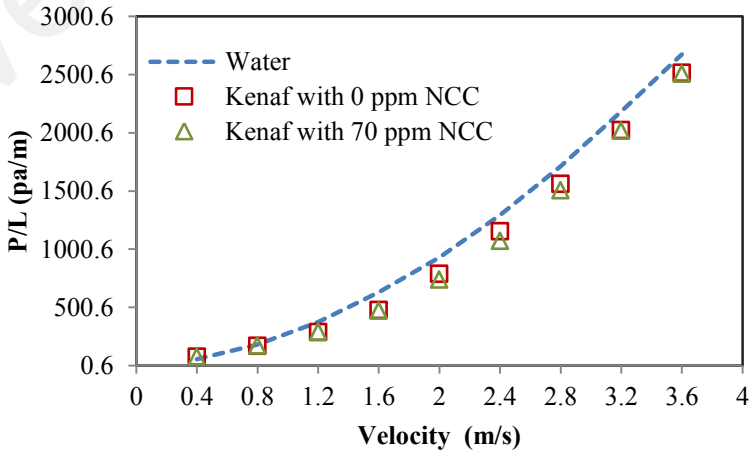

Figure 4.49: Pressure drop versus velocity for water, and Kenaf suspension with no NCC and 70 ppm NCC.

Drag ratio versus velocity diagrams are shown in Figures 4.50 and 4.51. The results show that suspension with very low NCC has higher drag ratio (lower drag reduction) compared to suspension with no NCC. The question remain here is that the increase in pressure loss comes from the reduction of pulp suspension concentration or is due to the addition of the NCC. Looking now at the drag ratio in Figure 4.51, it shows that the suspension containing more NCC has higher drag reduction than Kenaf suspension alone. It can be postulated that more NCC can interact more with the fibers and alter the mechanism of the pressure loss and overcome the increase of drag ratio due to reduction of fiber concentration. At low percentage of NCC loading the effect of reduction in fiber concentration is pronounced. The results are similar to that obtained for potato starch.

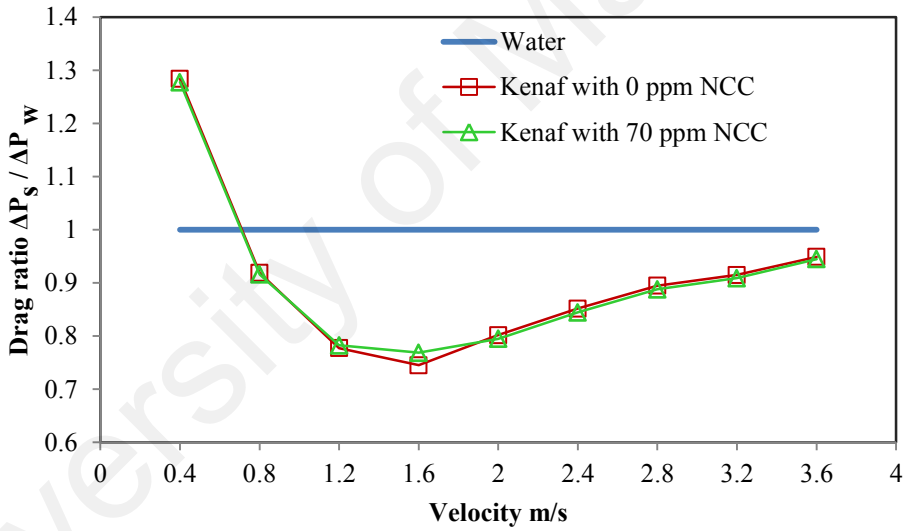

Figure 4.50: Drag ratio versus velocity for water, Kenaf suspension, and Kenaf suspension with 70 ppm NCC.

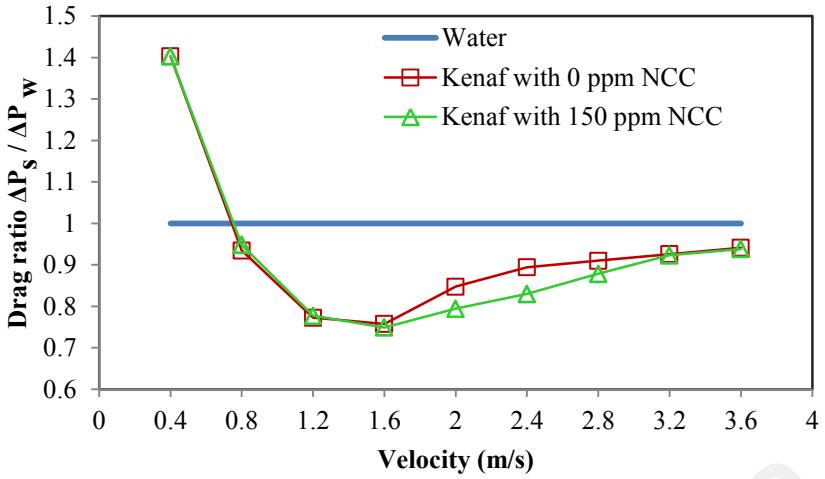

Figure 4.51: Drag ratio versus velocity for water, Kenaf suspension, and Kenaf suspension with 150 ppm NCC.

Comparison of the suspension containing pulp/CPAM and pulp/NCC, the one with NCC causes lower reduction in drag ratio. The maximum increase in drag reduction caused by addition of NCC was 7.1 %. The NCC with high concentration had less effect on increment of drag reduction than CPAM due to the polarity effect. CPAM with positive charge in dilute fiber suspensions promotes fiber-fiber bridging. It has been proposed previously that both interparticle bridging and charge reduction are important in flocculation mechanisms for fiber suspensions. CPAM can be absorbed at the fiber surface whereas no absorption between NCC particles with negatively charged cellulose occurred. Addition of NCC to fiber suspension decreases the bridging effect between fibers, increasing the effect of individual fibers, not fiber network on drag reduction.

4.9 Concerns associated with experimental procedures

There were several concerns and difficulties while the conducting the experimental works for heat transfer and pressure drop studies. The procedures being used to manage the relevant factors are reviewed in the following paragraphs.

4.9.1 Concentration of samples

Consistency of suspension was determined from the samples taken directly from the tank. For each experiment, two samples were collected from the tank while the suspension was flowing through the experimental flow loop, weighted, filtered, dried at 105 °C for 2 hours and reweighed. The same procedure was repeated at the end of the run to ensure that the concentration was constant during the experiment.

4.9.2 Flow rate and pressure drop control

Flow was measured by flow meter and the flow was controlled by using the inverter operated motor driven pump. Since flow meter shown fluctuation especially at high velocities, the target flow rates were considered at the upper range of fluctuated reading. For each flow rate the system needs time to become stable, in some cases a slight reduction in flow rate has been noted after some minutes while monitoring the flow rate during the run. Flow rate reduction was due to the air trapped inside the pipe. A valve was designed on the return line exactly before tank to release the air and rectify the flow rate. As a consequence, pressure drop detected by the pressure transducer was showing fluctuation as well. Generally at each velocity, pressure drops of low concentration samples were more stable than high concentration samples.

4.9.3 Heat flux and temperature control

Heat flux was regulated by the PLC. A monitor installed in the PLC box displays the power supply percentage of the total capacity of the heaters for controller regulated test section heating. Heat flux was monitored ad cross checked by using a clampmeter during the experiments to ensure constant heat flux at the test section. One of the important parameters was the bulk temperature. The heat transfer experiments were designed based on the bulk temperature at 30°C and it was attempted to keep the bulk

temperature constant. It should be noted that data collection had started at steady state when bulk temperature was maintained constant. In the initial stage it took some time to get the system stabilized. Increasing the velocity caused an increase in temperature where the lower chiller temperature was needed to keep the bulk temperature constant. Once the system reached to the steady-state condition, the bulk temperature remained constant.

4.9.4 Stirring time and multiple runs

One of the concerns associated with the experimental works was to define a proper procedure to run the pulp samples especially when the sample was containing the additives. As explained in chapter 3 polymer was added to the pulp sample in the tank which had been stirred for 2-3 hours before being recirculated in the system.

A supplementary experiment was conducted with EFB sample (0.2 wt.% concentration) and data were taken in the velocity range of 0.4-3.6 m/s at 30 °C (Figure 4.52) to examine the effect of soaking/ stirring time or multiple runs on the samples.

At the end of the first run, the sample was kept inside the tank under stirring. After 30 hours stirring, the second run was conducted in the same procedure. Results have shown insignificant difference between the pressure loss data taken from the first and second runs.

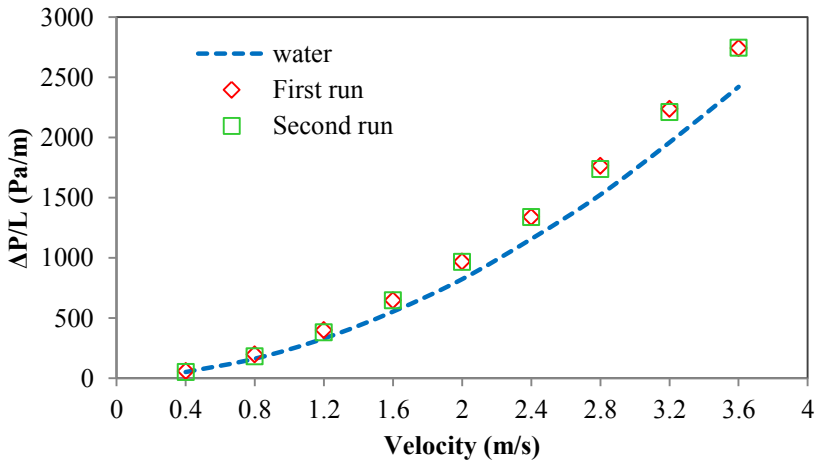

Figure 4.52: Frictional head loss as a function of velocity for two runs of EFB sample at concentration of 0.2 wt.% and bulk temperature of 30 °C.

4.10 Summary

Validation of the test rig was presented in this chapter. Before conducting the tests using the pulp suspension the water run data in form of Nusselt number and pressure loss were presented. The results obtained from the water run were compared with the existing correlations. The effect of fiber species, fiber concentration, velocity and beating degree on both heat transfer coefficient and pressure loss data was discussed in details. At the middle and high ranges of velocities the suspension with the lowest concentration (0.2 wt.%) tends to show the heat transfer coefficient higher than water. Suspensions with o.4 wt.% and 0.6 wt.% shown lower h_c value compared to that of water. In the case of pressure loss studies the suspensions at concentration of 0.2 and 0.4 wt.% presented the drag ratio data higher than the water line in the low and middle velocity range while the 0.6 wt.% sample exhibited drag reduction behavior. Moreover, Relationship of h_c and pressure drop data with fiber and paper properties are studied. Preparation and characterization of NCC was presented in this chapter and effect of additives such as CPAM, potato starch and NCC on pressure loss were presented and thoroughly discussed.

CHAPTER 5 CONCLUSION

5.1 Conclusion

The goals of the present work were to investigate the heat and momentum transfer of non- wood fiber suspensions in closed conduit flow. The following conclusions could be drawn from the obtained experimental data.

Fiber concentration and velocity had great influences on both the h_c and pressure drop of fiber suspensions flow in pipe. Presence of a small quantity (0.2 wt.%) of non-wood fibers in water flowing through a heated pipe resulted in a heat transfer enhancement. The h_c enhances at velocity around 1 m/s and continues up to the end of the investigated velocity range. The maximum increase in h_c occured at the maximum velocity and in the present case it is 3.6 m/s. At higher concentration of fibre in suspension such as 0.4 and 0.6 wt.% h_c decreased below water values. The effect of beating was examined on the heat transfer coefficient of Kenaf suspension. Low degree of beating (2000 degree for Kenaf sample) did not significantly affect h_c values throughout the velocity range while an increase in beating degree (4000 degree) reduced the h_c values. The h_c values obtained from same species of fibers at concentration of 0.6 wt.% and 1.2 m/s correlated well with fiber length, flexibility ratio and slender ratio. The results shown that h_c values would be decreased by a decrease in fiber length and fiber slender ratio or increase in flexibility ratio. An approximate linear relationship between h_c values and fiber/paper properties (from a specific non-wood fiber species) has shown that the specific fiber and paper properties could be predicted by monitoring heat transfer data. The efforts for correlating the h_c values with fiber and paper properties obtained from different species of fibers were not successful. This reveals that h_c or pressure loss data obtained from a specific fiber species cannot be used as an indicator for pulp and paper quality from other fiber species.

In the case of pressure loss studies, the pressure drop versus velocity curves for non-wood fibers were similar in shape comparing to those reported previously for wood fibers. Drag reduction was occurred at fiber concentration of 0.6 wt.% . Lower drag ratio provides higher drag reduction. The flow behavior of non-wood suspension in drag reduction region were similar to those reported for wood fiber samples where maximum drag reduction was followed by an increase in drag ratio to near the water line at higher velocities. Increase in beating degree would increase the drag reduction level where maximum drag ratio of 0.75 occurred at 1.6 m/s. Pressure loss data from the Kenaf samples correlated well with fiber and paper properties. Similar to the heat transfer data, the pressure loss data could be used to correlate fiber and paper properties with the suspension properties. CPAM and potato starch samples were used as the conventional additives to pulp suspensions. Concentrations of additives were set at 70 ppm and 150 ppm. Addition of CPAM has increased the drag reduction even at a very little quantity (70 ppm). Moreover, NCC as a new generation of additives has been synthesized successfully and characterized. Pulp suspension sample containing the NCC at low concentration (70 ppm) was shown no significant change on the drag reduction level. Drag reduction increased by an increase in NCC concentration (150 ppm). In comparison to the CPAM at 150 ppm concentration, NCC provided lower influence on enhancement of drag reduction due to polarity influence. Whereas positively charged CPAM being absorbed to negatively charged fibers enhance drag reduction.

5.2 Suggestion for further works

The research works presented in this thesis have presented new insights into the flow behavior of non-wood pulp fibers in pipe flow. Based on the present findings the following recommendations could be made:

Study of the flow behavior of non-wood fibers suspensions in very low velocities is suggested to investigate the flow behavior of non-wood pulp suspension in plug flow. Moreover, study on the flow behavior of other types of natural fibers, a mixture of wood and non-wood can be proposed to extend the research avenues. Meanwhile, investigation of other measurable fibre and paper properties could be conducted to correlate with heat transfer and pressure loss characteristics of fiber suspensions. The effect of other preferable types of additive materials e.g. Nanofibrillated cellulose on pressure loss behavior of pulp suspensions can be an area of interest. However two polymer concentrations were selected to study the effect of polymer concentration on the pressure loss trends, the considered concentrations of additives and even pulp fibers can be extended for the wider ranges of studies. Apart from these, study on the flow behavior of fiber suspensions with other nanomaterials e.g. conductive carbons can be suggested. Nanomaterial can be synthesized from the fibers and added into the fiber suspension. Especially in the case of conductive nanomaterials the extensive works can be done in the field of paper making or any other fields such as texture industry. Preparation of carbon from fibers was mentioned in the appendix F. The synthesized material will be used by our group for further studies on the flow behavior of fiber suspensions containing conductive nanomaterials.

References

Abe, K., & Yano, H. (2009). Comparison of the characteristics of cellulose microfibril aggregates of wood, rice straw and potato tuber. *Cellulose, 16*(6), 1017-1023.

Aloulou, F., Boufi, S., Belgacem, N., & Gandini, A. (2004). Adsorption of cationic surfactants and subsequent adsolubilization of organic compounds onto cellulose fibers. *Colloid and Polymer Science, 283*(3), 344-350.

Amin, N., Abdel-Aziz, M., & El-Ashtoukhy, E. Z. (2014). Effect of pulp fiber suspensions on the rate of mass transfer controlled corrosion in pipelines under turbulent flow conditions. *Chemical Engineering Research and Design, 92*(11), 2333-2338.

Araki, J., Wada, M., Kuga, S., & Okano, T. (2000). Birefringent glassy phase of a cellulose microcrystal suspension. *Langmuir, 16*(6), 2413-2415.

Ashori, A. (2006). Nonwood fibers—a potential source of raw material in papermaking. *Polymer-Plastics Technology and Engineering, 45*(10), 1133-1136.

Banavath, H. N., Bhardwaj, N. K., & Ray, A. (2011). A comparative study of the effect of refining on charge of various pulps. *Bioresource Technology, 102*(6), 4544-4551.

Baptista, P., Costa, A. P., Simões, R., & Amaral, M. E. (2014). Ailanthus altissima: An alternative fiber source for papermaking. *Industrial Crops and Products, 52*, 32-37.

Barnett, J., & Bonham, V. A. (2004). Cellulose microfibril angle in the cell wall of wood fibres. *Biological Reviews, 79*(2), 461-472.

Batchelor, W., Kjell-Arve, K., & Ouellet, D. (1999). Refining and the development of fibre properties. *Nordic Pulp and Paper Research Journal, 14*(4), 285-291.

Beck-Candanedo, S., Roman, M., & Gray, D. G. (2005). Effect of reaction conditions on the properties and behavior of wood cellulose nanocrystal suspensions. *Biomacromolecules, 6*(2), 1048-1054.

Beg, M. D. H., & Pickering, K. L. (2008). Mechanical performance of Kraft fibre reinforced polypropylene composites: Influence of fibre length, fibre beating and hygrothermal ageing. *Composites part A: Applied Science and Manufacturing, 39*(11), 1748-1755.

Beltramino, F., Roncero, M. B., Vidal, T., Torres, A. L., & Valls, C. (2015). Increasing yield of nanocrystalline cellulose preparation process by a cellulase pretreatment. *Bioresource Technology, 192*, 574-581.

Benhamou, K., Kaddami, H., Magnin, A., Dufresne, A., & Ahmad, A. (2015). Bio-based polyurethane reinforced with cellulose nanofibers: a comprehensive investigation on the effect of interface. *Carbohydrate Polymers, 122*, 202-211. doi: 10.1016/j.carbpol.2014.12.081

Bennington, C., Azevedo, G., John, D., Birt, S., & Wolgast, B. (1995). The yield stress of medium-and high-consistency mechanical pulp fibre suspensions at high gas contents. *Journal of Pulp and Paper Science, 21*(4), J111-J118.

Bennington, C., Kerekes, R., & Grace, J. (1990). The yield stress of fibre suspensions. *The Canadian Journal of Chemical Engineering, 68*(5), 748-757.

Bergander, A., & Salmén, L. (2002). Cell wall properties and their effects on the mechanical properties of fibers. *Journal of Materials Science, 37*(1), 151-156.

Bhardwaj, N. K., Duong, T. D., & Nguyen, K. L. (2004a). Pulp charge determination by different methods: effect of beating/refining. *Colloids and Surfaces A: Physicochemical and Engineering Aspects, 236*(1), 39-44.

Bhardwaj, N. K., Hoang, V., & Nguyen, K. L. (2007a). A comparative study of the effect of refining on physical and electrokinetic properties of various cellulosic fibres. *Bioresource Technology, 98*(8), 1647-1654.

Bhardwaj, N. K., Kumar, S., & Bajpai, P. K. (2004a). Effects of processing on zeta potential and cationic demand of kraft pulps. *Colloids and Surfaces A: Physicochemical and Engineering Aspects, 246*(1), 121-125.

Bhardwaj, N. K., Kumar, S., & Bajpai, P. K. (2004b). Effects of processing on zeta potential and cationic demand of kraft pulps. *Colloids and Surfaces A: Physicochemical and Engineering Aspects, 246*(1–3), 121-125.

Blomstedt, M. (2007). *Modification of cellulosic fibers by carboxymethyl cellulose: effects on fiber and sheet properties*: Helsinki University of Technology.

Bobkowicz, A., & Gauvin, W. (1965). The turbulent flow characteristics of model fibre suspensions. *The Canadian Journal of Chemical Engineering, 43*(2), 87-91.

Bondeson, D., Mathew, A., & Oksman, K. (2006). Optimization of the isolation of nanocrystals from microcrystalline cellulose by acid hydrolysis. *Cellulose, 13*(2), 171-180.

Bousfield, D. W. (2008). Rheological issues in the paper industry. *The brittish society of rheology, Rheology reviews*, 47-70.

Branch, C. A. (1991). *Heat transfer and heat transfer fouling in evaporators with kraft pulp black liquor.* University of Auckland.

Braun, B., Dorgan, J. R., & Chandler, J. P. (2008). Cellulosic nanowhiskers. Theory and application of light scattering from polydisperse spheroids in the Rayleigh− Gans− Debye regime. *Biomacromolecules, 9*(4), 1255-1263.

Brinchi, L., Cotana, F., Fortunati, E., & Kenny, J. (2013). Production of nanocrystalline cellulose from lignocellulosic biomass: technology and applications. *Carbohydrate Polymers, 94*(1), 154-169.

Carrasco, F., Mutje, P., & Pelach, M. (1996). Refining of bleached cellulosic pulps: characterization by application of the colloidal titration technique. *Wood Science and Technology, 30*(4), 227-236.

Charani, P. R., Dehghani-Firouzabadi, M., Afra, E., Blademo, Å., Naderi, A., & Lindström, T. (2013). Production of microfibrillated cellulose from unbleached kraft pulp of Kenaf and Scotch Pine and its effect on the properties of hardwood kraft: microfibrillated cellulose paper. *Cellulose, 20*(5), 2559-2567.

Chen, Y., Wan, J., Zhang, X., Ma, Y., & Wang, Y. (2012). Effect of beating on recycled properties of unbleached eucalyptus cellulose fiber. *Carbohydrate Polymers, 87*(1), 730-736.

Chinga-Carrasco, G. (2011). Cellulose fibres, nanofibrils and microfibrils: the morphological sequence of MFC components from a plant physiology and fibre technology point of view. *Nanoscale Research Letters, 6*(1), 1-7.

Clark, J. D. A. (1969). Fibrillation, Free Water, and Fiber Bonding. *Tappi J, 52*(2), 335-340.

Clarke, B., Ebeling, K., & Kropholler, H. (1985). Fibre coarseness: a new method for its characterisation. *Paperi Ja Puu, 67*(9), 490-499.

Colebrook, C., & White, C. (1937). Experiments with fluid friction in roughened pipes. *Proceedings of the royal society of london. series a, mathematical and Physical sciences*, 367-381.

Correa, A. C., de Morais Teixeira, E., Pessan, L. A., & Mattoso, L. H. C. (2010). Cellulose nanofibers from curaua fibers. *Cellulose, 17*(6), 1183-1192.

Courchene, C. E., Peter, G. F., & Litvay, J. (2006). Cellulose microfibril angle as a determinant of paper strength and hygroexpansivity in Pinus taeda L. *Wood and Fiber Science, 38*(1), 112-120.

Cui, Y., Pelton, R., & Ketelson, H. (2008). Shapes of polyelectrolyte titration curves. 2. The deviant behavior of labile polyelectrolytes. *Macromolecules, 41*(21), 8198-8203.

Daily, J. W., & Bugliarello, G. (1958). *The effects of fibers on velocity distribution, turbulence and flow resistance of dilute suspensions*: Hydrodynamics Laboratory, Department of Civil and Sanitary Engineering, Massachusetts Institute of Technology.

Dalpke, B., & Kerekes, R. (2005). The influence of fibre properties on the apparent yield stress of flocculated pulp suspensions. *Journal of Pulp and Paper Science, 31*(1), 39-43.

Daud, W. R. W., & Law, K. N. (2010). Oil palm fibers as papermaking material: Potentials and challenges. *BioResources, 6*(1), 901-917.

de Carvalho Mendes, C. A., Ferreira, N. M. S., Furtado, C. R. G., & de Sousa, A. M. F. (2015). Isolation and characterization of nanocrystalline cellulose from corn husk. *Materials Letters, 148*, 26-29.

De Gennes, P.-G. (1990). *Introduction to polymer dynamics*: CUP Archive.

Den Toonder, J., Hulsen, M., Kuiken, G., & Nieuwstadt, F. (1997). Drag reduction by polymer additives in a turbulent pipe flow: numerical and laboratory experiments. *Journal of Fluid Mechanics, 337*, 193-231.

Derakhshandeh, B. (2011). *Rheology of low to medium consistency pulp fibre suspensions.* University of British Columbia (Vancouver).

Dias, J., Taylor, M., Thompson, J., Brenkel, I., & Gregg, P. (1988). Radiographic signs of union of scaphoid fractures. An analysis of inter-observer agreement and reproducibility. *Journal of Bone & Joint Surgery, British Volume, 70*(2), 299-301.

Donaldson, L. (2007). Cellulose microfibril aggregates and their size variation with cell wall type. *Wood Science and Technology, 41*(5), 443-460.

Dong, X. M., Revol, J.-F., & Gray, D. G. (1998). Effect of microcrystallite preparation conditions on the formation of colloid crystals of cellulose. *Cellulose, 5*(1), 19-32.

Duffy, G., & Titchener, A. (1975). disruptive shear stress of pulp networks. *Svensk papperstidning*.

Duffy, G. G. (1972). *A study of the flow properties of New Zealand wood pulp suspensions.* ResearchSpace@ Auckland.

Duffy, G. G. (2006). Measurements, mechanisms and models: Some important insights into the mechanisms of flow of fibre suspensions. *ANNUAL TRANSACTIONS-NORDIC RHEOLOGY SOCIETY, 14*, 19.

Duffy, G. G., Kazi, S. N., & Chen, X. (2000). *Heat transfer to fibre suspensions in annular flow*. Paper presented at the Chemeca 2000: Opportunities and Challenges for the Resource and Processing Industries, Barton, A.C.T.: Institution of Engineers, Australia.

Duffy, G. G., Titchener, A., Lee, P., & Moller, K. (1976). Mechanisms of flow of pulp suspensions in pipes. *APPITA Aust Pulp Pap Ind Tech Assoc*.

Dutt, D., & Tyagi, C. (2011). Comparison of various eucalyptus species for their morphological, chemical, pulp and paper making characteristics. *Indian Journal of Chemical Technology, 18*(2), 145-151.

Ebringerova, A., Hromadkova, Z., & Heinze, T. (2005). Hemicellulose *Polysaccharides i* (pp. 1-67): Springer.

El Miri, N., El Achaby, M., Fihri, A., Larzek, M., Zahouily, M., Abdelouahdi, K., . . . Solhy, A. (2016). Synergistic effect of cellulose nanocrystals/graphene oxide nanosheets as functional hybrid nanofiller for enhancing properties of PVA nanocomposites. *Carbohydrate Polymers, 137*, 239-248.

Elazzouzi-Hafraoui, S., Nishiyama, Y., Putaux, J.-L., Heux, L., Dubreuil, F., & Rochas, C. (2007). The shape and size distribution of crystalline nanoparticles prepared by acid hydrolysis of native cellulose. *Biomacromolecules, 9*(1), 57-65.

Eyholzer, C., Bordeanu, N., Lopez-Suevos, F., Rentsch, D., Zimmermann, T., & Oksman, K. (2010). Preparation and characterization of water-redispersible nanofibrillated cellulose in powder form. *Cellulose, 17*(1), 19-30.

Fällman, M. C. (2009). Turbulence measurements in fiber suspension flows: experimental methods and results.

Fan, J.-s., & Li, Y.-h. (2012). Maximizing the yield of nanocrystalline cellulose from cotton pulp fiber. *Carbohydrate Polymers, 88*(4), 1184-1188.

Fardim, P., & Duran, N. (2003). Modification of fibre surfaces during pulping and refining as analysed by SEM, XPS and ToF-SIMS. *Colloids and surfaces a-physicochemical and engineering aspects, 223*(1-3), 263-276.

Fardim, P., Holmbom, B., Ivaska, A., Karhu, J., Mortha, G., & Laine, J. (2002). Critical comparison and validation of methods for determination of anionic groups in pulp fibres. *Nordic Pulp & Paper Research Journal, 17*(3), 346-351.

Fernando, D., Muhić, D., Engstrand, P., & Daniel, G. (2011). Fundamental understanding of pulp property development under different thermomechanical pulp refining conditions as observed by a new Simons' staining method and SEM observation of the ultrastructure of fibre surfaces. *Holzforschung, 65*(6), 777-786.

Ferreira, P. J., Matos, S., & Figueiredo, M. M. (1999). Size characterization of fibres and fines in hardwood kraft pulps. *Particle & particle systems characterization, 16*(1), 20-24.

Forgacs, O. (1957). *The hydrodynamic behaviour of paper-making fibres*.

Forgacs, O. (1963). The characterization of mechanical pulps. *Pulp Pap. Mag. Can, 64*, T89-T118.

Forsström, J., Torgnysdotter, A., & Wågberg, L. (2005). Influence of fibre/fibre joint strength and fibre flexibiity on the strentgh of papers from unbleached kraft fibres. *Nordic Pulp & Paper Research Journal, 20*(2), 186-191.

Gao, Y., Huang, F., Rajbhandari, V., Li, K., & Zhou, Y. (2009). Effect of separate refining and co-refining of bctmp/kp on paper properties. *Pulp and Paper Canada*.

Gärd, J. (2002). *The Influence of fibre curl on the shrinkage and strength properties of paper.* (master thesis), University of Technology, Luleå, Sweden.

Genco, J. M. (1999). *Fundamental processes in stock preparation and refining.* Paper presented at the Tappi Pulping Conference.

Gharehkhani, S., Sadeghinezhad, E., Kazi, S. N., Yarmand, H., Badarudin, A., Safaei, M. R., & Zubir, M. N. (2015). Basic effects of pulp refining on fiber properties-a review. *Carbohydrate Polymers, 115*, 785-803.

Gharehkhani, S., Shirazi, S. F. S., Jahromi, S. P., Sookhakian, M., Baradaran, S., Yarmand, H., . . . Basirun, W. J. (2015). Spongy nitrogen-doped activated

carbonaceous hybrid derived from biomass material/graphene oxide for supercapacitor electrodes. *RSC Advances, 5*(51), 40505-40513.

Gnielinski, V. (1976). New equations for heat and mass-transfer in turbulent pipe and channel flow. *International chemical engineering, 16*(2), 359-368.

Gonzalez-Labrada, E., & Gray, D. G. (2012). Viscosity measurements of dilute aqueous suspensions of cellulose nanocrystals using a rolling ball viscometer. *Cellulose, 19*(5), 1557-1565. doi: 10.1007/s10570-012-9746-9

González, I., Boufi, S., Pèlach, M. A., Alcalà, M., Vilaseca, F., & Mutjé, P. (2012). Nanofibrillated cellulose as paper additive in eucalyptus pulps. *BioResources, 7*(4), 5167-5180.

Grignon, J., & Scallan, A. (1980). Effect of pH and neutral salts upon the swelling of cellulose gels. *Journal of Applied Polymer Science, 25*(12), 2829-2843.

Gulsoy, S. K., & Tufek, S. (2013). Effect of chip mixing ratio of pinus pinaster and populus tremula on kraft pulp and paper Properties. *Industrial & Engineering Chemistry Research, 52*(6), 2304-2308.

Haavisto, S., Koskenhely, K., & Paulapuro, H. (2008). Effect of fiber flocculation and filling design on refiner loadability and refining characteristics. *BioResources, 3*(2), 403-424.

Haavisto, S., Liukkonen, J., Jäsberg, A., Koponen, A., Lille, M., & Salmela, J. (2011). Laboratory-Scale Pipe Rheometry: A Study of a Microfibrillated Cellulose Suspension. *Proc Papercon, 2011*, 704-717.

Habibi, Y., Lucia, L. A., & Rojas, O. J. (2010). Cellulose nanocrystals: chemistry, self-assembly, and applications. *Chem Rev, 110*(6), 3479-3500. doi: 10.1021/cr900339w

Hamad, W. Y., & Hu, T. Q. (2010). Structure–process–yield interrelations in nanocrystalline cellulose extraction. *The Canadian Journal of Chemical Engineering, 88*(3), 392-402.

Hartler, N. (1995). Aspects on curled and microcompressed fibres. *Nord. Pulp Paper Res. J., 10*(1).

Hassan, N. H. M., Muhammed, S., & Ibrahim, R. (2014). Properties of gigantochloa scortechinii paper enhancement by beating revolution. *Journal Of Tropical Resources And Sustainable Science, 2*, 59-67.

Hassan, N. H. M., Suhaimi, M., & Rushdan, I. (2013). Effect of soda-anthraquinone pulping conditions and beating revolution on the mechanical properties of paper made from gigantochloa scortechinii (semantan bamboo). *Malaysian Journal of Analytical Sciences, 17*(1), 75-84.

Helmerius, J., von Walter, J. V., Rova, U., Berglund, K. A., & Hodge, D. B. (2010). Impact of hemicellulose pre-extraction for bioconversion on birch Kraft pulp properties. *Bioresource Technology, 101*(15), 5996-6005.

Herrington, T. M., & Petzold, J. C. (1992). An investigation into the nature of charge on the surface of papermaking woodpulps 1. Charge/pH isotherms. *Colloids and surfaces, 64*(2), 97-108.

Heymer, J. O. (2009). *Measurement of heterogeneity in low consistency pulp refining by comminution modeling.* (PhD Thesis), University of British Columbia, Vancouver,BC, Canada.

Hirose, K., & Oka, T. (1971). On the Friction Factor for the Turbulent Flow of Dilute Aqueous Polymer Solutions. *Memoirs of the School of Engineering, Okayama University, 6*(1), 7-12.

Holt, B. L., Stoyanov, S. D., Pelan, E., & Paunov, V. N. (2010). Novel anisotropic materials from functionalised colloidal cellulose and cellulose derivatives. *Journal of Materials Chemistry, 20*(45), 10058-10070.

Horn, D., & Linhart, F. (1996). Retention aids *Paper Chemistry* (pp. 64-82): Springer.

Horvath, A. E. (2006). *The effects of cellulosic fiber charges on polyelectrolyte adsorption and fiber-fiber interactions.* (Doctoral of philosophy), Royal Institute of Technology, Stockholm, Sweden.

Horvath, A. E., & Lindstrom, T. (2007). Indirect polyelectrolyte titration of cellulosic fibers-surface and bulk charges of cellulosic fibers. *Nordic Pulp and Paper Research Journal, 22*(1), 87.

Hosseinpour, R., Fatehi, P., Latibari, A. J., Ni, Y., & Sepiddehdam, S. J. (2010). Canola straw chemimechanical pulping for pulp and paper production. *Bioresource technology, 101*(11), 4193-4197.

http://www.statista.com/statistics.

Hubbe, M. A., & Chen, J. (2004). Charge-related measurements–A reappraisal. Part 1. Streaming current. *Paper Technol, 45*(8), 17-23.

Hubbe, M. A., & Heitmann, J. A. (2007). Review of factors affecting the release of water from cellulosic fibers during paper manufacture. *BioResources, 2*(3), 500-533.

Hubbe, M. A., Nanko, H., & McNeal, M. R. (2009). Retention aid polymer interactions with cellulosic surfaces and suspensions: A review. *BioResources, 4*(2), 850-906.

Hubbe, M. A., & Wang, F. (2002). Where to add retention aid: Issues of time and shear. *Tappi journal, 1*(1), 28-33.

I'Anson, S., Karademir, A., & Sampson, W. (2006). Specific contact area and the tensile strength of paper. *Appita journal, 59*(4), 297.

Ingmanson, W., & Thode, E. (1959). Factors contributing to the strength of a sheet of paper. II. Relative bonded area. *Tappi, 42*(1), 83-93.

Jahan, M. S., Chowdhury, N., & Ni, Y. (2010). Effect of different locations on the morphological, chemical, pulping and papermaking properties of Trema orientalis (Nalita). *Bioresource Technology, 101*(6), 1892-1898.

Jäsberg, A. (2007). *Flow behaviour of fibre suspensions in straight pipes: new experimental techniques and multiphase modeling*: University of Jyväskylä.

Jiménez, L., Serrano, L., Rodríguez, A., & Sánchez, R. (2009). Soda-anthraquinone pulping of palm oil empty fruit bunches and beating of the resulting pulp. *Bioresource Technology, 100*(3), 1262-1267.

Johansson, A. (2011). Correlations between fibre properties and paper properties.

Jonoobi, M., Oladi, R., Davoudpour, Y., Oksman, K., Dufresne, A., Hamzeh, Y., & Davoodi, R. (2015). Different preparation methods and properties of nanostructured cellulose from various natural resources and residues: a review. *Cellulose, 22*(2), 935-969.

Joseph, D., Riccius, O., & Arney, M. (1986). Shear-wave speeds and elastic moduli for different liquids. Part 2. Experiments. *Journal of Fluid Mechanics, 171*, 309-338.

Joutsimo, O. (2004). *Effect of mechanical treatment on softwood kraft fiber properties.* Helsinki University of Technology.

Jovanović, J., Pashtrapanska, M., Frohnapfel, B., Durst, F., Koskinen, J., & Koskinen, K. (2006). On the mechanism responsible for turbulent drag reduction by dilute addition of high polymers: theory, experiments, simulations, and predictions. *Journal of Fluids Engineering, 128*(1), 118-130.

Kalia, S., Boufi, S., Celli, A., & Kango, S. (2014). Nanofibrillated cellulose: surface modification and potential applications. *Colloid and Polymer Science, 292*(1), 5-31.

Kamel, A., & Shah, S. N. (2009). Effects of salinity and temperature on drag reduction characteristics of polymers in straight circular pipes. *Journal of Petroleum Science and Engineering, 67*(1), 23-33.

Kang, T. (2007). *Role of external fibrillation in pulp and paper properties*: Helsinki University of Technology.

Karami, H., & Mowla, D. (2012). Investigation of the effects of various parameters on pressure drop reduction in crude oil pipelines by drag reducing agents. *Journal of Non-Newtonian Fluid Mechanics, 177*, 37-45.

Karppinen, A. (2014). Rheology and flocculation of polymer-modified microfibrillated cellulose suspensions.

Kazi, S. N. (2001). *Heat transfer to fiber suspensions-studies in fiber characterisation and fouling mitigation.* (Doctor of Philosophy), The University of Auckland.

Kazi, S. N., Duffy, G. G., & Chen, X. D. (1999). Heat transfer in the drag reducing regime of wood pulp fibre suspensions. *Chemical Engineering Journal, 73*(3), 247-253.

Kazi, S. N., Duffy, G. G., & Chen, X. D. (2014a). Study of the effect of entrance length on heat transfer to fibre suspensions in annular flow heat exchangers. *International Journal of Heat and Mass Transfer, 78*, 548-556. doi: 10.1016/j.ijheatmasstransfer.2014.06.081

Kazi, S. N., Duffy, G. G., & Chen, X. D. (2014b). Validation of heat transfer and friction loss data for fibre suspensions in a circular and a coaxial pipe heat exchanger. *International Journal of Thermal Sciences, 79*, 146-160. doi: 10.1016/Mthermalsci.2014.01.001

Kazi, S. N., Duffy, G. G., & Chen, X. D. (2015). Heat transfer coefficient of flowing wood pulp fibre suspensions to monitor fibre and paper quality. *Applied Thermal Engineering, 78*, 172-184.

Kerekes, R., & Schell, C. (1992). Characterization of fibre flocculation regimes by a crowding factor. *Journal of Pulp and Paper Science, 18*(1), J32-J38.

Kerekes, R., Soszynski, R., & Doo, T. (1985). *The flocculation of pulp fibres.* Paper presented at the Papermaking Raw Materials: Their Interaction with the Production Process and Their Effect on Paper Properties-Transactions of the Eighth Fundamental Research Symposium held at Oxford: September 1985.

Kerekes, R. J., & Olson, J. A. (2003). *Perspectives on Fibre Length Reduction in Refining.* Paper presented at the Proceedings of 7th PIRA International Refining Conference & Exhibition, Stockholm, Sweden.

Kerekes, R. J., Soszynski, R. M., & Doo, P. A. T. (2005). Characterizing refining action in PFI mills. *Tappi J, 4*(3), 9-13.

Khalil, H. A., Bhat, A., & Yusra, A. I. (2012). Green composites from sustainable cellulose nanofibrils: a review. *Carbohydrate Polymers, 87*(2), 963-979.

Kim, D. H., & Song, Y. S. (2015). Anisotropic optical film embedded with cellulose nanowhisker. *Carbohydrate Polymers*.

Kim, N. J., Kim, S., Lim, S. H., Chen, K., & Chun, W. (2009). Measurement of drag reduction in polymer added turbulent flow. *International Communications in Heat and Mass Transfer, 36*(10), 1014-1019.

Kline, S. J., & McClintock, F. (1953). Describing uncertainties in single-sample experiments. *Mechanical Engineering, 75*(1), 3-8.

Kočar, D., Pedersoli Jr, L., Strlič, M., Kolar, J., Rychlý, J., & Matisová-Rychlá, L. (2004). Chemiluminescence from paper: II. The effect of sample crystallinity, morphology and size. *Polymer Degradation and Stability, 86*(2), 269-274.

Kongdee, A., Bechtold, T., Burtscher, E., & Scheinecker, M. (2004). The influence of wet/dry treatment on pore structure-the correlation of pore parameters, water retention and moisture regain values. *Carbohydrate Polymers, 57*(1), 39-44.

Krochak, P., Ankerfors, M., Holm, R., & Lindstrom, T. (2011). *Drag Reduction Characteristics of Micro-Fibrillated Cellulose*. Paper presented at the papercon 2011, Northern Kentucky Convention Center in Covington, KY.

Kugler, D. (1990). Non-wood fiber crops: commercialization of kenaf for newsprint.

Kumar, A., Negi, Y. S., Choudhary, V., & Bhardwaj, N. K. (2014). Characterization of cellulose nanocrystals produced by acid-hydrolysis from sugarcane bagasse as agro-waste. *Journal of Materials Physics and Chemistry, 2*(1), 1-8.

Laine, J., Buchert, J., Viikari, L., & Stenius, P. (1996). Characterization of unbleached kraft pulps by enzymatic treatment, potentiometric titration and polyelectrolyte adsorption. *Holzforschung-International Journal of the Biology, Chemistry, Physics and Technology of Wood, 50*(3), 208-214.

Latifah, J., Ainun, Z., Rushdan, I., & Mahmudin, S. (2009). Restoring strength to recycled fibres by blending with kenaf pulp. *Malaysian Journal of Science, 28*(1), 79-87.

Lee, P., & Duffy, G. (1976a). Analysis of the drag reducing regime of pulp suspension flow. *Technical Association of Pulp & Pap Ind, Jour of, 59*(8).

Lee, P. F., & Duffy, G. G. (1976b). Relationships between velocity profiles and drag reduction in turbulent fiber suspension flow. *AIChE Journal, 22*(4), 750-753.

Leitner, J., Seyfriedsberger, G., & Kandelbauer, A. (2013). Modifications in the bulk and the surface of unbleached lignocellulosic fibers induced by a heat treatment without water removal: effects on fibre relaxation of PFI-beaten kraft fibers. *European Journal of Wood and Wood Products, 71*(6), 725-738.

Li, M. C., Wu, Q. L., Song, K. L., Lee, S., Qing, Y., & Wu, Y. Q. (2015). Cellulose Nanoparticles: Structure-Morphology-Rheology Relationships. *ACS Sustainable Chemistry & Engineering, 3*(5), 821-832.

Lindström, T. (1989). Some fundamental chemical aspects on paper forming. *Fundamentals of Papermaking, 1*, 309-412.

Liu, D., Chen, X., Yue, Y., Chen, M., & Wu, Q. (2011). Structure and rheology of nanocrystalline cellulose. *Carbohydrate Polymers, 84*(1), 316-322.

Loijas, M. (2010). Factors Affecting the Axial Force in Low-Consistency Refining. *Tampere University pf Applied Science, Paper Technology, Tampere, Finland: Valkeakoski Service Center*.

Lu, A., Hemraz, U., Khalili, Z., & Boluk, Y. (2014). Unique viscoelastic behaviors of colloidal nanocrystalline cellulose aqueous suspensions. *Cellulose, 21*(3), 1239-1250.

Lu, P., & Hsieh, Y.-L. (2010). Preparation and properties of cellulose nanocrystals: rods, spheres, and network. *Carbohydrate Polymers, 82*(2), 329-336.

Luettgen, C. O., Lindsay, J. D., & Stratton, R. A. (1991). Turbulent dispersion in pulp flow: preliminary results and implications for the mechanisms of fiber-turbulence interactions.

Lumiainen, J. (1990). New theory can improve practice. *Pulp and Paper International, 32*(7), 46-54.

Lumiainen, J. (2000). Refining of chemical pulp. *Papermaking part, 1*, 86-122.

Lumley, J. L. (1969). Drag reduction by additives. *Annual Review of Fluid Mechanics, 1*(1), 367-384.

Lyytikäinen, K., Saukkonen, E., Kajanto, I., & Kayhko, J. (2010). The effect of hemicellulose extraction on fiber charge properties and retention behavior of kraft pulp fibers. *BioResources, 6*(1), 219-231.

Ma, H., Zhou, B., Li, H.-S., Li, Y.-Q., & Ou, S.-Y. (2011). Green composite films composed of nanocrystalline cellulose and a cellulose matrix regenerated from functionalized ionic liquid solution. *Carbohydrate Polymers, 84*(1), 383-389.

MacKenzie, J., Martinez, D. M., & Olson, J. A. (2014). A quantitative analysis of turbulent drag reduction in a hydrocyclone. *The Canadian Journal of Chemical Engineering, 92*(8), 1432-1443.

Main, N. M., Talib, R. A., Ibrahim, R., Rahman, R. A., & Mohamed, A. Z. (2015). Linerboard Made from Soda-Anthraquinone (Soda-AQ) Treated Coconut Coir Fiber and Effect of Pulp Beating. *BioResources, 10*(4), 6975-6992.

Manzanares, M., Tenorio, J., & Ayerbe, L. (1997). Sowing time, cultivar, plant population and application of N fertilizer on Kenaf in Spain's central plateau. *Biomass and Bioenergy, 12*(4), 263-271.

Marin, F., Sanchez, J., Arauzo, J., Fuertes, R., & Gonzalo, A. (2009). Semichemical pulping of Miscanthus giganteus. Effect of pulping conditions on some pulp and paper properties. *Bioresource Technology, 100*(17), 3933-3940.

Martinelli, R. C. (1947). Heat transfer to molten metals. *Trans. ASME, 69*(8), 947-959.

Martinez, D., Kiiskinen, H., Ahlman, A.-K., & Kerekes, R. (2003). On the mobility of flowing papermaking suspensions and its relationship to formation. *Journal of Pulp and Paper Science, 29*(10), 341-347.

Meier, H. (1962). Chemical and morphological aspects of the fine structure of wood. *Pure and applied chemistry, 5*, 37-52.

Middis, J., Muller-Steinhagen, H., & Duffy, G. (1994). Heat transfer and frictional pressure drop characteristics of model nylon fibre suspensions. *Appita, 47*(2), 154-158.

Min, T., Yul Yoo, J., Choi, H., & Joseph, D. D. (2003). Drag reduction by polymer additives in a turbulent channel flow. *Journal of Fluid Mechanics, 486*, 213-238.

Miyanishi, T. (1995). On-line zeta potential analyses of a fine paper machine and a newsprint paper machine. *Tappi Journal, 78*.

Moayed, A. R. (1999). Characterization of Fibre Suspension Flows at Papermaking Consistencies.

Mohlin, U., Miller, J., Mohlin, U., & Miller, J. (1995). *Industrial refining-effects of refining conditions on fibre properties.* Paper presented at the Proc. 3rd international refining conference.

Mohlin, U. B., & Alfredson, C. (1990). Fiber deformation and its implications in pulp characterization. *Nordic Pulp and Paper Research Journal, 5*(6), 105-111.

Moller, K., & Duffy, G. (1978). An equation for predicting transition-regime pipe friction loss [Pulp suspensions flowing]. *Tappi [Technical Association of the Pulp and Paper Industry](USA)*.

Moller, K., & Elmqvist, G. (1980). Head losses in pipe bends and fittings. *TAPPI, 63*(3), 101-104.

Mosse, W. K., Boger, D. V., Simon, G. P., & Garnier, G. (2012). Effect of cationic polyacrylamides on the interactions between cellulose fibers. *Langmuir, 28*(7), 3641-3649.

Mossello, A. A., Harun, J., Resalati, H., Ibrahim, R., Shams, S. R. F., & Tahir, P. M. (2010). New approach to use of kenaf for paper and paperboard production. *BioResources, 5*(4), 2112-2122.

Mossello, A. A., Harun, J., Shamsi, S. R. F., Resalati, H., Tahir, P. M., Ibrahim, R., & Mohmamed, A. Z. (2010). A Review of Literatures Related to Kenaf as a Alternative for Pulpwoods. *Agricultural Journal, 5*(3), 131-138.

Mossello, A. A., Harun, J., Tahir, P. M., Resalati, H., Ibrahim, R., Shamsi, S. R. F., & Mohmamed, A. Z. (2010). A review of literatures related of using kenaf for pulp production (beating, fractionation, and recycled fiber). *Modern Applied Science, 4*(9), p21.

Mou, H., Iamazaki, E., Zhan, H., Orblin, E., & Fardim, P. (2013). Advanced Studies on the Topochemistry of Softwood Fibres in Low-Consistency Refining as Analyzed by FE-SEM, XPS, and ToF-SIMS. *BioResources, 8*(2).

Mutjé, P., Pèlach, M. A., García, J. C., Presta, S., Vilaseca, F., & Jimenez, L. (2006). Comparison of cationic demand between olive wood organosolv pulp and eucaliptus kraft pulp. *Process Biochemistry, 41*(7), 1602-1607.

Nagalakshmaiah, M., Mortha, G., & Dufresne, A. (2016). Structural investigation of cellulose nanocrystals extracted from chili leftover and their reinforcement in cariflex-IR rubber latex. *Carbohydrate Polymers, 136*, 945-954.

Navaee-Ardeh, S., Mohammadi-Rovshandeh, J., & Pourjoozi, M. (2004). Influence of rice straw cooking conditions in the soda–ethanol–water pulping on the mechanical properties of produced paper sheets. *Bioresource technology, 92*(1), 65-69.

Nayeri, M. D., Paridah, M. T., Harun, J., Abdullah, L. C., Bakar, E. S., Jawaid, M., & Namvar, F. (2013). Effects of temperature and time on the morphology, pH, and buffering capacity of bast and core kenaf fibres. *BioResources, 8*(2), 1801-1812.

Neto, W. P. F., Silvério, H. A., Dantas, N. O., & Pasquini, D. (2013). Extraction and characterization of cellulose nanocrystals from agro-industrial residue–Soy hulls. *Industrial Crops and Products, 42*, 480-488.

Nugroho, D. D. P. (2012). *Low consistency refining of mixtures of softwood & hardwood bleached kraft: Effects of refining power.* Asian Institute of Technology.

Oksanen, T., Pere, J., Buchert, J., & Viikari, L. (1997). The effect of Trichoderma reesei cellulases and hemicellulases on the paper technical properties of never-dried bleached kraft pulp. *Cellulose, 4*(4), 329-339.

Oksman, K., Etang, J. A., Mathew, A. P., & Jonoobi, M. (2011). Cellulose nanowhiskers separated from a bio-residue from wood bioethanol production. *Biomass and Bioenergy, 35*(1), 146-152.

Olson, J., Robertson, A., Finnigan, T., & Turner, R. (1995). An analyzer for fibre shape and length. *Journal of Pulp and Paper Science, 21*(11), J367.

Orts, W., Godbout, L., Marchessault, R., & Revol, J.-F. (1998). Enhanced ordering of liquid crystalline suspensions of cellulose microfibrils: A small angle neutron scattering study. *Macromolecules, 31*(17), 5717-5725.

Paavilainen, L. (1993). Conformability, flexibility and collapsibility of sulphate pulp fibres. *Paperi Ja Puu, 75*(9-10), 689-702.

Page, D. H. (1985a). The mechanism of strength development of dried pulps by beating [fiber kinking, crimping, upgrading]. *Svensk Papperstidning, 88*.

Page, D. H. (1989a). *The beating of chemical pulps–the action and the effects.* Paper presented at the 9th Fundamental Research Symposium on Fundamentals of paper-making.

Page, D. H. (1989b). The beating of chemicals pulps - The action and the effects. *Papermaking Raw Materials, Trans. of the 9th, Fundamental Research Symposium,*

Cambridge, UK, 1-37.

Page, D. H. (1989c). Fundamentals of papermaking transactions of the ninth fundamental research symposium (cf baker and vw punton, eds.): Mechanical Engineering Publications, London.

Page, D. H. S., R.S., Jordan, B.D., Barbe, M.C. . (1985b). *Curl, crimps, kinks and microcompressions in pulp fibers- their origin, measurements and significance. Paper making rawmaterials: their interaction with the production process and their effect on paper properties.* . Paper presented at the Transactions of the 8th Fundamental Research Symposium, Oxford , Punton.

Pande, H., Rao, N., Kapoor, S., & Roy, D. (1999). Hydrodynamic behavior of nonwood fiber suspensions. *Tappi journal, 82*(6).

Pandey, J. K., Kim, C.-S., Chu, W.-S., Lee, C. S., Jang, D.-Y., & Ahn, S.-H. (2009). Evaluation of morphological architecture of cellulose chains in grass during conversion from macro to nano dimensions. *e-Polymers, 9*(1), 1221-1235.

Paradis, M. A., Genco, J. M., Bousfield, D. W., Hassler, J. C., & Wildfong, V. (2002). Determination of drainage resistance coefficients under conditions of known shear rate. *Tappi J., 1*(8), 12-18.

Pattara, P. S. (2012). *Low Consistency Refining of Chemical Pulp, Investigating the Effect of Intensity on Fibre Cutting.* (Master Thesis).

Peng, F., & Johansson, L. (1996). Characterization of mechanical pulp fibres. *Journal of Pulp and Paper Science, 22*(7), J252-J257.

Penniman, J. G. (1992). Comparison of pulp pad streaming potential measurement and mobility measurement. *Tappi Journal, 75*(8), 111-115.

Petit-Conil, M., Cochaux, A., & De Choudens, C. (1994). Mechanical pulp characterization: a new and rapid method to evaluate fibre flexibility. *Paperi ja puu, 76*(10), 657-662.

Petukhov, B. (1970). Heat transfer and friction in turbulent pipe flow with variable physical properties. *Advances in Heat Transfer, 6*(503), i565.

Pirmahboub, H., Talebizadeh-Rafsanjani, A., Charani, P. R., & Morvaridi, R. (2015). Eco-friendly pulping of rice stem by twin-screw extruder: optimization of cooking time and naoh concentration. *Cellulose Chemistry and Technology, 49*(5-6), 485-495.

Pokhrel, C. (2010). Determination of Strength Properties of Pine and Its Comparison with Birch and Eucalyptus.

Polan, M. (1993). Effects of Refining on the Flocculation of Chemical Pulp Suspensions. *Institute of Papermaking, Darmstadt, Germany and Pulp and Paper Centre, The University of British Columbia*.

Ptasinski, P., Nieuwstadt, F., Van Den Brule, B., & Hulsen, M. (2001). Experiments in turbulent pipe flow with polymer additives at maximum drag reduction. *Flow, Turbulence and Combustion, 66*(2), 159-182.

Pulkkinen, I. (2010). From eucalypt fiber distributions to technical properties of paper.

Pulkkinen, I. F., J.; Aittamaa, J. . (2007). The effect of refining on fiber transverse dimension distributions of eucalyptus pulp species. *O Papel, 68*(5), 58-66.

Ramezani, O., & Nazhad, M. M. (2005). The effect of refining on paper formation. *Tappsa Journal, Archive, 2*.

Rånby, B. G. (1951). Fibrous macromolecular systems. Cellulose and muscle. The colloidal properties of cellulose micelles. *Discussions of the Faraday Society, 11*, 158-164.

Rene, E., Ulrich, H., & Wolfgang, B. (2006). A Method to determine Fibre Wall Damage induced by Refining. *Pulp and Fibre Technology Graz University of Technology, Institute for Paper, Graz, Austria*.

Revol, J.-F., Bradford, H., Giasson, J., Marchessault, R., & Gray, D. (1992). Helicoidal self-ordering of cellulose microfibrils in aqueous suspension. *International Journal of Biological Macromolecules, 14*(3), 170-172.

Richter, V., Orlandini, S., Caobianco, S., Scognamiglio, C., Lopopolo, S., Grossi, B., . . . Focher, B. (1996). *Non-wood plant pulps. Morphology and papermaking properties*. Paper presented at the Fourth European Workshop on Lignocellulosics and Pulp.

Rodríguez, A., Moral, A., Serrano, L., Labidi, J., & Jiménez, L. (2008). Rice straw pulp obtained by using various methods. *Bioresource Technology, 99*(8), 2881-2886.

Rodríguez, A., Sánchez, R., Requejo, A., & Ferrer, A. (2010). Feasibility of rice straw as a raw material for the production of soda cellulose pulp. *Journal of Cleaner Production, 18*(10), 1084-1091.

Roman, M., & Winter, W. T. (2004). Effect of sulfate groups from sulfuric acid hydrolysis on the thermal degradation behavior of bacterial cellulose. *Biomacromolecules, 5*(5), 1671-1677.

Rosli, W. D. W., Mazlan, I., & Law, K. N. (2011). Effect of Lignin on Acacia Mangium Kraft Pulp Refining Behaviour. *Cellulose Chemistry and Technology, 45*(9-10), 643-648.

Roy, A., & Larson, R. G. (2005). A mean flow model for polymer and fiber turbulent drag reduction. *Applied Rheology, 15*(6), 370-389.

Rushdan, I. (2003). Effect of refining on fibre morphology and drainage of soda pulp derived from oil palm empty fruit bunches. *Journal of Tropical Forest Products, 9*(1/2), 26-34.

Rushdan, I., Latifah, J., Hor, W., & Mohd Nor, M. (2007). Commercialscale production of soda pulp and medium paper from oil palm empty fruit bunches. *Journal of Tropical Forest Science, 19*(3), 121.

Rusu, M., Mörseburg, K., Gregersen, Ø., Yamakawa, A., & Liukkonen, S. (2011). Relation between fibre flexibility and cross sectional properties. *BioResources, 6*(1), 641-655.

Saikia, C., Goswami, T., & Ali, F. (1997). Evaluation of pulp and paper making characteristics of certain fast growing plants. *Wood Science and Technology, 31*(6), 467-475.

Sarrazin, P., Beneventi, D., Chaussy, D., Vurth, L., & Stephan, O. (2009). Adsorption of cationic photoluminescent nanoparticles on softwood cellulose fibres: effects of particles stabilization and fibres' beating. *Colloids and Surfaces A: Physicochemical and Engineering Aspects, 334*(1), 80-86.

Sasaki, S. (1991). Drag reduction effect of rod-like polymer solutions. I. Influences of polymer concentration and rigidity of skeltal back bone. *Journal of the Physical Society of Japan, 60*(3), 868-878.

Seth, R., & Page, D. (1988). Fiber properties and tearing resistance. *Tappi Journal, 71*(2), 103-107.

Sha, J., Nikbakht, A., Wang, C., Zhang, H., & Olson, J. (2015). The Effect of Consistency and Freeness on the Yield Stress of Chemical Pulp Fibre Suspensions. *BioResources, 10*(3), 4287-4299.

Shafeiei-Sabet, S., Hamad, W. Y., & Hatzikiriakos, S. G. (2013). Influence of degree of sulfation on the rheology of cellulose nanocrystal suspensions. *Rheologica Acta, 52*(8-9), 741-751.

Shafiei-Sabet, S., Hamad, W. Y., & Hatzikiriakos, S. G. (2012). Rheology of nanocrystalline cellulose aqueous suspensions. *Langmuir, 28*(49), 17124-17133.

Shafiei Sabet, S. (2013). Shear rheology of cellulose nanocrystal (CNC) aqueous suspensions.

Shirazi, S. F. S., Gharehkhani, S., Yarmand, H., Badarudin, A., Metselaar, H. S. C., & Kazi, S. N. (2015). Nitrogen doped activated carbon/graphene with high nitrogen level: Green synthesis and thermo-electrical properties of its nanofluid. *Materials Letters, 152*, 192-195.

Shopsowitz, K. E., Qi, H., Hamad, W. Y., & MacLachlan, M. J. (2010). Free-standing mesoporous silica films with tunable chiral nematic structures. *Nature, 468*(7322), 422-425.

Sixta, H. (2008) *Handbook of Pulp* (pp. 2-19): Wiley-VCH Verlag GmbH.

Sreenivasan, K. R., & White, C. M. (2000). The onset of drag reduction by dilute polymer additives, and the maximum drag reduction asymptote. *Journal of Fluid Mechanics, 409*, 149-164.

Sridach, W. (2010). Pulping and paper properties of Palmyra palm fruit fibers. *Sonklanakarin Journal of Science and Technology, 32*(2), 201.

Stoere, P., Nazhad, M., & Kerekes, R. J. (2001). An experimental study of the effect of refining on paper formation. *Tappi Journal, 84*(7).

Šturcová, A., Davies, G. R., & Eichhorn, S. J. (2005). Elastic modulus and stress-transfer properties of tunicate cellulose whiskers. *Biomacromolecules, 6*(2), 1055-1061.

Sutton, P., Joss, C., & Crossely, B. (2000). *Factors affecting fiber characteristics in pulp.* Paper presented at the 2000 pulping / process & product quality conference.

TAPPI. (1993). Consistency (concentration) of pulp suspensions, T 240 om-93

TAPPI. (1999). T 227 om-99, Freeness of pulp (Canadian standard method).

TAPPI. (2002). Forming handsheets for physical tests of pulp: TAPPI.

TAPPI. (2006). Folding endurance of paper (MIT tester) (Vol. T 511 om-02).

technology, F. r. (2001). Introduction to stock prep refining. *www.fibrelab.ubc.ca/files/2012/07/FINEbar-Training_Manual.pdf.*

Thomas, L. H., Forsyth, V. T., Šturcová, A., Kennedy, C. J., May, R. P., Altaner, C. M., . . . Jarvis, M. C. (2013). Structure of cellulose microfibrils in primary cell walls from collenchyma. *Plant Physiology, 161*(1), 465-476.

Toms, B. A. (1948). *Some observations on the flow of linear polymer solutions through straight tubes at large Reynolds numbers.* Paper presented at the Proceedings of the 1st International Congress on Rheology.

Tschirner, U., Ramaswamy, S., & Goel, A. (2002). *Effect of cereal straw fiber addition to papermaking furnish.* Paper presented at the Annual meeting-pulp and paper technical association of canada.

Tschirner, U. W., Barsness, J., & Keeler, T. (2007). Recycling of chemical pulp from wheat straw and corn stover. *BioResources, 2*(4), 536-543.

Vaezi, M., Katta, A. K., & Kumar, A. (2014). Investigation into the mechanisms of pipeline transport of slurries of wheat straw and corn stover to supply a bio-refinery. *Biosystems Engineering, 118*, 52-67.

Vaseleski, R. C., & Metzner, A. (1974). Drag reduction in the turbulent flow of fiber suspensions. *AIChE Journal, 20*(2), 301-306.

Ventura, C., Blanco, A., Negro, C., Ferreira, P., Garcia, F., & Rasteiro, M. (2007). Modeling pulp fiber suspension rheology. *Tappi journal, 6*(7), 17-23.

Ververis, C., Georghiou, K., Christodoulakis, N., Santas, P., & Santas, R. (2004). Fiber dimensions, lignin and cellulose content of various plant materials and their suitability for paper production. *Industrial Crops and Products, 19*(3), 245-254.

Wågberg, L., & Lindström, T. (1987). Flocculation of cellulosic fibers by cationic polyacrylamides with different charge densities [polyelectrolytes, kinetics].

Wai, N., Nanko, H., & Murakami, K. (1985). A morphological study on the behavior of bamboo pulp fibers in the beating process. *Wood Science and Technology, 19*(3), 211-222.

Wan, J., Yang, J., Ma, Y., & Wang, Y. (2011). Effects of the pulp preparation and papermaking processes on the properties of occ fibers. *BioResources, 6*(2), 1615-1630.

Wathén, R. (2006). Studies on fiber strength and its effect on paper properties.

Williams, W. C. (2007). *Experimental and theoretical investigation of transport phenomena in nanoparticle colloids (nanofluids).* Massachusetts Institute of Technology.

Wilson, E. E. (1915). A basis for rational design of heat transfer apparatus. *Trans. ASME, 37*(47), 47-82.

Wistara, N., & Young, R. (1999). Properties and treatments of pulps from recycled paper. Part I. Physical and chemical properties of pulps. *Cellulose, 6*(4), 291-324.

Xu, Q., Gao, Y., Qin, M., Wu, K., Fu, Y., & Zhao, J. (2013). Nanocrystalline cellulose from aspen kraft pulp and its application in deinked pulp. *International Journal of Biological Macromolecules, 60*, 241-247.

Yacob, S. (2007). *Progress and challenges in utilization of oil palm biomass.* Paper presented at the Paper presented Asian Science and Technology Seminar, sponsored by Japan Science and Technology Agency.

Yang, D. K., West, J. L., Chien, L. C., & Doane, J. W. (1994). Control of reflectivity and bistability in displays using cholesteric liquid crystals. *Journal of Applied Physics, 76*(2), 1331-1333.

Ye, Y.-S., Zeng, H.-X., Wu, J., Dong, L.-Y., Zhu, J.-T., Xue, Z.-G., . . . Mai, Y.-W. (2016). Biocompatible reduced graphene oxide sheets with superior water dispersibility stabilized by cellulose nanocrystals and their polyethylene oxide composites. *Green Chemistry*.

Yuan, L., Wan, J., Ma, Y., Wang, Y., Huang, M., & Chen, Y. (2013). The Content of Different Hydrogen Bond Models and Crystal Structure of Eucalyptus Fibers during Beating. *BioResources, 8*(1).

Zeng, X., Retulainen, E., Heinemann, S., & Fu, S. (2012). Fibre deformations induced by different mechanical treatments and their effect on Zero-Span Strength. *Nordic Pulp and Paper Research Journal, 27*(2), 335.

Zhang, Y., Sjögren, B., Engstrand, P., & Htun, M. (1994). Determination of charged groups in mechanical pulp fibres and their influence on pulp properties. *Journal of Wood Chemistry and Technology, 14*(1), 83-102.

Zimmermann, T., Bordeanu, N., & Strub, E. (2010). Properties of nanofibrillated cellulose from different raw materials and its reinforcement potential. *Carbohydrate Polymers, 79*(4), 1086-1093.

Zubir, M. N. B. M. (2015). *Facile and highly scalable approach to enhance the stability of colloidal system for thermal application.* University of Malaya.

List of publications and papers presented

Gharehkhani, S., Sadeghinezhad, E., Kazi, S. N., Yarmand, H., Badarudin, A., Safaei, M. R., & Zubir, M. N. M. (2015). Basic effects of pulp refining on fiber properties—A review. Carbohydrate polymers, 115, 785-803

Gharehkhani, Samira; Seyed Shirazi, Seyed Farid; yarmand, hooman; Gharehkhani, Abdolreza; Badarudin, Ahmad; Ibrahim, Rushdan; Kazi, Salim Newaz. (2016). Preparation and characterization of nanocrystalline cellulose from Acacia mangium. International conference on micro and nano technology.

Gharehkhani, S., Shirazi, S. F. S., Jahromi, S. P., Sookhakian, M., Baradaran, S., Yarmand, S.N.Kazi & Basirun, W. J. (2015). Spongy nitrogen-doped activated carbonaceous hybrid derived from biomass material/graphene oxide for supercapacitor electrodes. RSC Advances,5(51), 40505-40513.

Gharehkhani, Samira; yarmand, hooman; Seyed Shirazi, Seyed Farid; Nashrul Mohd Zubir, Mohd; Amiri, Ahmad; Solangi, Khalid Hussain; Ibrahim, Rushdan; Kazi, Salim Newaz (2016). Insights into flow behavior of a non-wood plant (Kenaf) fibre suspension in straight pipe for pulp and paper industry.

Gharehkhani, S., Nouri-Borujerdi, A., Kazi, S. N., & Yarmand, H. (2014). Extension of weighted sum of gray gas data to mathematical simulation of radiative heat transfer in a boiler with gas-soot media. The Scientific World Journal.

Shirazi, S. F. S., Gharehkhani, S., Yarmand, H., Badarudin, A., Metselaar, H. S. C., & Kazi, S. N. (2015). Nitrogen doped activated carbon/graphene with high nitrogen level: Green synthesis and thermo-electrical properties of its nanofluid. Materials Letters, 152, 192-195.

Yarmand, H., Gharehkhani, S., Shirazi, S. F. S., Amiri, A., Montazer, E., Arzani & Kazi, S. N. (2016). Nanofluid based on activated hybrid of biomass carbon/graphene

oxide: Synthesis, thermo-physical and electrical properties. International Communications in Heat and Mass Transfer, 72, 10-15.

Yarmand, H., Gharehkhani, S., Shirazi, S. F. S., Amiri, A., Alehashem, M. S., Dahari, M., & Kazi, S. N. (2016). Experimental investigation of thermo-physical properties, convective heat transfer and pressure drop of functionalized graphene nanoplatelets aqueous nanofluid in a square heated pipe. Energy Conversion and Management, 114, 38-49.

Shirazi, S. F. S., Gharehkhani, S., Metselaar, H. S. C., Nasiri-Tabrizi, B., Yarmand, H., Ahmadi, M., & Osman, N. A. A. (2016). Ion size, loading, and charge determine the mechanical properties, surface apatite, and cell growth of silver and tantalum doped calcium silicate. RSC Advances, 6(1), 190-200.

Yarmand, H., Gharehkhani, S., Ahmadi, G., Shirazi, S. F. S., Baradaran, S., Montazer, & Dahari, M. (2015). Graphene nanoplatelets–silver hybrid nanofluids for enhanced heat transfer. Energy Conversion and Management,100, 419-428.